Univerzita Karlova v Praze

1. lékařská fakulta

Doktorské studijní programy v biomedicíně

Studijní obor: Biochemie a patobiochemie

Mgr. Jan Ševčík

The functional *in vitro* analysis of the BRCA1 alternative splicing variants

Funkční *in vitro* analýza alternativních sestřihových variant genu BRCA1

Dizertační práce

Vedoucí závěrečné práce: Doc. MUDr. Zdeněk Kleibl, PhD.

Ústav biochemie a experimentální onkologie, 1. LF UK v Praze

Praha, 2012

Prohlášení:

Prohlašuji, že jsem závěrečnou práci zpracoval/a samostatně a že jsem řádně uvedl/a a citoval/a všechny použité prameny a literaturu. Současně prohlašuji, že práce nebyla využita k získání jiného nebo stejného titulu

Souhlasím/~~Nesouhlasím~~* s trvalým uložením elektronické verze mé práce v databázi systému meziuniverzitního projektu Theses.cz za účelem soustavné kontroly podobnosti kvalifikačních prací.

V Praze, 04.07.2012

JAN ŠEVČÍK

Podpis

*Nehodící se vypusťte

Identifikační záznam:

ŠEVČÍK Jan. Functional *in vitro* analysis of the BRCA1 alternative splicing variants Praha, 2012. 105 s., 0 příl. Dizertační práce (PhD.). Univerzita Karlova v Praze, 1. lékařská fakulta, Ústav biochemie a experimentální onkologie. Vedoucí práce: Doc. MUDr. Zdeněk Kleibl, PhD.

Abstrakt:

Úvod: Inaktivace tumor supresorového genu BRCA1 je predispozičním faktorem vzniku karcinomu prsu a ovaria. Vznik funkčně odlišných nádorově specifických alternativních sestřihových variant může být možným mechanismem snižujícím aktivitu BRCA1 v procesu reparace dvouřetězcových zlomů DNA (DDSB). V této práci jsme funkčně charakterizovali dvě alternativní sestřihové varianty BRCA1Δ14-15 a BRCA1Δ17-19, nalezené v průběhu genetického screeningu jedinců s vysokým rizikem vzniku karcinomu prsu.**Metody**: Pro funkční *in vitro* analýzu jsme vytvořili modelový systém klonů buněčné linie MCF-7 stabilně exprimujících zkoumané varianty. Pomocí comet assay a konfokální imunomikroskopie jsme v tomto systému sledovali vliv BRCA1Δ14-15 a Δ17-19 variant na kinetiku reparace DDSB a proliferaci. Aktivita DNA reparačních procesů byla stanovena přímo pomocí *in vitro* NHEJ assay a nepřímo testem senzitivity na mitomycin C. Proliferační aktivita byla stanovena klonogenním testem a růstovými křivkami. **Výsledky**: Exprese BRCA1Δ14-15 a Δ17-19 zvyšuje v MCF-7 buňkách úroveň endogenního poškození DNA, zpomaluje reparaci DDSB, negativně ovlivňuje tvorbu reparačních komplexů v počáteční fázi reparace a prodlužuje jejich trvání. Varianty BRCA1Δ14-15 a Δ17-19 rozdílně ovlivňují aktivitu HR, NHEJ a radiosensitivitu MCF-7 buněk. **Závěr**: Zvýšení exprese BRCA1Δ14-15 nebo Δ17-19 má v MCF-7 buňkách dominantně negativní vliv na reparaci DDSB. Možným mechanismem je narušení procesu vzájemné komunikace hlavních DDSB reparačních pochodů – HR a NHEJ. Důsledkem toho je ztráta flexibility procesu reparace DDSB a tím i snížení stability genomu. Výsledky naší práce ukazují, že alternativní sestřihové varianty BRCA1Δ14-15 a Δ17-19 v MCF-7 buňkách negativně ovlivňují aktivitu BRCA1 v procesu udržování genomové homeostazi.

KLÍČOVÁ SLOVA: karcinom prsu, *BRCA1*, alternativní mRNA sestřih, homologní rekombinace, NHEJ, genomová stabilita, IRIF, proliferační aktivita.

Abstract:

BACKGROUND: The inactivation of the tumor suppressor gene BRCA1 is a predisposing factor for a breast/ovarian cancer development. Formation of cancer-specific alternative splicing variants with aberrant biological properties can represent additional mechanism decreasing the overall BRCA1 activity in DNA double strand break (DDSB) repair. In this study, we analyzed BRCA1 alternative splicing variants BRCA1Δ14-15 and Δ17-19 ascertained previously during the screening of high-risk breast cancer individuals. **METHODS**: We established a stable MCF-7 cell line-based model system for an *in vitro* analysis of BRCA1 variants. Using this system, we analyzed the impact of BRCA1Δ14-15 and Δ17-19 variants on DNA repair kinetics using comet assay and confocal immunomicroscopy. The capacity of DNA repair was assessed directly by an *in vitro* NHEJ assay and indirectly by a mitomycin C sensitivity test. The proliferation activities were determined by a clonogenic assay and growth curves. **RESULTS**: Overexpression of BRCA1Δ14-15 and Δ17-19 increases the endogenous level of DNA damage, slows down the DDSB repair, and decelerates the initial phase of radiation-induced foci formation and prolongs their persistence. Moreover, BRCA1Δ14-15 and Δ17-19 differentially influence the activity of HR and NHEJ and sensitivity of MCF-7 cells to ionizing radiation. **CONCLUSIONS**: The overexpression of BRCA1Δ14-15 or Δ17-19 impairs the DNA repair capacity in a dominant-negative fashion. We hypothesize, that BRCA1Δ14-15 and Δ17-19 impair the balance and communications between main DDSB repair pathways – HR and NHEJ. This leads to the loss of flexibility in DDSB repair and could contributes to the increased genomic instability. We conclude that alternative splicing variants BRCA1Δ14-15 and Δ17-19 negatively influence the BRCA1 functions in maintaining of genome homeostasis in MCF-7 cells.

KEYWORDS: breast cancer, *BRCA1*, alternative mRNA splicing, homologous recombination, NHEJ, genome stability, IRIF, cell cycle checkpoint, proliferation.

Acknowledgment:

The thesis summarizes results obtained during my long term stay at the Institute of Biochemistry and Experimental Oncology of the 1st Faculty of Medicine, Charles University, Prague.

I would like to use this opportunity to thank all people, who helped, supported and pursed me during my Ph.D. studies; above all my supervisor Doc. Zdeněk Kleibl, Ph.D., Petra Kleiblová M.D., Ph.D., Martin Falk Dr. Ph.D and all my colleagues from the Institute of Biochemistry and Experimental Oncology without whose great encouragement and kind guidance this work could not have been accomplished.

This work has been supported by following grants: GAČR P301/12/1850; IGA MZ ČR NT12280; GAUK 428711, and PRVOUK-P27/LF1/1.

INDEX

1 INTRODUCTION

The BRCA1 gene (Breast cancer 1 gene; OMIM*113705) was first cloned in 1994 after being mapped to 17q21.31 chromosome by a genetic linkage analysis as high-penetrant breast and ovarian cancer predisposition gene [1].

1.1 The structure of *BRCA1* gene

The *BRCA1* gene contains 23 exons spanning the total area of 81 kb. The structure of *BRCA1* is unique due to an unusually large central exon 10 that constitutes more than 60% of the entire *BRCA1* coding sequence. The unusual high number of the *Alu* repetitions located in intronic sequences contributes to the elevated frequency of the intragenic rearrangements [2].

The *BRCA1* 5' site lies in a duplicated part of the 17q21 chromosome. Within this region lies BRCA1 1A, 1B and 2 exons with corresponding intronic sequences respectively. As a result of this duplication a *BRCA1* pseudogene (ψBRCA1) is localized 30 kbp upstream of a *BRCA1* gene [3].

1.2 BRCA1 transcript variants

The *BRCA1* gene contains 22 constitutive coding exons, one alternative coding exon (exon 13) and two distinct forms of non-coding exon 1 (exon 1a and 1b, respectively). The expression is driven by two independent promoters marked as α and β, respectively [4]. Their usage governs the inclusion of certain form of the exon 1. In both transcripts differing in the exon 1, the BRCA1 coding sequence starts within exon 2 at the same position. Except to this arbitral translation initiation codon at exon 2, there other translation initiation sites were described in the BRCA1 variants containing exon 1b. The variable 5' UTR BRCA1 mRNA sequence was shown to be an important regulator of BRCA1 translation [5]. The promoter selection, together with additional posttranscriptional processing of pre-mRNA, determines formation of six different naturally occurring BRCA1 transcription variants.

The transcription variant 1 (NM_007294), also known as BRCA1a (Fig.1), represents the most frequently occurring variant. It contains the exon 1a plus 22 constitutive coding exons

in the 7224 bp long transcript translated into the full-length protein (220 kDa). The transcription variant 2 (NM_007300.3) contains the alternative coding exon 13 resulting in the longest BRCA1 transcript, that is translated into the protein with additional 31 amino acids. The transcription variant 3 (NM_007297.3) contains the 1b non-coding exon and lacks the exon 3. Though in-frame, the skipping of the exon 3 leads to the formation of premature termination codon at the exon 2 – exon 4 junction. However, the BRCA1 transcription variant 3 uses an alternative down-stream translation start localized in the exon 4. The resulting protein is N-terminally shortened for 102 amino acids. The transcript variant 4 (NM_007298.3) generally marked as BRCA1Δ11b (or BRCA1Δ11q) is the shortest transcription variant of BRCA1 gene. It lacks the exon number 1 and uses an alternative 3' splicing site within the central exon 10b.[1] The primary transcript contains a short exon 10a that consists of 116 bp only. The transcription variant 5 (NM_007299.3) contains the 1b and 10a exons and additionally lacks the exon 22. The skipping of exon 22 shifts the original ORF and results in the formation of BRCA1 protein isoform with different and partially truncated C-terminal part.

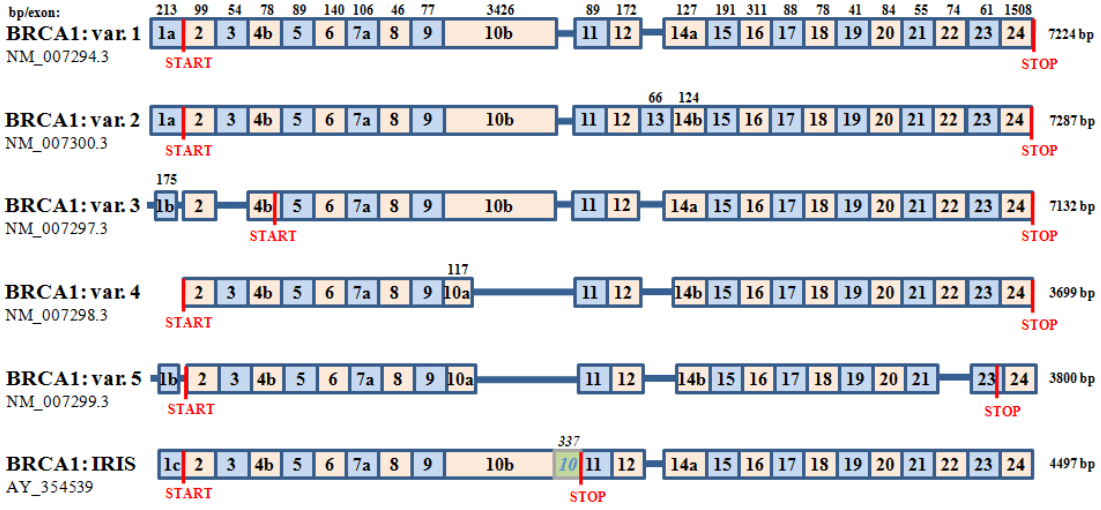

Figure 1: The BRCA1 transcription variants. *The BRCA1 gene contains 24 exons. The exon 1 is non-coding and exist in two alternative variants (1a and 1b, respectively) differing in their length. The alternative exon 13 is exclusively present in transcription variant 2. BRCA1 is naturally transcribed in* ***5 variants*** *differing in the exon composition, translation initiation (START), termination (STOP) and length. The* ***BRCA1 IRIS*** *is a specific isoform transcribed from the same gene that uses an alternative 3' splicing site within exon 10b resulting in partial inclusion of the sequence from intron* ***10*** *and premature termination following 34 amino acids at the C-terminus of IRIS.*

[1] *BRCA1* exons in this text are numbered according to the currently recommended classification. In former (and yet widely used) classification system, the exon 10b was denoted as exon 11.

The BRCA1 IRIS (AY354539.2) is a specific isoform that is generally not included between the BRCA1 transcriptional variants [6]. However, it originates from the same gene and differs from the BRCA1 transcription variant 1 by presence of variant exon 1c and usage of an alternative splicing site beyond the exon 10b resulting in inclusion of 337 nucleotides from intron 11 and premature termination of translation. Truncated IRIS protein contains 1365 identical amino acids to the N-terminus of full length BRCA1 and a novel part with 34 amino acids at IRIS C-terminus.

1.3 Structure of the BRCA1 protein

The BRCA1 is a large multidomain phosphoprotein consisting of 1863 amino acids in its full-length form. The activities of BRCA1 are determined by certain protein motifs localized separately within the protein molecule (Fig. 2).

Besides the localization signals, DNA binding domain (DBD) and serine rich region, BRCA1 contains three different conservative protein-interaction modules. The N-terminally localized RING finger domain, the coiled-coil domain and a tandem of two C-terminally-localized BRCT domains. Though the conformation of the entire BRCA1 protein has not been determined yet the crystallographic data of the structure of RING and BRCT domains are available [7,8].

The BRCA1 RING finger domain is a protein interaction motif consisting of RING finger and two flanking α-helixes encompassing the amino acids 1 – 109 (exons 2 – 6 respectively). The first 100 amino acids residues are highly conserved within the BRCA1 gene indicating the importance of RING finger domain. The RING finger is a zinc-binding protein interaction motif containing conserved sequence of 24 – 64 amino acids where seven cysteine and one histidine residues binding coordinately two Zn2+ ions stabilizing the RING structure. The N- and C-terminal α-helixes are responsible for binding of BARD1- another RING-containing protein. Beside the direct interaction with other RING finger containing proteins (BARD1, BRAP2), the RING finger domain alone was shown to generally possess an E3 mono-ubiquitin ligase activity [9]. This BRCA1 enzymatic activity is dramatically

elevated upon interaction and formation of a stable heterodimer with BARD1 [10]. It is highly probable that the only BRCA1-BARD1 heterodimer is able to catalyze the ubiquitinylation of certain substrates.

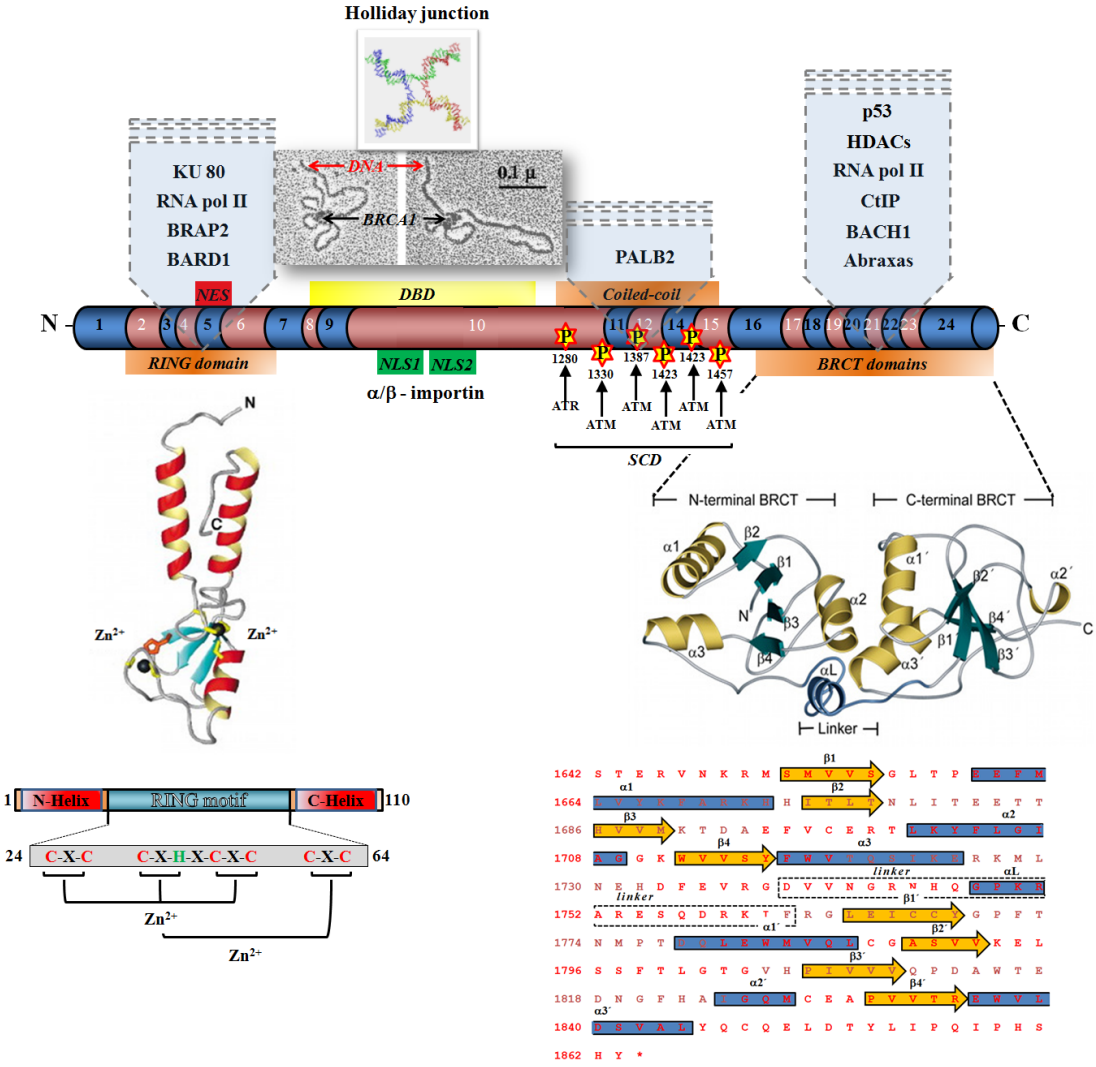

Figure 2: Structure of BRCA1 protein. *BRCA1 is a large nuclear phosphoprotein consisting of 1863 amino acids. The intracellular localization of BRCA1 protein is driven by two* ***nuclear localization signals (NLS)*** *mediated the interaction with nuclear α/β - importin receptor.* ***Nuclear export signal (NES)*** *facilitating the shuttling of BRCA1 between cytoplasm and nucleus by interaction with CRM1 receptor is located at the N – terminal part of BRCA1. Activities of these opposite localization signals are highly influenced by binding of BARD1 and BRAP1. The exact intranuclear (re)localization of BRCA1 is mediated by interaction with specific proteins participating directly on DNA damage response processes (RNA pol II, Ku 80, Abraxas). These proteins interact with BRCA1 by its three independent protein-protein interaction motifs: N-terminal* ***RING domain****, C-terminal* ***coiled-coil domain*** *and a tandem of two C-terminal* ***BRCT domains****. These highly conserved binding modules are often presented within the proteins participating on the DNA repair processes. The RING domain*

*forms an active site of **E3 ubiquiting ligase activity** of BRCA1/BARD1 heterodimer. The coiled-coil domain binds PALB2 which ensures the linking of BRCA1 and BRCA2. The **serine containing domain (SCD)** of BRCA1 is a target of phosphorylation for various kinases (including ATM, ATR, Chk2). The biological properties of BRCA1 including its binding capacity or localization are regulated on the phosphorylation-dependent manner. BRCA1 is capable bind to DNA directly via its **DNA binding domain (DBD)**. This binding is DNA-structure but not DNA-sequence-specific. The affinity of BRCA1 is higher to branched DNA structures. When bounded, BRCA1 causes the structural changes in DNA molecule forming a four-way complex resembling a Holliday junction.*

The BRCA1 is a nuclear-cytoplasm shuttling protein. Nuclear export of BRCA1 is secured by a nuclear export sequence (NES) localized on the C-terminal helix of RING domain (amino acids 81 – 99; exon 6) [11]. Due to this immediate proximity to RING domain, binding of BARD1 physically covers the BRCA1's NES and thus causes its nuclear retention [12]. The active nuclear localization of BRCA1 is mediated by two nuclear localization signals (NLS) at the BRCA1 N-terminal part (amino acids 501 – 507 NLS1 and 607 – 614 NLS2, respectively; exon 10) recognized by the importin-α receptor [13]. NLS1 is more critical for BRCA1 nuclear transport as mutations in this sequence (but not in NLS2) abrogate the interaction of BRCA1 with nuclear transport machinery.

The central region of BRCA1 was shown to directly interact with DNA. Naseem et all. [14] described that the amino acids residues 230 – 534 are responsible for DNA binding activity while Paull et all. [15] determined the DBD activity to the amino acids 452 – 1079. Though the data are inconsistent and the structure of BRCA1 putative DBD is largely unknown, it has been proven that BRCA1 displays rather structural then sequence preference in DNA binding. It was shown, that affinity of BRCA1's DBD is markedly higher to the branched DNA structures then to intact linear DNA [15]. Moreover, binding of BRCA1 causes significant structural changes in DNA molecule forming a four-way junction with BRCA1 protein in the centre. The DNA binding capacity of BRCA1 is enhanced by its interaction with BARD1 and decreased by binding of the p53 protein. Additionally, BRCA1 tethered to the DNA was shown to inhibit the nuclease activity of MRE11-Rad50-Nbs1 (MRN) complex. This together indicates that BRCA1 binds to the DNA intermediates in the collapsed replication fork and DNA double strand breaks (DDSB). The presence of BRCA1 stabilizes the structure of damaged DNA and prevents the nucleolytic attack directed to the naked DNA intermediates.

The BRCA1 phosphoprotein is a substrate for various protein kinases. The majority of BRCA1 phosphorylation sites clusters into the serine-containing domain (SCD) which spans

the region between amino acids 1280 – 1540 (exons 10 – 15) [16]. The phosphorylation status was shown to selectively influences intracellular and intranuclear localization of BRCA1 and its biological activity regulating the cell-cycle checkpoints (Tab.1)[17]. The functional importance of SCD was further supported by a finding that mutated BRCA1 protein lacking two phosphorylation sites (S1423 and S1524) failed to rescue the radiation hypersensitivity of a BRCA1-deficient cell line [18].

Besides to the direct phosphorylation activities, the SCD exhibits certain protein-binding activity mediated by the coiled-coil domain (CCD) spanning the amino acids 1280 – 1524 (exons 10 – 14) [19]. Similarly to RING domain, the binding specificity of CCD is determined by a presence of another CCD within the molecule of binding partner. The PALB2 protein interacts directly with BRCA1 in this way. PALB2 bridges the BRCA1 and BRCA2 proteins and thus facilitates the loading of Rad51 and subsequent DNA strand exchange [20]. Because the CCD is a part of SCD, it is tempting to speculate that certain phosphorylation events within this region may influence the BRCA1 binding capacity or a binding partner preference.

***Table 1**: The BRCA1 phosphorylation sites with relevant kinases and biological consequences.*

Akt	ATM	ATR	Cdk	Chk2	DNA-PK_{CS}	Biological consequence
Thr509						localization
				Ser988		Binding capacity
		Ser1148				*unknown*
	Ser1189					*unknown*
		Ser1280				*unknown*
	Ser1298					*unknown*
	Ser1330					*unknown*
	Ser1387	Ser1387			Ser1387	S phase checkpoint
	Ser1423					G2/M checkpoint
	Ser1457					*unknown*
	Ser1466					*unknown*
			Ser1497			*unknown*
	Ser1524					Caspase 3 activation

The BRCA1 C-terminal domain (BRCT) is a highly conserved phosphoprotein-specific interaction module originally described in BRCA1[21,8]. Later it has been found that BRCT is also presented in multiple other proteins involved in the DNA repair processes. According to the ability to recognize phosphoproteins, the BRCT domains are classified into two categories. Class-I BRCT domain recognizes exclusively the phosphorylated Serine residues

(pSer), while the class-II can recognize pSer as well as pThr residues. The BRCA1 contain a tandem of two identical class-I BRCT domains recognizing the pSer–X–X–Phe motif, separated by a short linker (BRCT1: amino acids 1,642-1,735; BRCT2: amino acids 1,755-1,855). Proteins with this phosphorylation motif are frequent targets of ATM/ATR kinases. Multiple BRCT repeats could bring together several different phosphorylated proteins. Hence, the BRCT-containing proteins represent the flexible scaffolding elements capable of specific enrichment of various proteins at the heart of the large, multiprotein complexes [22]. BRCA1 interacts via BRCT domains with BACH1, CtIP or Abraxas in mutually exclusive manner; however, growing evidence indicates the importance of BRCT domains in localization, DNA binding and transcriptional activity of BRCA1.

1.3.1 Intracellular localization of BRCA1

In concord with the fact, that the majority of BRCA1 functions is directly connected to the genome (DNA repair, transcription or the regulation of the cell cycle progression), BRCA1 has been defined as a predominantly nuclear protein. However, many independent experiments showed that BRCA1 localizes also into the cytoplasm and mitochondria where actively participates on the mitotic chromosome segregation or apoptosis (Fig. 3).

The nuclear localization of BRCA1 is crucial for its tumor-suppressing function and is ensured by the nuclear localization signal (NLS). The BRCA1 NLS binds to the α/β-importin receptor complex that is responsible for translocation of NLS-containing proteins through the nuclear envelope. However, the experiments with mutant BRCA1 variants showed that the nuclear localization is not exclusively dependent on the presence of BRCA1 NLS [23]. Later it was found that the interaction of BRCA1 with BARD1 stimulates the nuclear localization, while the interaction with BRAP2 stimulates the cytoplasmic retention [12]. Therefore, BARD1 acts as the BRCA1 escorting protein providing its own NLS for translocation of the heterodimer to the nucleus while binding of BRAP2 masks the BRCA1's NLS and thus disable the interaction with importin complex.

The certain BRCA1 intranuclear targeting to the site of requirement is mainly ensured by interactions with various BRCA1 binding partners. The interaction with Ku80 brings BRCA1 to the site of DNA single-strand breaks, interaction with RAP80 and MDC1 to the site of DNA double-strand breaks, and interaction with RNA polymerase II and PCNA to the site of active transcription or stalled replication fork [24,25]. The cooperative action of both

BRCA1 protein-interaction motifs, the RING finger and BRCT domains, are necessary for targeting of BRCA1 to the sites of requirement in this way.

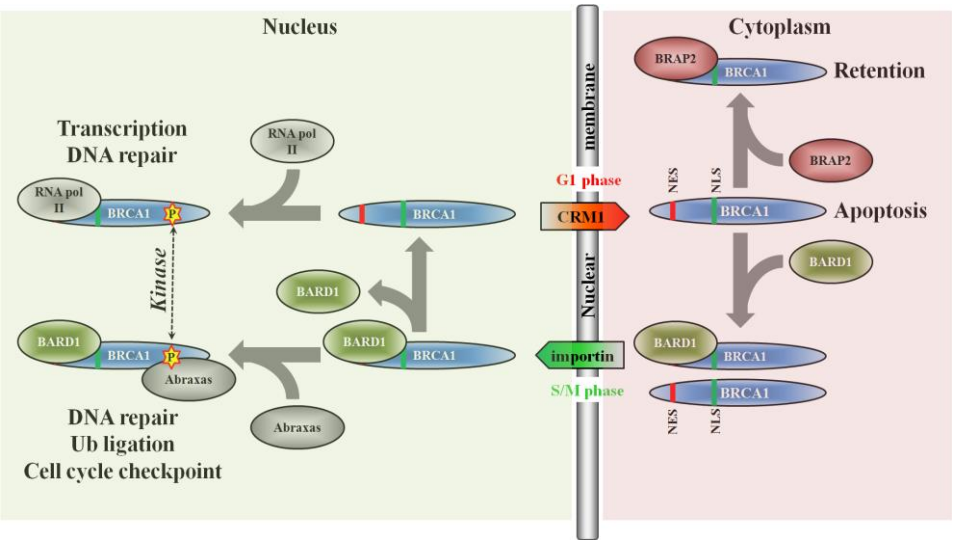

Figure 3: Intracellular shuttling of BRCA1 protein. *BRCA1 is predominantly localized in the nucleus, however a part of the BRCA1 pool accumulates in the cytoplasm and mitochondria. The intracellular (re)localization of BRCA1 is cell cycle phase-dependent. During the S/M phase BRCA1 accumulates in the nucleus, while during the G1 phase BRCA1 is exported to the cytoplasm. The nuclear import of BRCA1 protein is enabled by two* ***nuclear localization signals (NLS)*** *via their interaction with* ***α/β-importin receptor****. Besides that, formation of* ***BRCA1/BARD1*** *complex masks the BRCA1's* ***nuclear export signal (NES)*** *and leads to a rapid* ***relocalization*** *of the heterodimer to the nucleus. Contrary to that, binding of* ***BRAP2*** *physically constrains the interaction with BARD1 and causes the* ***retention of BRCA1 in cytoplasm****. While in nucleus, the BRCA1 protein is phosphorylated by various protein kinases. The exact intranuclear localization of BRCA1 to the sites of requirement is driven mainly by* ***various protein-protein interactions*** *with certain binding partners (RNA pol II, PCNA, Abraxas, BACH1 etc.). The formation of different protein complexes designates the participation of BRCA1 within various processes (transcription, cell cycle check point, DNA repair). When linked to the BARD1 or other nuclear proteins, the nuclear export of BRCA1 is blocked. The dissociation of BRCA1 from protein complexes discloses its nuclear export signal and leads to translocalization to the cytoplasm via the* ***CRM1 receptor****. In the cytoplasm BRCA1 is either degraded in the proteasome in the ubiquitin dependent manner or participates on the apoptosis.*

The nuclear export of BRCA1 is dependent on its association with CRM1 receptor. Recently, the nuclear export signal (NES) was described in the BRCA1 protein explaining the observation of full-length BRCA1 protein in the cytoplasm [11]. The BRCA1 NES is localized in a proximity to RING finger domain. The direct interaction with BARD1 masks the BRCA1's NES and disables its interaction with nuclear export receptor [26].

The BRCA1 nuclear accumulation and export to the cytoplasm depends on the cell cycle phase, protein structure and phosphorylation status. Certain BRCA1 variants with altered protein structure were shown to fail in nuclear localization indicating the importance of the BRCA1 protein structure on its localization [27]. Moreover the nuclear localized BRCA1 is hyper-phosphorylated in contrast to the BRCA1 in the cytoplasm. This together indicates that BRCA1 subcellular localization is the important determinant of its activity. It is now accepted that the exact localization of BRCA1 is a dynamic process and its shuttling between particular cellular compartments is tightly regulated.

1.3.2 BRCA1-containing complexes

The BRCA1 protein participates in an unusually broad spectrum of intracellular processes. Targeting a single molecule to the different biological processes requires an existence of several activation states of this molecule turned on/off by various upstream regulatory pathways. Though the phosphorylation status or intracellular localization was shown to directly influence the biological activity of BRCA1, it does not explain its exact targeting to the sites of requirement. Assuming the biological activities of BRCA1, a protein-protein interaction modulator, are determined by a complex of BRCA1 binding partners and their binding is a target for regulation.

The BRCA1 promiscuously interacts with various proteins (376 different proteins were evidenced to interact with BRCA1 so far)2. However, it was shown that within different cellular processes BRCA1 (in phosporylation-dependent manner) physically co-localizes with certain proteins to form specific supercomplexes [28,29]. DNA damage or replication blockage causes redistribution of BRCA1 among these complexes. In 2006, Greenberg et all. described three BRCA1-containing supercomplexes and suggested their functions (Tab.2) [30]. All BRCA1-containing supercomplexes are assembled in nucleus and their core consists of the BRCA1/BRAD1 heterodimer. The complexes were marked according to the exclusive interaction partner: A (Abraxas), B (Bach1), and C (CtIP) (Tab. 2).

[2] http://kueckgen677s09.weebly.com/protein-interactions.html. (accessed 2012-05-15)

Table 2: *The BRCA1 containing super complexes, compositions, activities and biological relevancies.*

Complex	Composition	Activity	Biological relevance
BRCA1-A	BRCA1/BARD1, **A**braxas, RAP80, BRCC36, BRCC45, NBA1	E3 ubiquitin ligase, deubiquitinase	G2/M checkpoint, HR
BRCA1-B	BRCA1/BARD1, **B**ACH1, TopBP1	Helicase, topoisomerase inhibition	Intra S checkpoint, HR
BRCA1-C	BRCA1/BARD1, **C**tIP, MRN	Nuclease	HR, NHEJ

The **BRCA1-A complex** contains at least seven different components. The complex core constitutes of Abraxas bounded to the BRCA1 BRCT domain through its C-terminus in a phosphorylation dependent manner (p-Ser406). The Abraxas serves as a central molecule that bridges interaction of each member of the BRCA1-A complex. The members of BRCA1-A complex contain an ubiquitin interaction motives (UIM) together with E3 ubiquitin ligase activity (BRCA1/BARD1 heterodimer) and deubiquitinase BRCC36. The site of DNA damage is subjected to a site of extensive ubiquitination. The localization of particular members of DNA repairing complex depends on the protein modifications including the ubiquitination. When the DNA is completely restored, dismantle of reparation complex is probably driven by the deubiquitination. Though it has not been proved yet, the BRCA1-A probably serves as a specific ubiquitinating/deubiquitinating complex organizing the proper folding/disassembling of DNA repair complex.

The **BRCA1-B complex** is required for the replication stress induced checkpoint control and DNA interstrand cross-linking repair. The BRCA1-B complex is formed through phosphorylated Ser990 of BACH1 binding to the BRCA1 BRCT. BACH1 is a DNA-dependent ATPase catalyzing the unwinding of DNA in a 5'-to-3' direction and its phosphorylation depends on the cell cycle phase. The localization of BACH1 to the site of DNA damage is mediated by the interaction of BRCA1 with MDC1 (containing FHA and BRCT motifs) tethered to the ubiquitinated γH2AX. Once presented at the site of DNA damage, the BACH1 (in cooperation with TopBP1) catalyzes the ssDNA regions extension and RPA loading for resolution of stalled replication forks. Moreover, BACH1 is required for activation of G2 phase checkpoint after the DNA damage.

The **BRCA1-C complex** consists of CtIP and the MRN complex bounded to the BRCA1 by the BRCT domain in a phosphorylation-dependent manner. The CtIP is a nuclease which promotes the DNA end resection generating the ssDNA regions important for the homology-directed DNA repair. BRCA1 brings the active CtIP to the site of DNA break and is probably responsible for the regulation of DNA resection - a crucial step in the selection of DNA repair pathway.

Ability to form specific protein super complexes is a key factor targeting BRCA1 activity to different cellular processes. However the exact signals regulating the trans-localization of BRCA1 within these complexes is not known yet.

1.4 Functions of BRCA1

BRCA1 is a large and predominantly nuclear phosphoprotein with E3 ubiquitin ligase activity. The majority of the BRCA1 functional studies have shown that the BRCA1 protein serves as a protein-protein interaction modulator with a central position in the DNA damage signaling pathway. The best described is its direct participation in the homology-directed DDSB repair [31]. Besides that, it has been proposed that BRCA1 also participates on other DDSB repair mechanisms including non-homologous end joining (NHEJ) and single strand annealing (SSA) [32]. Additionally, BRCA1 was described to have a direct transcriptional activity [33] and a regulatory function in post-transcriptional mRNA processing via its interaction with RNA polymerase II [34,35]. Moreover, BRCA1 participates in cell cycle and apoptosis regulation in response to DNA damage [36]. All together, functions of BRCA1 are strongly associated with the molecular response to genotoxic stress indicating the key position of BRCA1 in the maintenance of genomic integrity.

1.4.1 Maintenance of the genomic integrity

During the cell live, the chromosomal DNA is frequently damaged by numerous endogenous and exogenous factors. These physical, chemical, or biological agents introduce various types of the DNA damage including looses or modifications of nitrogen bases, introduction of mismatched bases, covalent inter-strand cross-linking or single- and double-strand DNA breaks. Gradual accumulation of genomic insults can leads to a malignant transformation [37].

The maintenance of genomic integrity relies on an activation of precise signalization in response to particular genomic insult. Irrespectively to the type of DNA damage, the signaling cascade involves three separate levels. The response pathway is initiated by sensors, a group of proteins that are capable to detect and identify particular DNA lesion. The initial signal is transferred to mediators that are responsible for the activation of effectors that execute the specific DNA repair mechanisms. Mediators represent an important signaling interface responsible for synchronization of DNA-repair mechanisms with activation of cell cycle checkpoints allowing the cell to repair the lesions and together with apoptosis ensuring that the genetic errors are not transmitted to the daughter cells.

1.4.1.1 The repair of DNA double strand breaks

DDSB belongs to the most deleterious DNA lesions. Though not very frequent in their occurrence, even single unrepaired DDSB can cause a cell death. DDSB can be induced by several mechanisms including exogenous (exposure to ionizing radiation) or endogenous (collapse of stalled replication fork encountering a single strand break in a DNA template or an immunoglobulin VDJ recombination events during meiosis) [38,39]. The average frequency of endogenous DDSB is seven per cell cycle, while the dose of 1 Gy of ionizing radiation causes approximately 30 DDSB per nucleus [40]. Unrepaired or mis-repaired DDSB can causes genomic instability by a promotion of gross chromosomal rearrangements or formation of bicentric or acentric chromosomes respectively [41]. To ensure the rapid and effective repair of DDSB two major mechanisms evolved NHEJ and HR. The key difference between the mechanisms of these DDSB repair pathways is their dependence on a DNA homology. The homology between long 3'-single strand sections of damaged DNA and the intact sister chromatid is required for HR that ensures the error-free repair accuracy with no loss of genetic information. On the contrary, NHEJ uses little or no sequence homology and some loss of DNA sequence is probable during this error-prone, but in eukaryotic cells predominant, repair mechanism.

Prevalence of usage of these DDSB repair pathways depends on several factors. HR plays the major role during late S and G2 phases when sister chromatids are in close proximity and thus available for homology-directed repair, whereas NHEJ is more prominent during G1 and early S phases [42]. Moreover, a detail analyzes of the DDSB repair kinetics revealed that the entire process of DNA repair involves fast component being active within first 2 – 3 hours after the genotoxic insult and a slow component which function for up to 48 hours

after the DNA damage [43,44]. This different kinetics depends on chromatin constitution [45,46,47]. While the fast DDSB repair typically occurs in a relatively easy accessible euchromatin, DDSB in tightly packed heterochromatin prioritize the slow component. A NHEJ is the prevailing mechanism for reparation of "simple" and easily accessible DDSB ensuring the necessary rapidity of repair process and it constitutes the major repair pathway in euchromatin. Those DDSB which are difficult to repair by the pathways of first choice – NHEJ, or occurring in a tightly packed heterochromatin parts are fixed by a precise but slower HR.

Despite the distinct mechanisms, NHEJ and HR are not fully independent. To some degree these pathways collaborate on DNA repair in coordinated action [48,49] in order to repair a DDSB rapidly and with minimal error. Thus the aberrant signaling unnaturally preferring one pathway to another can harm a subtle balance between rapidity and accuracy of DDSB repair with potentially detrimental impact on a genomic stability. Moreover, it is suggested that both pathways constitute a double secured mechanism [50,51]. So when NHEJ is impaired the activity of HR increases and vice versa [52,53]. Thus, despite their seeming redundancy, both HR and NHEJ are required to maintain the genomic integrity.

1.4.1.1.1 DNA double strand breaks sensing

The initial step of global cellular response to a genotoxic insult is a detection of the DNA damage. Although the entire process of DDSB recognition has not been fully unraveled yet, there is a generally accepted paradigm for DNA damage-induced checkpoint activation in which a sensor detects the DNA damage and the signal is transmitted to adapter molecules, typically protein kinases. Considering the two major DDSB repair pathways, there are two distinct mechanisms for DNA damage detection.

The key sensor for DDSB recognition in homology-directed repair pathway is a heterotrimeric complex consisting of MRE11, Rad50 and Nbs1 (MRN complex) [54]. The MRE11 and Rad50 proteins are highly evolutionary conserved through archeal to higher metazoans. On the contrary, Nbs1 is a protein specific for eukaryotes in which regulates cell cycle checkpoints. MRE11 represent scaffolding of the complex that ensures its indispensable protein-protein and protein-DNA interactions. It binds simultaneously Rad50 and Nbs1 and tethers them to the DNA. Beside that MRE11 possess a dsDNA 3'-to-5' exonuclease, annealing, and unwinding activities important for further HR processing [55].

Rad50 protein has a unique structure containing a "head" domain (at the N-terminus) responsible for MRE11 binding, large central coiled-coil structure and a C-terminal "hook" domain [56]. Nbs1 acts as a linker facilitating the interaction with an ATM kinase. At the site of DDSB, MRE11-Rad50 (MR) heterodimer core initially associates with both ends of broken DNA and simultaneously with the homologous sequence on the sister chromatid. By the MRE11-MRE11 linkage, resulting MR-MR tetramer prevents the separation of broken DNA ends [57]. Alongside this, the coiled-coil filaments of Rad50 invade surrounding chromatin and RAD50 hook domains of MR-complexes assembled at a site of broken DNA and homologous portion of sister chromatid clamps them together (Fig. 4). Once the chromatids and free DNA ends are tethered, the ATM is bounded by the Nbs1 to the site of DDSB. This binding activates ATM by autophosphorylation [58]. Activated ATM in turn phosphorylates H2AX histones of proximal nucleosomes and thus starts propagation of the initial signal [59]. Phosphorylated H2AX (γH2AX) are subsequently recognized and bounded by MDC1 that brings to the DDSB site an ubiquitin ligase RNF8 catalyzing the polyubiquitinylation of γH2AX in the imminent proximity to the DDSB and simultaneously binds another molecule of ATM phosphorylating distal H2AXs [60]. Ubiquitinylation of γH2AX enables binding of Rap80 and other protein factors necessary for subsequent HR processing, while the additional phosphorylation of H2AX within several kbp from the DDSB site ensures the mediation and amplification of signal and a large scale chromatin remodelation [61].

Sensing of DDSB repaired by NHEJ pathway depends on a high binding affinity of Ku proteins to free DNA ends. Two members of Ku protein family the 70 kDa Ku70 (XRCC6) and 86 kDa Ku80 (XRCC5) form a ring-shape heterodimer (Fig. 4) [62]. This heterodimer binds in several copies to free ends of broken DNA and holds them together by weak electrostatic interactions. Further this complex is stabilized by a DNA-PKcs bridging free DNA ends [63]. Formation of Ku-DNA-PKcs heteromeric complex (DNA-PK) activates its kinase activity and enables ATM binding. When bound to DNA-PK, ATM is stabilized in its inactive dimeric form. Activities of these kinases subsequently ensure the signal propagation to an appropriate response [64].

1.4.1.1.2 Mechanisms for DDSB repair pathway selection

The most important decisive factor of DDSB repair pathway selection is the initial processing of free DNA ends. While NHEJ requires no or minimal processing of free DNA

ends prior to ligation, HR involves interacion of long homologous sequences between damaged parental and intact sister chromatids ensured by a single strand invasion. Therefore, when free DNA ends are largely resected (in 3'-to-5' direction), relevant free DNA ends undergo HR. On the contrary, when the resection of free DNA ends is suppressed, DNA is directly ligated by NHEJ (Fig. 4). Thus the ultimate decision relays on the protection of free DNA ends or promotion of single strand resection [65].

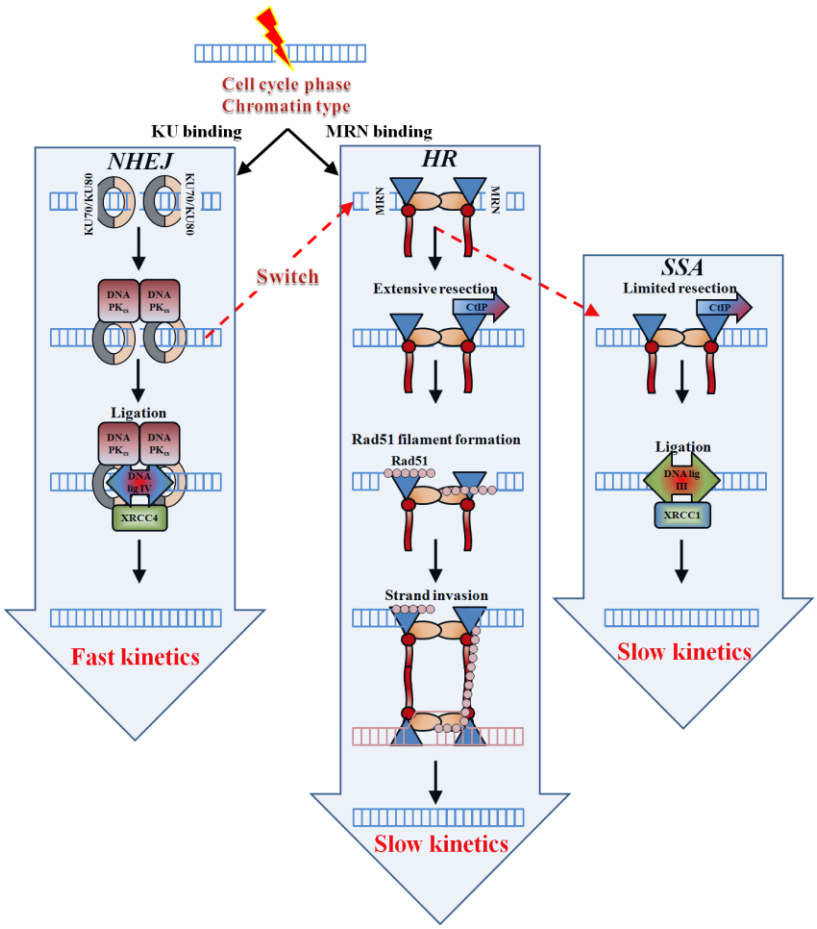

Figure 4: The DDSB repair pathway selection. *The initial processing of free DNA ends at the site of DDSB is the main regulating step for DDSB repair pathway selection. In relation to the actual cell cycle phase and exact localization of DDSB within chromatin either* ***Ku70/Ku80*** *or* ***MRN complex*** *binds to the DNA. In a phosphorylation-dependent manner mediated by an activity of DNA-PK or ATM, the repair process further progresses either by the direct ligation within* ***fast but error-prone NHEJ*** *or by strand resection within* ***slow but exact HR****. Degree of the free DNA end resection leads to the usage of HR or a single strand annealing (SSA), a process that uses a short homology between broken DNA ends without invasion to the sister chromatid. Particular repair pathways are linked together and cooperate on the repair of DDSB.*

Both key sensors, the Ku in the NHEJ pathway and the MRN in the HR pathway, possess a high affinity to the free DNA ends and probably directly compete for their occupation. It has been shown that both these protein complexes are presented at the site of DDSB during the early stages of repair pathway. While the interaction of Ku70/Ku80 heterodimers with DNA ends physically blocks additional processing of broken DNA ends, the MRN promotes their additional processing by the exonuclease-mediated resection.

In DDSB repair processed by NHEJ pathway, the DNA-PK complex suppresses activation of the ATM and thereby inhibits HR [53]. On the contrary, when DNA-PKcs is released the Ku70/Ku80 complex disintegrates. Competing MRN complex fully restore ATM activity which causes unblocking of HR. The dissociation of DNA-PKcs from the DNA is dependent on its phosphorylation, though the relevant kinase is not known yet. The effect of DNA-PKcs on the selection of further repair mechanism in this manner was proved by the observation that HR is elevated in DNA-PKcs null cells [66]. It is tempting to speculate that the activity of such kinase can be dependent on the cell cycle phase and thus govern the preferential usage of NHEJ in G1 and S phases. Regulation of DDSB repair in a cell cycle-dependent manner was described in case of CtIP which is responsible for large scale resection of free DNA ends. The CtIP is held in the site of DDSB by its interaction with BRCA1. This interaction is dependent on CtIP phosphorylation at Ser327 by CDK1 during S/G2 phases [67]. Thus, regulation of DNA-PKcs and ATM activities and consequently their downstream mediators govern the final decision of DDSB repair pathway selection that secures the balance between rapidity and fidelity of the DDSB repair [50].

1.4.1.1.3 Homologous Recombination (HR)

HR repair of DDSB is generally considered as an error-free mechanism. The high accuracy of this process is based on the homology-directed formation of the temporary heteroduplex between corresponding portions of damaged parental and intact sister chromatids. The sister chromatid template ensures a complete repair without loss of genetic information.

Detection of DDSB is initialized by the MRN sensor complex recruiting the ATM kinase as described previously in 1.4.1.1.1. The anatomy of DNA at the break site influences the final conformation of MRN complex [54]. The symmetric shape of MRN homodimer caused by the “blunt-ended” DDSB stably tethers the active ATM. On the contrary, the “cohesive-

ended" DDSB leads to formation of asymmetric MRN homodimer and release of active ATM diffusing into the intranuclear space [64]. The binding status of ATM was shown to directly influence its substrate specificity. The conformation of MRN complex and its interaction with ATM was shown to be a base for different signalization in double and single strand breaks.

All these events take place within a minute after the DNA damage and result in a formation of protein complex termed as early ionizing radiation-induced focus (IRIF). In the subsequent steps of DDSB response pathway, the γH2AX proteins are recognized and bounded by a MDC1 molecule. The MDC1 serves as a platform attracting additional ATM phosphorylating the distal H2AX causing the "wave-like" spreading of signalization within the region of several kbp apart from the site of DDSB [68]. This additional H2AX phosphorylation is an important factor for a large scale chromatin remodeling in HR [69]. Besides that, the MDC1 allows binding of ubiquitin ligase RNF8 which catalyzes the polyubiquitinylation of H2AX at the Lys63 [70]. Arising polyubiquitin chain serves as an anchor for binding of proteins responsible for the free DNA end-processing and mediation of signal to the downstream effectors. The BRCA1-A complex (see 1.3.2) localizes to the site of DDSB by interaction with RAP80 which binds the polyubiquitin chain by its UIM domain. Subsequently, BRCA1 enables the 5'-to-3' resection by binding a CtIP exonuclease. A newly-formed 3' overhangs are rapidly protected by RPA proteins subsequently exchanged by the Rad51 monomers. Loading of Rad51, a central recombinase in the homology-directed DDSB repair, is ensured by mutual activity of BRCA2 and PALB2 [71]. The long filaments of Rad51-coated ssDNA invade the sister chromatid held in the proximity by the MRN complex (Fig. 4). This strand exchange results in a formation of a D-loop where broken DNA ends hybridize to the denatured complementary sequences of sister chromatid. Missing polynucleotide sequence of the strand with DDSB is refilled from the D-loop-formed heteroduplex DNA in 5'-to-3' direction by DNA polymerase and reunified by DNA ligase. Once both DNA strands of broken chromatid are fully restored, the D-loop is dismantled. Two mechanisms ensure the D-loop resolution. A holliday junction cleavage leads to the exchange of relevant portion of DNA between sister chromatids or denaturation with subsequent synthesis dependent strand annealing without any exchange of genetic information between sister chromatids.

1.4.1.1.3.1 Role of BRCA1 in homologous recombination (HR)

Direct connection of BRCA1 to the homology-directed DDSB repair was elucidated due to its well documented interactions with many HR protein factors in situ. Recently, it becomes clear that BRCA1 participates on all phases of HR from initiation to termination and, moreover, governs the step wise manner of HR [72].

The central event in HR represents mutual pairing of homologous portions of the sister chromatids forming a structure termed as D loop. Thus, the 5'-to-3' resections and strands invasions are crucial steps of the successful repair. Moreover, when completely repaired, the cell must also have a mechanism disengaging the invading strands (allowing the HR repair) to minimize frequency of crossing-over events that may complicate chromosome segregation and potentially results in chromosomal rearrangements. Failure in this final dismantling of IRIF following an accomplished HR repair is linked with a phenomenon called hyper homologous recombination which could be as dangerous to genomic stability as non-functional HR [73].

BRCA1 localizes to the DDSB sites repaired by HR through the association of BRCA1-A complex (see 1.3.2) with modified histones in an ubiquitinylation-dependent manner [24]. When anchored to the sites of DNA damage, BRCA1 participates in HR initiation by promoting the 5'-end resection. This activity is enabled by tethering the CtIP nuclease via its interaction with BRCA1 BRCT domains forming the BRCA1-C complex. It has been shown, that the activity of CtIP is strongly dependent on its binding to the BRCA1 [74]. Because NBS1 nuclease from MRN complex possesses only 3'-to-5' exonuclease activity, the additional processing of free DNA ends enabling resection and subsequent strand invasion relies on CtIP bounded to BRCA1. Thus, any defect in BRCA1 capacity to form a BRCA1-C complex (caused either by BRCA1 mis-localization, or its altered binding capacity) can result in the HR failure and progressive DNA damage.

During the strand-invasion step, the homology-directed DNA-DNA interactions between single-strand overlaps (generated by resection) and homologous sequence on a sister chromatid are mediated mainly by the Rad51 recombinase. The Rad51 molecules are loaded onto the RPA-coated ssDNA overlaps in many copies forming the long filaments capable to recognize and invade a homologous sequence. Loading of Rad51 is ensured by BRCA2 which localizes to the site of DDSB through its interaction with PALB2 protein [75]. This BRCA2/PALB2-loading complex is held in a proper position by its interaction with a BRCA1-C complex. Phosphorylation of BRCA1 at Ser988 by the CHK2 kinase is required

for this interaction [76]. By loading of Rad51, enabled just after formation of ssDNA overlaps, HR can proceed to the next step. Thus, BRCA1 not only participates in a strand invasion but also governs correct progression of HR.

The repair complex contains number of proteins participating in the crossing-over. Therefore, once the DDSB is completely repaired, it is necessary to suppress further HR and dismantle the repair complex to avoid an inappropriate crossing-over event. Though the procedure of complete IRIF dissociation is poorly understood yet, the deubiquitinilation seems to be it critical component. Delayed disassembling of HR repair complexes was observed in cells expressing the BRCA1 variant with mutation in BRCT domain [73]. This suggests that in late phases of HR BRCA1 binds a specific deubiquitinase via its BRCT domain. One of the best candidates for the putative deubiquitinase is a BRCC36 which was shown to co-localize to DDSB through its interaction with BRCA1-A complex.

1.4.1.1.4 Non-Homologous End Joining (NHEJ)

Due to the minimal requirements on DNA homology, NHEJ is a predominant repair mechanism within the eukaryotic cells with sophisticated chromatin structure. The core of this, generally considered error-prone mechanism, consists of Ku proteins, DNA-PKcs, LigIV and its cofactor XRCC4. The free DNA ends are first recognized by Ku heterodimers consisting of Ku70 and Ku80. The ring-like structure of Ku heterodimer thread with a high affinity around free DNA ends within seconds after the genotoxic insult [77]. The rapidity of binding probably prevents the separation of relevant DNA ends and thus ensures ligation of corresponding parts of the DNA molecule. Ku heterodimers bounded to the both DNA ends in several copies then recruit two molecules of DNA-PKcs displacing Ku into the 10 bp interior [78]. Formation of DNA-PK holoenzyme complex consisting of Ku70/Ku80 and DNA-PKcs on the DNA ends results in activation of its kinase activity. Activated DNA-PK in turn phosphorylates several DNA-binding proteins including XRCC4, WRN, MRE11, and Artemis. Phosphorylated XRCC4 forms a complex with DNA ligase IV which binds to the Ku70/Ku80 heterodimers and together with DNA-PK promotes end-to-end association of disrupted DNA [78,79]. The final ligation catalyzed by DNA ligase IV is enabled upon autophosphorylation of DNA-PK that in turn dissociates from DSB site. In addition, DNA ligation is regulated by the activity of the WRN helicase and nucleases MRE11 and Artemis responsible for opening of the hairpin loops and generation or shortening of 3’ and 5’

overhangs on DNA strands. The accuracy as well as introduction of errors during NHEJ probably relies on the regulation of activity of these nucleases [80].

1.4.1.1.4.1 Role of BRCA1 in Non-Homologous End Joining (NHEJ)

The participation of BRCA1 in other then HR pathways has been investigated following the results of studies showing contradictory influence of BRCA1-/- and BRCA1-mutant cells on NHEJ [81,82,83].

BRCA1 is known to interact and co-localize at the site of DDSB with both sensors of main DNA repair pathways – Ku and MRN complex [25,74]. This co-localization takes place within the initial phase of the DDSB repair response and is probably dependent on the formation of precise BRCA1-containing protein complexes. Assuming the BRCA1 as a platform protein, its presence at the DDSB site can tethered additional proteins responsible for further processing of the free DNA ends or enhancing the DNA repair pathway progression. Presence of BRCA1-C complex promotes the 5'-to-3' resection that leads to formation of the long homology regions between sister chromatids resulting in slow but error-free HR event. The low rate resection (mediated probably by MRN complex in the absence of BRCA1-bounded CtIP) leads to the finding of a small homology between both ends of broken DNA resulting in SSA and loss of non-homologous portions. The absence of BRCA1-C complex leads to 53BP1-mediated blocking of nuclease activity resulting in a rapid but error-prone non-canonical NHEJ pathway [84].

Neither HR, nor NHEJ are fully dependent on the presence of the intact BRCA1 suggesting its supportive rather than indispensable function. In concord with this concept is a finding, that BRCA1 null cells has mainly unchanged activity of NHEJ, however, frequently exerts increased error rate within the global DNA repair process [85]. Thus the spatio-temporal regulation of BRCA1 localization and binding capacity at the site of DDSB seems to be a factor tuning both rapidity and accuracy of the DNA end joining.

1.4.2 Regulation of transcription

It has been documented that depletion of BRCA1 results in transcriptional changes in more than 1000 genes [86]. Surprisingly, the chromatin immunoprecipitation analysis reveals that only a minority of genes' promoters are bounded to BRCA1. Both evidences

suggest that direct as well as indirect mechanisms may contribute to the BRCA1-mediated regulation of transcription.

Binding of BRCA1 to the transcriptional machinery via BRCA1 C-terminal domains was the first activity ascribed to the BRCA1 protein [87]. Since then, the experiments shown, that the C-terminus of BRCA1 recruits RNA polymerase II (RNA polII) to the synthetic reporter indicating a role of BRCA1 in transcriptional regulation [88]. It was shown that BRCA1 physically interacts only with such RNA polII that is hyper-phosphorylated [89]. This typically occurs in highly-processive transcription units. On the contrary, phosphorylation of BRCA1 (upon DNA damage) causes its dissociation from the core transcriptional machinery. Finding that BRCA1 interacts almost exclusively with the catalytically active RNA polII, but not with free RNA polII in vivo suggests that BRCA1 has a specific role within the post-promoter events rather than during the initiation of transcription.

Based on these findings, Lane et al proposed that BRCA1 binds to the active RNA polII as a part of the genome-scanning complex [90]. Proposed BRCA1 role in this complex is to enhance the security of chromatine structure in regions with highly-active transcription. The DNA damage (e.g. DNA cross-linking) causes the stalling of RNA polII and RNA processing. To make such a site of DNA damage accessible for the repair apparatus, the active transcription complex must be withdrawn. Translocalization of BRCA1 from RNA polII complex to the DNA repair complex in the phosphorylation-dependent manner enables specific degradation of stalled transcription complex by the BRCA1/BARD1-mediated ubiquitinylation (Fig.5) [91]. This scenario was further supported by findings that BRCA1 ubiquitinates RNA polII, and that deletion of the BRCA1 N-terminus bearing the E3 ubiquitin-ligase activity abrogated BRCA1 ability to interact with active transcription complex [92].

Moreover, BRCA1 can regulate signaling pathways that affect the activity of specific transcription factors. It has been described that BRCA1 interacts with estrogen receptor α (ERα) abrogating the ERα signaling and thus repressing the expression of ERα-dependent genes [93]. Besides that, phosphorylated BRCA1 is required for the ATM-mediated phosphorylation of p53 in DNA damage response and subsequent p53-dependent transactivation of G1/S checkpoint genes.

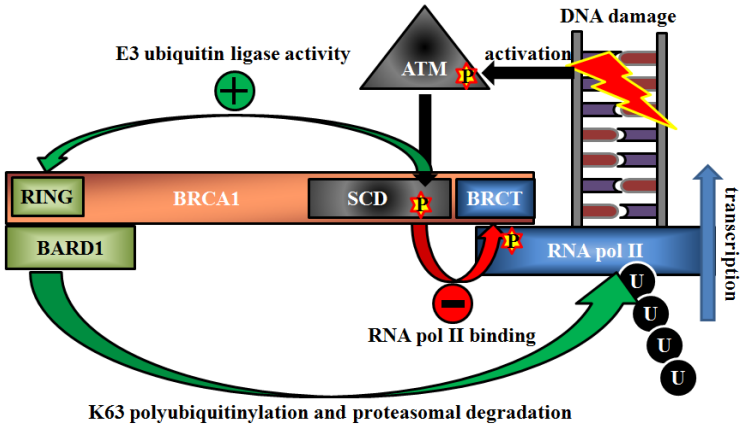

Figure 5: BRCA1 mediated regulation of transcription. *BRCA1 binds to highly processive RNA polymerase II (RNA polII) via the BRCT protein interaction motif in a phosphorylation dependent manner (P). When encountering a DNA damage the active transcription complex stalls and must be dismantled to enable a DNA repair. Activated ATM phosphorylates the BRCA1 on serine 1423 residue in the serine containing domain (SCD. This causes the dissociation of BRCA1 from transcription complex. Free BRCA1 in complex with BARD1 than in turn catalyzes the polyubiquitinylation (U) and subsequent proteasomal degradation of RNA polII to enable a DNA repair process to take place.*

Regarding to the presence of DBD in the BRCA1 protein, it was suggested that BRCA1 can regulate transcription of specific genes by direct binding of some promoter regions. This specific binding was proved by number of experiments [15]. However, no sequence specificity of the BRCA1 DBD has been described so far. Thus, recruitment of BRCA1 to promoter regions must be specifically directed by additional mechanism. In consistence with this assumption it has been shown that BRCA1 interacts with a number of transcription factors (e.g. STAT1, c-Myc or ZBRK1) [94]. With respect to these findings it has been suggested that BRCA1 is presented on promoters of specific genes as a part of regulatory complex ready to respond to upstream stimuli.

Although BRCA1 is generally considered as a DNA repair protein it also participates in transcription as a co-activator or co-repressor and also this function contribute to its overall role in the maintenance of genomic integrity.

1.4.3 Cell cycle checkpoints

The ability to control the order and timing of cell cycle events precisely is essential for successful cell division. To prevent transmission of damaged DNA to daughter cells,

chromatin is carefully monitored during the whole cell division. Encountering the DNA damage, the cell is arrested in certain stage of the cell cycle until the damage is fully repaired. The cellular machineries mediating cell cycle arrest are collectively termed as cell cycle checkpoints. The proper function of the cell cycle checkpoints is critically important for the maintenance of genomic integrity. During the cell cycle phases, BRCA1 is differentially expressed [95] and undergo various different phosphorylation events [96]. Moreover, the intracellular shuttling of BRCA1 protein as well as formation of specific complexes is cell cycle-dependent [13]. This may suggests that BRCA1 participates on the cell cycle regulation.

Experiments with anti-sense RNA-mediated BRCA1 downregulation showed that BRCA1 participates in the G1/S arrest in response to DNA damage [97]. The key G1/S checkpoint regulator is the p53 tumor suppressor that controls the transcription of CDK's inhibitor p21waf1. The p21 was also identified as a key downstream target of BRCA1 in the process of G1/S checkpoint [98]. Direct transcriptional regulation of p21 by BRCA1 depends on the formation of BRCA1-C complex in a phosphorylation-dependent manner [99]. Beside that BRCA1 was reported to regulate the transcription of p21 indirectly via p53. In this process, BRCA1 in complex with its binding partner BARD1 serves as a scaffold protein enabling phosphorylation of p53 on Ser 15 by activated ATM upon DNA damage [97]. This leads to the p53-mediated induction of p21 and subsequent G1/S arrest.

The BRCA1 null cell line HCC1937 is known to be defective in the S phase checkpoint. Revealing that this defect in HCC1937 is fully restored upon complementation of BRCA1 function indicates the role of BRCA1 in the S phase checkpoint [100]. Further, experiment with BRCA1 mutants showed that ATM-mediated phosphorylation of BRCA1 on Ser 1387 is specifically required for the S phase checkpoint following ionizing radiation-induced DNA damage [101]. Though the precise mechanism has not been fully explored yet, it is tempting to speculate that phosphorylated BRCA1 may recruit functional partners for governing the S phase checkpoint. This further supports that BRCA1 interacts with many proteins directly involved in the S phase checkpoint (i.e. H2AX, MDC1, 53BP1 or MRN complex) [102]. Additionally to that, BRCA1 was shown to regulate the ATM activity by promoting its autophosphorylation [103]. BRCA1 co-localizes with the MRN complex at the site of DDSB. This sensor complex is the mostly responsible for the ATM activation [104]. Though the activation of ATM is not exclusively dependent on the presence of BRCA1, it seems that BRCA1 performs the role of auxiliary activation-enhancing factor.

In addition to G1/S and intra S phase checkpoints, certain DNA damage also induces the G2/M checkpoint. Loss of this checkpoint allows the cell with damaged DNA proceed to the M phase and increases the likelihood of passing of abnormal chromosomes to the daughter cells. Experiments with embryonic cell lines showed, that cells lacking BRCA1, or cells expressing altered BRCA1 exhibited no reduction in the mitotic index after ionizing radiation-induced DNA damage [105]. This suggests a role of BRCA1 in G2/M checkpoint. Phosphorylation of BRCA1 at Ser 1423 has been identified as the key determinant of BRCA1-mediated regulation of G2/M checkpoint [100]. This phosphorylation is important for activation of Chk1 and Chk2 [106] that in turn phosphorylate Wee1 and Cdc25A/B/C kinases suppressing the activity of Cdc2 and cyclin B for mitosis entry. Beside that BRCA1 transcriptionally regulates the 14-3-3σ protein that sequesters active Cdc25C to cytoplasm [107].

Disability to pass through the cell cycle checkpoint due to the severe cellular or genomic insult leads to the apoptosis. Loss of control mechanisms triggering this cellular ultimate emergency break causes an uncontrolled cellular division with accumulation of DNA damage. Though the exact mechanism is not known, BRCA1 was shown to participate in the regulation of apoptosis through H-ras/MAPK/JNK pathways resulting in induction of GADD45 and activation of caspase 9 [108,109].

BRCA1 is an important cell cycle checkpoint factor and the loss of its expression or changes in its protein structure can lead to developmental abnormalities, genetic instability or tumorigenesis.

1.5 Alternative pre-mRNA splicing

The human genome contains a relatively small number of protein-coding genes (approximately 20,000 – 25,0003). The significantly increased repertoire of biologically active molecules of proteins in eukaryotes is provided by post-transcriptional processing of precursor-messenger RNA (pre-mRNA) in the pre-mRNA splicing. Except the constitutive splicing that results in formation of full-length mRNA, it is estimated that almost 60% of human genes undergo alternative splicing leading to the formation of different mRNA iisoforms from a single primary transcript [110]. The process of alternative pre-mRNA splicing can affect the biological activity of relevant transcript by alteration of protein-

[3] http://www.ornl.gov/sci/techresources/Human_Genome/project/info.shtml

coding sequences, introduction of premature stop codon, or changes in the 5' or 3' untranslated regions of mRNA.

The majority of alternative splicing events occur within the mRNA protein-coding regions. Alternative splicing introduces changes in mRNA by complete or partial withdrawal of exons coding for particular protein domain(s) or by insertion of new protein-coding sequences by adding of alternative exons. Alternative usage of exons and/or introns makes the alternative splicing a versatile system capable to alter a structure of a gene product in terms of insertion or deletion of specific protein parts. Translations of alternatively spliced mRNAs lead to formation of proteins containing variable set of functional domains. Therefore, the final protein variants differ from that derived from constitutively proceed mRNA in their structure and properties including enzymatic or signaling activity [111,112], association with binding partners [113], intracellular localization [114], or stability [115].

Containing a premature stop codon, the mRNA could be degraded by a nonsense-mediated decay (NMD). [116,117]. The NMD is activated when premature stop codon occurs within the region of approximately 50 nucleotides upstream from splicing–generated exon–exon junction. Such mRNAs are immediately marked by exon junction complex (EJC) and swiftly degraded preventing production of truncated protein. Several lines of evidence show the connections between NMD and alternative splicing. The process of pre-mRNA splicing is a major source of premature stop codon introduction into mRNAs making it together with NMD an important control mechanisms for the abundance of cellular transcripts [118].

The untranslated regions (UTRs) of eukaryotic mRNAs play an important role in post-transcriptional regulation of gene expression by modulating nucleocytoplasmic mRNA transport, translation efficiency, and mRNA stability. Many examples prove a decreased stability of primary mRNA transcript with subsequent impact on protein production due to changes in UTR regions caused by regulated pre-mRNA splicing [119].

Why so many genes are regulated at the level of mRNA processing by alternative splicing? The aim of the process, enabling production of distinct protein isoforms differing in their polypeptide architecture and therefore biological properties and functions from a single primary transcript, is to react on variable cellular requirements via formation of the most suitable protein isoform(s) in tissue-, cell-, or state-(disease)-specific manner [120]. Proteins generated from alternatively spliced mRNAs frequently exerts antagonistic functions to their full-length isoform [121]. Usually, several mRNA isoforms are generated by alternative splicing besides the formation of dominant mRNA isoform coding for full-length protein.

Alternatively spliced mRNA isoforms and their protein products, respectively, commonly represent a minor component of particular gene expression; however, upon specific intracellular conditions, formation of alternatively spliced mRNAs translated into the functionally altered proteins could be broadly increased. Hence, the pre-mRNA splicing affecting the final protein formation in qualitative and quantitative manner represents one of the major sources of genetic diversity in eukaryotes that enables rapid changes in protein composition from subtle modification to complete loss/change of function under the transforming environmental condition.

1.5.1 Spliceosome complex and its assembly

Removing of intron is mostly mediated by a large macromolecular complex – spliceosome – co-localized within the cell in so called "RNA factory", a dynamic structure linking transcription, pre-mRNA splicing, and mRNA posttranscriptional modifications [122]. Catalytic spliceosome core involves five basic splicing factors from the family of small nuclear ribonucleoprotein particles (snRNP U1, U2, U3, U4, and U6) containing uridyl-rich small nuclear RNAs (snRNAs) and a cortege of associated proteins contributing to spliceosome complex stabilization and splice site selection [123].

The basic snRNPs interacts with specific pre-mRNA cis-regulatory elements to build up spliceosome in stepwise manner with the assistance of numerous [124] additional protein factors (Fig. 6). In completely assembled spliceosome (complex C), the catalytic center is formed by U2 snRNP together with U5-U6 snRNPs bound to a mandatory pre-mRNA cis-regulatory elements – 5' splice site, branch point site, and 3' splice site preceding by a polypyrimidine tract – located in intronic sequence [125].

Because 5' splice site are usually far away from branch point site followed by polypyrimidine tract and 3' splice site, it is necessary to bring them together. This action requires that both exon-flanking intronic sequences (the 5' splice site and the branch point site) have to be first marked by their association with snRNPs and then bring into the catalytic conformation in a set of specific interactions. Final catalytically-active spliceosome is stabilized by a complex array of non-covalent interactions involving specific RNA–RNA interactions and protein–RNA and protein–protein interactions. Because these interactions are week and splice sites and the branch point site sequences are only slightly conserved, more than just one alternative for splicing exists frequently. Therefore, a crucial task of

alternative splicing process is the selection of proper splice site. This is broadly influenced by activity of associated splicing factors, their current expression within the cell, phosphorylation of spliceosome components and presence of facultative RNA cis-regulatory elements (enhancers/silencers) [127,128,129].

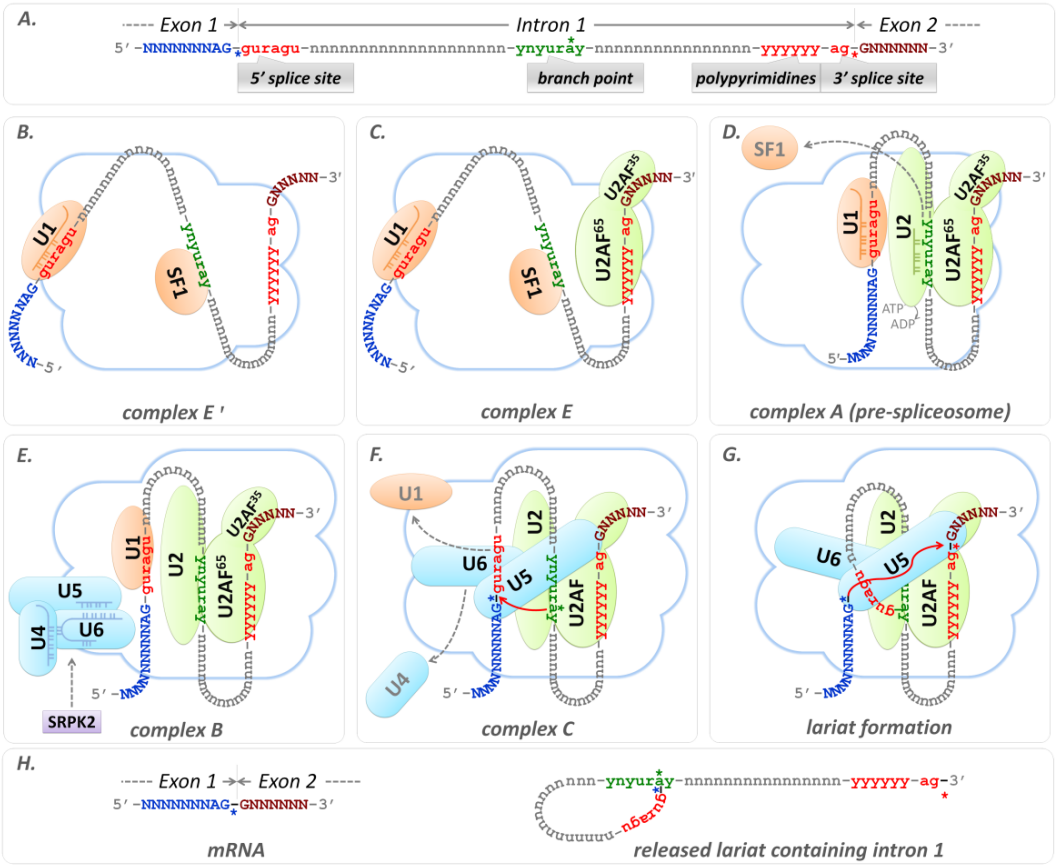

Figure 6. Schematic representation of basic pre-mRNA cis-elements (A), spliceosome assembly and its catalytic activity (B-H). A. *Pre-mRNA molecule consists of variable amount of exons interrupted by non-coding introns. Several basic cis-regulatory elements are required for pre-mRNA splicing including the donor 5' splice site (consensus sequence GURAGU), the branch point, a motif with consensus sequence YNYURAY localized 17–40 nucleotides upstream of the Y-AG sequence of the acceptor - 3' splice site (indicating the end of an intron) and a polypyrimidine tract (located in the vicinity of 3' splice site) serves as a binding site for the splicing factor U2AF (U2 snRNA auxiliary factor; consisting of 65 kD and 35 kD subunits).*
Spliceosomes are built de novo on a pre-mRNA. Several splicing complex-intermediates are distinguished during spliceosome formation.
B. *In the initial step is formed the complex H consisting of various hnRNPs, however, formation of early complexes E' and E is usually considered as the commitment to splicing pathway. The complex E' assembles by recruiting U1 snRNP to 5' splice site and splicing factor 1 (SF1) to the branch point site.*
C. *Binding of the U2AF to a polypyrimidine tract and 3' splice site results in formation of complex*

E.

***D**. Further conformation change accompanied formation of the pre-spliceosome (complex A) involves ATP-dependent association of U2 hnRNP (in cooperation with RNA-tethered RS domain of SF1) with the branch point site replacing the SF1 molecule. U2AF65 (via its RS domain) adheres to branch point sequence, simultaneously.*

***E**. Later, the preassembled complex of U4/U6-U5 hnRNPs tightly base-paired by their snRNAs enters pre-spliceosome to form penta-snRNP-containing complex B. For proper integration of the U4/U6-U5 tri-snRNP into the spliceosome is required phosphorylation of the PRP28 helicase (also denoted as DDX23) by SR protein kinase 2 (SRPK2).*

***F**. Catalytically active form of spliceosome (complex C) results from recruitment of additional protein factors and a large rearrangement of the complex during which U4 releases from U6 that binds to U2 displacing U1 in binding to 5' splice site. The U5 snRNP bridges both 5' end of exon 1 and 3' end of exon 2.The first transesterification reaction (red arrow) occurs between 5' splice site (blue *) and the adenosine (red *) in branch site pulled together by RNA–RNA interactions of the U4/U6 snRNPs complex. The 2' hydroxyl group on the branch point adenosine attacks the phosphate group at the junction between exon 1 and intron 1. This transesterification results in formation of lariat structure (5' end phosphate of intron 1 is bind to ribose 2' OH group of adenosine in branch site) and free 3' OH group of the last guanosine in exon 1.*

***G**. In subsequent second transesterification reaction (red arrow) the 3' OH group at the end of exon 1 attacks the phosphodiesteric bond between the last guanosine on the 3' end of intron 1 and first nucleotide of exon 2.*

***H**. The second transesterification joins exons 1 and 2 and releases intronic lariat [126].*

1.5.1.1 Splicing factors governing splice sites selection

In the pre-spliceosome, 5' splice site is marked by U1 snRNP binding GURAGU motif (where the only first GU dinucleotide is highly conserved) by base pairing that involves 3–4 base pairs only [130,131]. Branch point site is sequentially recognized by an essential splicing factor U2AF (interacting with pre-mRNA by RS domain in U2AF65 subunit) and U2 snRNP bound by snRNA – pre-mRNA base pairing. Both U2AF subunits simultaneously bind polypyrimidine tract and 3' splice site via their RNA-recognition motifs (RRMs). These interactions are supported and stabilized by basic and auxiliary splicing factors. Except the basic splicing factors (represented by snRNPs), auxiliary splicing factors are necessary for both constitutive splicing and splice site selection in alternative splicing. The two main classes of auxiliary splicing factors include serine–arginine rich (SR) (together with SR-related) proteins [132,133] and heterogenous nuclear ribonucleoproteins (hnRNPs) [134]. Auxiliary splicing factors bind to facultative pre-mRNA cis-regulatory elements – splicing enhancers or silencers localized within exons and introns (exon/intron splicing enhancer – ESE/ISE; exon/intron splicing silencer – ESS/ISS) [135,136,137]. The SR and SR-related proteins generally associate with splicing enhancers promoting splicing between the closest 5' and 3' splicing sites, while hnRNPs recognize splicing silencers inhibiting usage of 3' splice sites or promoting the use of more distant 5' splicing sites. Presence of

protein-binding and RNA-binding motifs in auxiliary splicing factors promotes changes in secondary pre-mRNA structure that enables approaching various 5' and 3' splice sites to spliceosome core complex by molecular mechanisms discussed later. The importance of secondary pre-mRNA structure in splicing events is supported by evidence that several RNA helicases influence spliceosome complex formation [138].

The SR proteins are relatively abundant nuclear phosphoproteins containing either one or two N-terminal ribonucleoprotein type RRMs and a C–terminal serine-arginine dipeptide-rich RS domain of variable length. The SR proteins (via RS domains interactions) form a functional protein net scaffolding spliceosome catalytic core and stabilize entire spliceosome complex [139,140]. Specific binding of their RRMs domains with pre-mRNA ESE/ISE elements controls these interactions in a spatial manner. The importance of protein–protein interactions on splicing process is evidenced by exon-independent function of RS domains showing *in vitro* that RS domain alone is sufficient for (low level) splicing [141,142,143]. It has been also proposed that RS domains in SR proteins are indispensable for spliceosome formation since initial steps [144,145,146]. It is assumed that the RS domains enhance assembling of basic splicing factors by influencing thermodynamic stability of base-paired RNA duplexes in spliceosome (i.e. U2 snRNP and branch point site, U1 snRNP and 5' splice site and U2 snRNP and U5/U6 snRNPs) [147]. Experiments using fusion proteins combining different RS domains with different RRM show that the functions of particular RS domains are interchangeable in spliceosome assembly [148,149]. Therefore, the RRM domains represent carriers of the SR protein-specificity to the targeted pre-mRNA cis-regulatory elements [150].

The hnRNP factors comprise the large group (at least 20 hnRNPs; A1 to U) of predominantly nuclear RNA-binding ribonucleoproteins containing RRMs (with different pre-mRNA sequence-binding preferences) and glycine-rich domains (GRD; mediating protein-protein interactions) [151]. The hnRNP factors rapidly associate with nascent pre-mRNA transcripts and are involved in whole mRNA metabolism. Moreover, they are also implicated in DNA-binding processes through their RRM and GRD motives contributing to DNA replication and repair processes [152]. The hnRNP proteins can both hinder or assist to the splice site selection through their direct interactions with RNA cis-regulatory elements (usually splicing silencers) acting antagonistically to SR proteins [153,154,155]. The three main mechanisms of action of hnRNPs in splicing regulation has been hypothesized [156]. (i) The hnRNPs prevents splice site recognition by binding to splicing silencer sequences that are frequently overlapped with splicing enhancer motives disabling recognition of

ESE/ISE sites by positively acting splicing factors [157]. (ii) Binding of hnRNPs to pre-mRNA ISS/ESS elements (localized around or within a silenced exon) is followed by multimerization of tethered proteins that causes formation of the loop containing skipped exon(s) protruding from spliceosome, and thus make silenced exon(s) sterically unavailable for splicing [158]. (iii) It has been shown that the hnRNP A1 protein binds with a high affinity to ESS site resulting in rapid cooperative assembly of further inhibitory hnRNPs complexes coating the pre-mRNA molecule [159]. This cooperative binding of hnRNPs interferes directly with association of basic snRNPs and U2AFs at the initial steps of spliceosome assembly.

While the SR and SR-related proteins endorse entry of flanking splice sites to spliceosome, the hnRNPs promote exclusion of their targeted pre-mRNA sequences from splicing (Fig. 7). Thus, the ratio between intranuclear concentrations of "pro-splicing" SR and "splicing-inhibitory" hnRNPs critically contribute to formation of various mRNA isoforms [160].

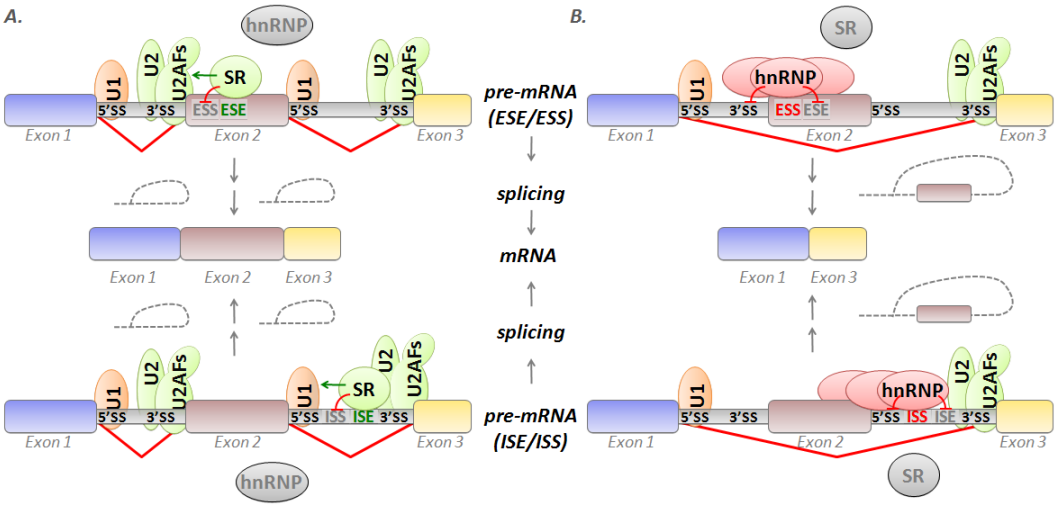

Figure 7. Activity of SR protein and hnRNPs in regulation of alternative splicing. *The association of SR proteins to ESE blocks accessibility of hnRNPs to ESS located in proximity and facilitates recruitment of basal splicing factors to obligatory 3' spice site sequences.* ***A.*** *In presented hypothetical case (upper panel) resulting in intron 1 removal, the U1 snRNP binds to 5' splice site and the most proximal 3' splice site (located in intron 1) is selected. Similar result provides accession of SRs to ISE (lower panel).* ***B.*** *High activity of hnRNPs bound to ESS (upper panel) and in turn multimerization of other hnRNPs disable binding of SRs to ESE and interfere with recognition of 3' splice site by U2AFs/U2 snRNP complex leading to the selection of distant 3' splice site and resulting in excision of exon 2 during splicing. Analogically, in case of hnRNPs binding to ISS (lower panel), the distant 5' splicing site is selected resulting in same situation.*

Using an *in vitro* model it has been shown that a member of SR protein family called alternative splicing factor (ASF)/splicing factor 2 (SF2) (aka splicing factor, arginine/serine-rich, 1; SFRS1) interferes directly with the hnRNPs family member hnRNPA1 for binding to artificial pre-mRNA containing two introns. The abundance of ASF/SF2 enhanced binding of U1 snRNP to both possible 5' splice sites. Simultaneous occupancy of both possible 5' splice sites by U1 snRNP enabled selection of the most proximal 5' splice site to 3' splice site resulting in formation of full-length mRNA. Contrary to that, higher concentration of hnRNP A1 bound to pre-mRNA led to a loop formation sterically inhibiting U1 snRNP binding at both possible splice sites, resulting in selection of the distal one [161]. According to this concept, the pre-mRNA cis-regulatory elements acts as units that increasing local concentration of particular auxiliary splicing factors resulting in either alternative exon/intron excision, or retention. Thus, the additional information required for intron-exon boundary definition is partly contained in these cis-acting regulatory sequences.

Except the above mentioned mechanisms, several studies indicated that other factors may affect splice site selection (further in 1.5.2). It has been shown that different RNA polymerases could involve splice site selection providing the evidence about connection of splicing to transcription in "RNA factory" by so far unknown mechanisms [162,163]. Several studies also indicate correlation between presence of a premature stop codon and splicing events leading to alteration in splice site preference avoiding a protein truncation [164]. Three possibilities have been suggested in this way. First, the presence of nonsense codon can disrupt a cis-regulatory element in pre-mRNA causing a change in intrinsic strength of splice site. Second, the nonsense codon could be recognized by translating ribosome influencing the splicing via the NMD-associated factor up-frameshift mutation 1 (Upf1; also regulator of nonsense transcripts 1; RENT1) in so called nonsense-associated altered splicing. Last, the premature stop codon could be recognized before translation by nuclear scanning mechanism within spliceosome in so called suppression of splicing.

1.5.1.2 RNA cis-regulatory elements

RNA cis-regulatory elements are directly involved in splicing processes. Both splice sites, and the branch point site serve as substrates for transesterifications joining exons and releasing introns in mRNA formation. Together with polypyrimidine tract, they form obligatory binding sites for core spliceosome snRNPs. The facultative pre-mRNA cis-regulatory elements are represented by splicing enhancers or silencers. Localization, primary

sequences, and occurrence of splicing silencers/ enhancers (antagonizing each other in exons and/or introns) directly influence splice site selection by titration of RS domains indispensable for spliceosome assembling at particular exons. In fact, the splicing enhancers are necessary for both constitutive and alternative splicing. Using *in vitro* and *in vivo* approach Stadler et al [165] discovered diverse array of purine–rich and pyrimidine–rich sequences that can act as ESS/ESE, identifying short (6–8 nucleotides) RNA motifs. Both ESS and ESE sequences were shown to be highly degenerated and sometimes partially overlapping. The affinity of splicing factors to pre-mRNA (and thus intrinsic strength of splicing enhancer/silencer) depends on both "complementarity" between cis-regulatory element and RRM of splicing factor and frequency of cis-regulatory elements within exon and intron [166]. Statistical analyses of ESE motifs distribution revealed that occurrence of ESEs positively correlates with probability of splicing in flanking splice site, and, vice versa, the low frequency of ESEs nearby the particular splice site make this one low probable for splicing/spliceosome formation [167]. Comparison between constitutively- and alternatively-spliced exons demonstrated slightly weaker splice site scores as well as significantly fewer ESE motifs in a group of alternatively spliced exons [168,169]. Assuming that the ESE-dependent splicing factors form a protein net stabilizing basic splicing factors bound to pre-mRNA, in alternative splicing this bound is weaker and easily influenceable by local concentrations of specific splicing factors.

Splicing silencers are suggested to play an important role in prevention of pseudoexon(s) inclusion in matured transcripts and in definition of constitutive exons by suppression of nearby decoy splice site [170,171]. This hypothesis is supported by results of several recent studies systematically identifying silencer elements within genes showing that pseudoexons seems to be enriched in ESS compared to constitutive exons [172]. Silencers are also more abundant in sequences containing decoy 3' splice sites [173]. Similar to splicing enhancers, silencers exert their activity through binding of specific auxiliary splicing factors, typically hnRNPs and PTBs (polypyrimidine tract binding proteins). The action of splicing factors through silencer sequences might be either direct competition for an important cis-regulatory element (such as splice site or polypyrimidine tract) with positively-acting factors, or introduction of such secondary structure to pre-mRNA molecule that constrains spliceosome assembly [174], as we discussed previously (chapter 1.5.1.1).

1.5.2 Regulation of alternative splicing and its regulatory function

Regulated mRNA splicing is the process that enables alternative usage of various splice sites within the primary mRNA transcript upon different cellular condition. Arising splicing variants thus reflect certain cellular responses to distinct stimuli and could play an important role in the regulation of relevant response pathways. Regarding the importance of splicing, there is a surprising contrast between well known signal transduction pathways controlling transcription and relatively poor knowledge of those regulating pre-mRNA processing. From the matter of the process, alternative splicing can be regulated on two distinct levels – the transcription-splicing coupling and activity of auxiliary protein splicing factors.

Structure and certain conformation of pre-mRNA molecule can be influenced mainly by the rapidity of RNA synthesis. Splicing takes place co-transcriptionally and thus the regulation of RNA polymerase activity/velocity directly reflect the splicing outcome [175]. Slower polymerization of RNA causes formation of bigger pre-lariat structure that is formed due to prolonged time for utilization of weaker cis-regulatory sites for auxiliary splicing factors. Compared to that, normal (high) rate of RNA synthesis utilize the strongest cis-regulatory elements upon a time pressure (Fig. 8) [176]. This hypothesis was supported by the finding that alternative splicing events of human fibronectin is not only controlled by the activity of SR proteins, but can also be modulated by the promoter occupation by certain RNA polymerase-containing complexes or phosphorylation of RNA polymerase molecule [177,178].

Regulation of alternative splicing by this mechanism plays a critical role in the DNA damage response. It has been described that UV irradiation causes the formation of pro-apoptotic isoforms of certain genes (Bcl-x, caspase-9) [35]. It is known that DNA damage causes the stalling of RNA polymerase complex and thus inhibits the 3'-end mRNA formation and related co-transcriptionally-coupled processes. Moreover, affection of alternative splicing following UV treatment is not dependent on the p53-mediated transcription indicating the superiority of alternative splicing events in DNA damage response. Additionally, a detail chip analysis revealed that more than 80% of genes that changed their expression following UV-mediated DNA damage also changed their splicing pattern [196]. This together suggests that modulation of alternative splicing through its coupling with transcription is a key feature in a DNA damage response.

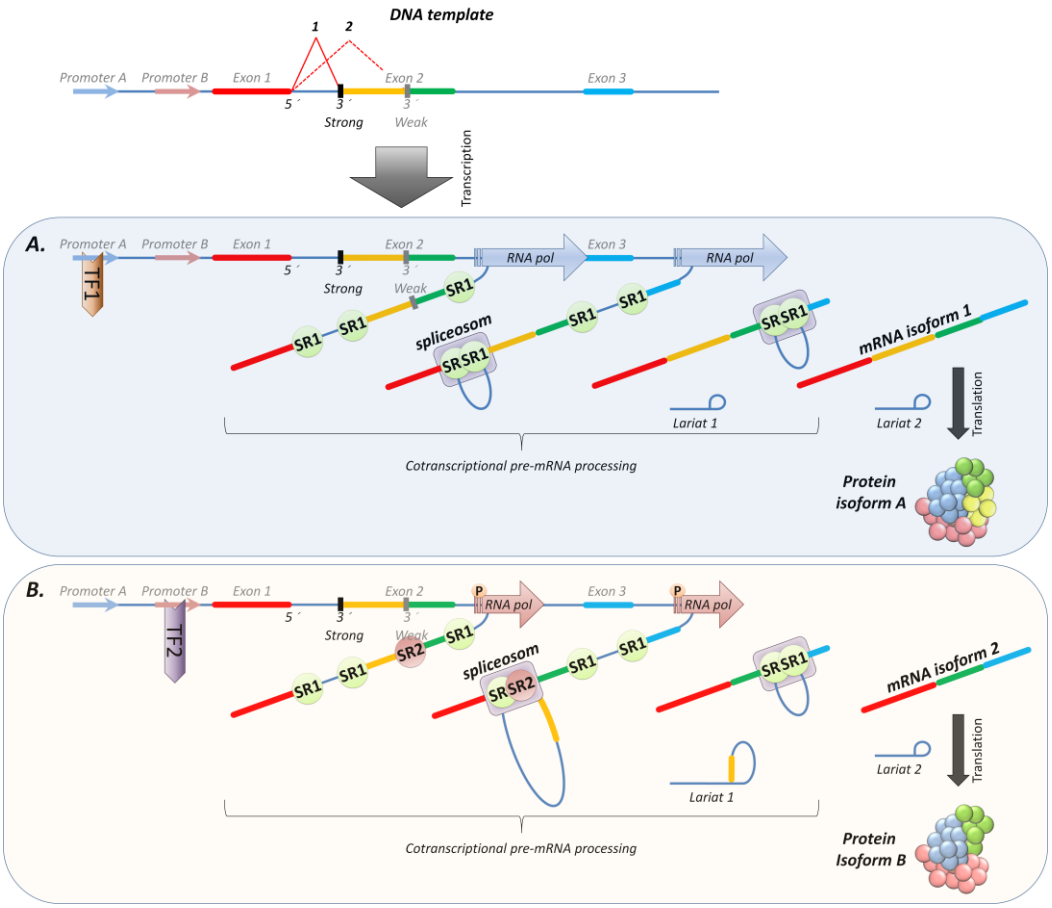

Figure 8. Regulation of alternative splicing by its coupling with transcription. *The activity of RNA polymerase during transcription is one of the key determinants of alternative splicing events. Usage of different gene promoter, depending on their occupancy by certain transcription factors (**TF1/2**), influences final activity of RNA polymerase (**RNA pol**). Beside that the rate of transcription can be regulated by the phosphorylation status (**P**) of the RNA polymerase's C-terminal domain. This typically occurs upon DNA damage and causes stalled transcription and delayed 3'-end pre-mRNA processing. **A**. Fast transcription provides to the co-transcriptional machinery "just" enough time to use stronger or proximal 3' splice site. **B**. Slower transcription allows the usage of alternative splicing factors (**SR1/SR2**) leading to more profound selection of 3' splice sites.*

As was shown in previous text, simultaneous or competing occupation of RNA cis-regulatory elements by auxiliary splicing factors is well described determinant of splice site selection. The interaction of splicing factors with pre-mRNA can be influenced by their spatiotemporal accessibility. It has been shown that the SR proteins co-localize with specific kinases in nuclear speckles [179]. Their clustering or releasing from nuclear speckles depends on phosphorylation of their RS domains [180]. Phosphorylation of serine residues within RS domains affects interaction of SR proteins with pre-mRNA cis-regulatory elements and proteins engaged in spliceosome assembly [181]. Furthermore,

(hyper)phosphorylation also regulates intracellular turnover of SR proteins targeting them for proteasome-mediated degradation [182]. Splicing factors from hnRNP family shuttle rapidly between nucleus and cytoplasm using nuclear transport receptors/transportin system. Phosphorylation of hnRNP directly influences its binding capacity to transportin and thus its nuclear import [183].

Several kinases responsible for the phosphorylation of SR proteins have been described including SR protein kinase (SRPK) and cyclin–like kinase or serine/threonine/tyrosine kinase (Clk/Sty) that constitutes highly conserved families with related but distinct substrate specificities. These kinases are directly involved in regulation of splicing process [184,185]. Moreover, other kinases (e.g. AKT kinases) were shown to phosphorylate certain splicing factors [186,187]. The enzymatic activities, substrate specificity, and subcellular localization of these kinases are regulated by upstream molecules [188].

Using the CD44 protein, Konig et al. showed that inclusion of the alternative exon v5 is enabled by cooperation of SR-related nuclear matrix protein 160 (SRm160) with relevant ESE [189]. On the contrary, exon v5 skipping is governed by hnRNP A1 binding to specific ESS [190]. Activity and subcellular localization of both these antagonistic splicing factors are affected by their phosphorylation. When overexpressed, hnRNP A1 inhibited inclusion of alternative exon v5, however, this inhibition was abolished upon activation of T-Cell Receptor (TCR) signal transduction pathway. On the contrary the inclusion of exon v5 was enhanced by the artificial activation of Ras/Rac/Raf/MEK signal transduction pathway. In model cell line ectopically expressed splicing factor SRm160 increased exon v5 inclusion only upon Ras protein activation. Moreover, changes in splicing pattern were protein synthesis-independent. This together indicates that activity of auxiliary splicing factors is governed by an upstream signalization and is regulated on the posttranscriptional level (Fig. 9).

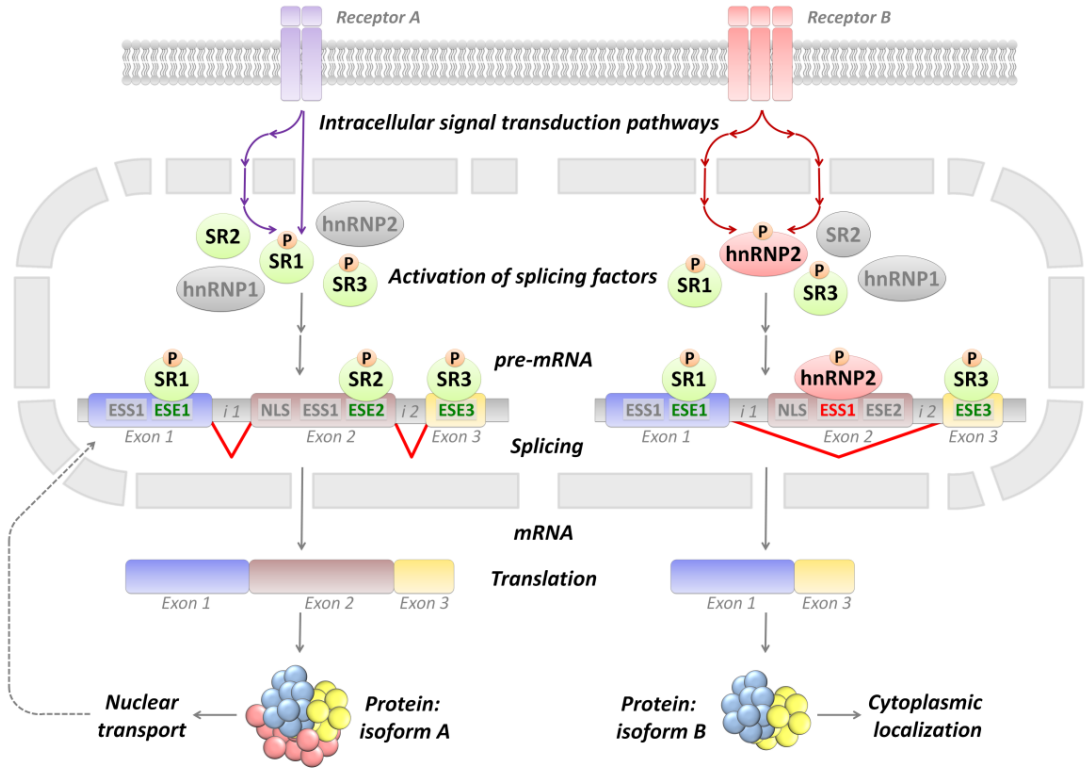

Figure 9. Regulation of alternative splicing by upstream signal-transduction events regulating phosphorylation of auxiliary splicing factors. *Specific signal transduction pathways transfer different initial signals to terminal kinases that directly control spatial concentration and activity of splicing factors by releasing them from nuclear speckles, or relocalizing them from cytoplasm in a phosphorylation-dependent manner. Splicing factors together with cis-acting elements (e.g. splicing enhancers/silencers) influence a splice site selection in a qualitative as well as quantitative manner. As a final result of the upstream signaling events, protein isoforms with modified properties are produced.*

Since that several other reports have shown that alternative splicing pattern could be changed by activation of specific signaling pathways. Number of experiments linked the alternative splicing events with activation of various signal transduction pathways consisting of cascade of specific kinases. The alternative splicing controlled by this mechanism has been demonstrated to influence multiple cellular functions including growth regulation, apoptosis, adhesion or migration [191,192].

1.5.3 Splicing alterations in cancer

Malignant transformation is governed by genomic DNA alterations accompanied by epigenetic insults. In cancer cells, splicing processes could be perturbated at various levels

[193,194,195]. Gene mutations could directly modify sites coding for pre-mRNA cis-regulatory elements. Mutation in genes coding for upstream regulators of auxiliary splicing factors or in genes coding for auxiliary splicing factors themselves could result in aberrant splicing of targeted pre-mRNAs. Except that, splicing of particular genes could be affected due to mis-regulation of signaling pathways accompanying malignant transformation. These mechanisms results in four major splicing modes: exon(s) skipping, 5' alternative splicing, 3' alternative splicing, and intron retention.

It is now estimated that at least 15% of all point mutations result in splicing defects [196]. Splice sites could be negated by a single nucleotide change or deletion. Similarly, function or intrinsic strength of others cis-regulatory elements could be changed or completely abolished. Finally, nonsense mutations causing introduction of premature stop codon into primary mRNA transcript are able to alter splicing pattern.

Few examples indicated possible links between splicing control and oncogenic signaling pathways [197]. Moreover, changes in quantity of splicing factors and activity of their kinases have been documented in some cancer types [198,199]. These facts together with observations that many oncogenes and tumor suppressor genes are spliced into isoforms with distinct or completely different functions [200,201] indicate that alterations in splicing during malignant transformation could be a part of its pathogenic mechanism.

1.5.4 BRCA1 alternative splicing variants and breast cancer

Individuals carrying a germ-line mutation in the BRCA1 gene are predisposed to early-onset breast and/or ovarian cancer. Regarding to its tumor suppressor function, loss of BRCA1 expression causes the BRCA1-associated cancers. Beside to the inactivating mutations, large deletions, genomic rearrangements, and epigenetic changes, production of alternative splicing variants can be another mechanism altering BRCA1 mRNA and protein levels.

Large number of different BRCA1 splicing variants has been non-systematically described so far [202,203]. The majority is represented by aberrant splicing variants resulting from genomic alterations affecting the consensus cis-regulatory splicing elements. Indeed, number of aberrant splicing variants is considered as pathogenic due to obvious inactivating structural changes. Many uncharacterized BRCA1 splicing variants are formed during the posttranscriptional modification of primary transcript as a result of noisy splicing [204]. The

frame-shifting aberrant splicing variants are frequently withdrawn by NMD eliminating their translation into the protein product [205]. However, this could decrease BRCA1 activity by decreasing its transcription rate. In various cell lines and tissues it has been described that expression of full length BRCA1 form is accompanied by three frequently-occurring alternative splicing variants – BRCA1Δ8-9; Δ10q and Δ8-10q [206]. Though the systematic and exact expression analysis of BRCA1 alternative splicing variants has not been done yet, it is known that expression rate of these predominant alternative splicing variants depends on cell cycle phase and is cell line specific. This may indicate an important function of alternative splicing variants in processes governed by the BRCA1. Beside the above-mentioned predominant BRCA1 alternative splicing variants, functions of several others were studied:

BRCA1Δ8-9 lacks a part of central DBD. Additionally, a number of proteins have been described to interact with BRCA1 via this region. It can be supposed that BRCA1Δ8-9 may exhibit changed protein-binding capacity, though the functional consequences are not known. The BRCA1Δ10q and BRCA1Δ8-10q were shown to have decreased transactivation activity and to possess both distinct and overlapping activity to full length BRCA1 [207].

The BRCA1Δ10 was shown to increases the genomic instability in mouse embryonic cells. Further analysis reveals the block of Rad51 filament loading during the HR of DDSB in cells expressing this BRCA1 alternative splicing variant [208]. Despite contradictory results, it is apparent that the BRCA1Δ10 has a potential to control the proliferative activity of cells [209].

BRCA1-IRIS (in-frame reading of BRCA1 intron 10 splice variant) is the alternative splicing variant generated by usage of cryptic 3' splice site in intron 10. Resulting protein product has identical 1365 N-terminal amino acids with full length BRCA1 followed by novel C-terminus consisting of 34 amino acids. Interestingly, the expression of BRCA1-IRIS prevails the expression of full length BRCA1 five times in lymphocytes [6]. While full length BRCA1 forms the discrete nuclear foci upon DNA damage, BRCA1-IRIS does not. Even though BRCA1-IRIS contain intact RING finger domain it does not associate with BARD1. BRCA1-IRIS positively influences the DNA replication, as it associates with proteins that bind to initiation sites of DNA replication, such as ORC1, Cdc6 and MCM2. Besides that, BRCA1-IRIS was shown to promote cellular proliferation by formation of complexes with nuclear receptor co-activators SRC1 and SRC3 that are recruited to the cyclin D1 promoter and triggering its expression and by inhibition of DNA replication

suppressor geminin [210]. In DNA damage response pathway, BRCA1-IRIS abrogates the p38MAPK/p53/WIP1 pathway increasing survival and proliferation of cells upon genotoxic stress [211]. This together indicates that contrary to full length BRCA1 that inhibits the cell cycle progression and in turn cellular proliferation, BRCA1-IRIS acts as a proto-oncogene.

A number of BRCA1 alternative splicing variants do not retain the original ORF and are predicted to be a subject for NMD. However, some experiments indicated that certain variants containing premature termination codon are expressed and possess unique features. For instance the BRCA1Δ22 has been shown to be expressed in mouse and human cell lines and be defective in transcriptional activation [202].

The expression of alternatively spliced BRCA1 isoforms in normal and malignant tissue is poorly understood. Several studies published conflicting results in such context [212,213] However the various surprising features possessed by distinct BRCA1 splicing variants prove the relevance of further functional studies in the context of BC development and progression.

2 THE WORKING HYPOTHESIS AND THE AIMS OF THE STUDY

During the ongoing genetic screening program of high risk breast/ovarian cancer families, performed at the Institute of Biochemistry and Experimental Oncology, various splicing variants of the main hereditary BC predisposing gene BRCA1 have been repeatedly detected at mRNA level. The absence of relevant gDNA rearrangement and a relatively broad spectrum of variants missing discrete exons indicate their origin in the mis-regulated pre-mRNA alternative splicing process.

Alternative splicing of pre-mRNA is capable to generate protein isoforms which can exert different properties and thus can markedly influence biological processes regulated by a full-length isoform. There is a growing evidence of possible role of mis-regulated splicing in malignant transformation. However, the majority of experiments have been focused on functional analyzes of point mutations and variants resulting from aberrant mRNA splicing while products of alternative pre-mRNA splicing and their functional impact are almost unknown.

The aim of this project was to functionally analyze two BRCA1 alternative splicing variants Δ14-15 and Δ17-19 retaining the original BRCA1 open reading frame and lacking short exons in areas coding for the important BRCA1 structural motifs: a serine-containing domain (SCD) in BRCA1Δ14-15 and first of tandem BRCT domains in BRCA1Δ17-19. Both these variants have been ascertained during the screening of high risk BC individuals. Thus their detail analyses would be beneficial for understanding the role of alternative pre-mRNA splicing in malignant transformation.

The purpose of this study was:

- Establishing of a reliable system for the *in vitro* functional analysis of the BRCA1 sequence variants
- Determining of the effect of BRCA1Δ14-15 and BRCA1Δ17-19 alternative splicing variants on the DNA repair and growth properties of cells stably expressing analyzed variants.

The obtained results will be used for evaluation of the BRCA1 alternative splicing variants in the process of mammary malignant transformation.

3 MATERIAL AND METHODS

MCF-7 cells were used as a model system for functional analysis of **selected BRCA1 sequence variants (BRCA1Δ14-15 and BRCA1Δ17-19**). Their coding sequences were constructed by **PCR-splicing approach** using a plasmid containing the entire human BRCA1 full-length coding sequence. Endogenous wtBRCA1 expression in MCF-7 cells was downregulated by **shRNA-mediated RNAi**. **Stable clones** expressing studied variants with/without coincidental downregulation of endogenous wtBRCA1 expression were selected after **calcium-phosphate transfection**. Expressions of BRCA1Δ14-15, BRCA1Δ17-19, and wtBRCA1 in constructed stable clones were quantified on mRNA level by **qPCR** and on protein level by **western blotting**.

Functional analysis was initiated by estimation of overall repair capacity following ionizing radiation induced DDSB by **comet assays.** Kinetics of DNA repair complexes was scored by **immunofluorescence confocal microscopy** evaluating formation and decomposition of γH2AX/53BP1 foci. Impairment of HR and NHEJ repair capacities were analyzed by **mitomycine C sensitivity test** and ***in vitro* NHEJ assay**, respectively. Influences of analyzed splicing variants on cellular growth were analyzed by **clonogenic assays** and **growth curves** under the standard cultivation conditions and following γ-irradiation.

3.1 Construction and characterization of stable clones

3.1.1 Expression system and construction of expression vectors

A pcDNA3.1. Hygro (Invitrogen) expression vector was used for expression of studied sequence variants (BRCA1Δ14-15 and BRCA1Δ17-19). The Rc_BRCA1 plasmid containing the entire human BRCA1 full-length coding sequence was provided by a generous gift from Paul D. Harkin (Dept. of Oncology, Queen's University Belfast) [214]. The entire BRCA1 coding sequence was re-cloned into the pcDNA3.1 vector by HindIII/XhoI double-digestion and subsequent ligation to pcDNA 3.1 vector linearized by the same restriction enzymes to prepare the pcDNA3.1-wtBRCA1 construct.

Expression constructs of particular BRCA1 splicing variants (BRCA1Δ14-15; BRCA1Δ17-19) were subsequently prepared by PCR splicing approach (Fig. 10) using pcDNA3.1-wtBRCA1 as a template (Fig. 10). The BRCA1Δ14-15 and BRCA1Δ17-19 inserts with skipped exons were prepared by a two-step PCR. In the first step the two inner primers with

overlapping sequences to the exons 13 and 16 for BRCA1Δ14-15 (14-15del F: 5'-GAACAAAGCACATCAGAAAAAGAGGGAACCCCTTACCTGGAATC–3', and 14-15del R: 5'-GATTCCAGGTAAGGGGTTCCCTCTTTTTCTGATGTGCTTTGTTC–3' respectively), and 16 and 20 for BRCA1Δ17-19 (17-19del R: 3'-GGACTGG GGTCTTCTTAAAGTACTAAAACTTCAGTCTC–5', and 17-19del F: 3'-GAGACTGAAGTTTTAGTACTTTAAGAAGACCCCAGTCC–5' respectively) were used together with outer primers with adjacent sequences containing the BamHI and XhoI restriction sites (forward 5'-AGCGTCCAGAAAGGAGAGCTTAGCAG–3' and reverse 5'-ATCCCCCACAGCCACTACTGAGTAACTCGAGTAGTTATTAC – 3'). A pcDNA3.1-wtBRCA1 expression construct, 0.5 mM of each primer and 0.5 U TaKaRa La Taq polymerases was cycled 25 times in 95°C - 30s; 56°C - 30s; 72°C - 1 min with the initial denaturation at 95°C 1 for min and the terminal elongation at 72°C for 10 min. For the second step, 100 ng of each of the first step PCR products, 0.5 mM of each of the outer primers, and 0.5 U TaKaRa La Taq polymerases were cycled 16 times at 95°C - 30s; 56°C - 10s; 68°C - 2 min with the initial denaturation at 95°C for 1 min and the terminal elongation at 72°C for 10 min. The PCR product was subsequently purified by a PCR purification kit (Genomed), double digested by BamHI and XhoI and ligated into a pcDNA3.1 vector linearized by the same restriction enzymes using a T4 DNA ligase (Fermentas) at 21°C overnight.

The whole volume of ligation reaction was then transformed into the TOP $10F^-$ competent cells (Invitrogen). Freshly thaw competent cells were mixed with ligation reaction and incubated on ice for 20 minutes. Then the heat shock at 42°C for 30 seconds exactly was done, cells were recovered in S.O.C medium at 37°C for 2 hours and finally seeded onto the LB agar plates containing 100 μg/ml ampicillin. After growing a single colony was picked up, grown in liquid LB medium with 100 μg/ml ampicillin and mini preparated using a Plasmid MINI preparation kit (Qiagen).

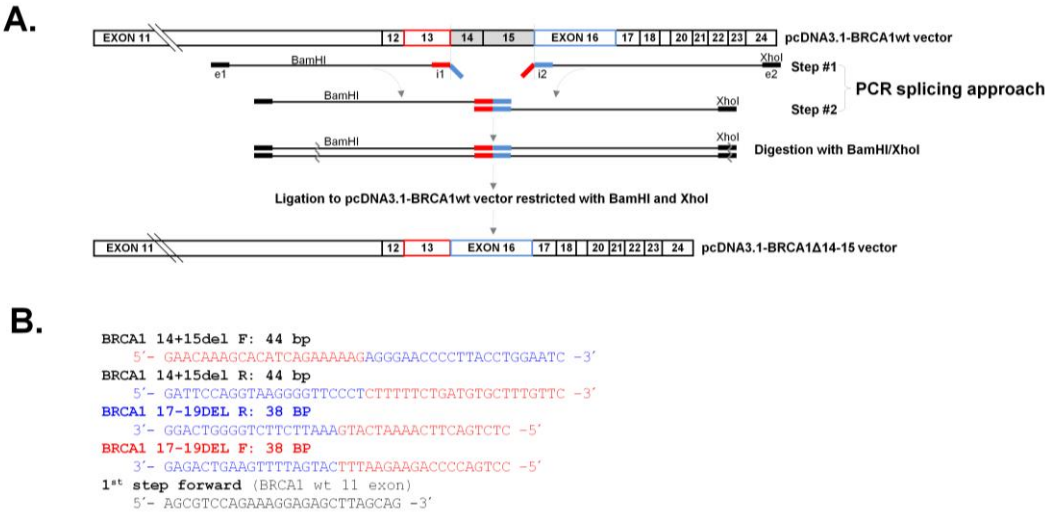

Figure 10: PCR splicing approach. *A two step PCR approach used for the generation of BRCA1Δ14-15 and BRCA1Δ17-19 inserts for pcDNA 3.1 expression system.* ***A.*** *In the first step are amplified two DNA areas enclosing the target skipped sequence* ***B*** *(exons 14-15 in the case of BRCA1Δ14-15; and exons 17-19 in the case of BRCA1Δ17-19 respectively) using inner primers (depicted here in a red/blue colors with respect to complementary areas) with overlapping sequences to the border exons. In the second step the two products of first PCR reaction are annealed together and further amplified using two outer primers.*

The whole insert length was sequenced using primer complementary to the pcDNA3.1 hygro plasmid and BRCA1 sequences (BRCA1 complementary 5'-AGCGTCCAGAAAGGAGAGCTTAG CAG–3'; pcDNA3.1 hygro complementary: 5'-TAGAAGGCACAGTCGAGGC–3').

Table 3: *A list of used oligonucleotides for the engineering of pSUPER-based anti-BRCA1 shRNA vectors. The shRNA sequence complementary to the target are* ***highlighted****.*

shRNA designation	Sequences of the pSUPER vector insert
shRNA 4834 (exon 15)	5'–GATCCCC**CACGATTTGACGGAAACAT**TTCAAG AGAATGTTTCCGTCAAATCGTGTTTTTGGAAC–3'
shRNA 4836 (exon 15)	5'–GATCCCC**CGATTTGACGGAAACATCT**TTCAAG AGAAGATGTTTCCGTCAAATCGTTTTTGGAAC–3'
shRNA 5196 (exon 17)	5'–GATCCCC**GTACAAGTTTGCCAGAAAA**TTCAAG AGATTTTCTGGCAAACTTGTACTTTTTGGAAC–3'
shRNA 5331 (exon 18)	5'–GATCCCC**GAAAATGGGTAGTTAGCTA**TTCAAG AGATAGCTAACTACCCATTTTCTTTTTGGAAC–3'

A pSUPER.retro.puro (Oligoengine) vector system with human H1 promoter driven expression of interfering RNA was used for short hairpin RNA (shRNA) mediated downregulation of endogenous wtBRCA1 expression. Interfering RNAs were targeted to exonic sequences missing in particular BRCA1 splicing variants (Tab. 3) and were designed according to generally accepted conventions for effective interfering RNA [215,216]. Each shRNA was synthesized as 60 nucleotides fragment (GeneriBiotech) (Fig. 11). Two complementary shRNA oligonucleotides were annealed and subsequently inserted into the BglII/HindIII-linearized pSUPER.retro.puro vector using a T4 DNA ligase (Fermentas) at 21°C overnight.

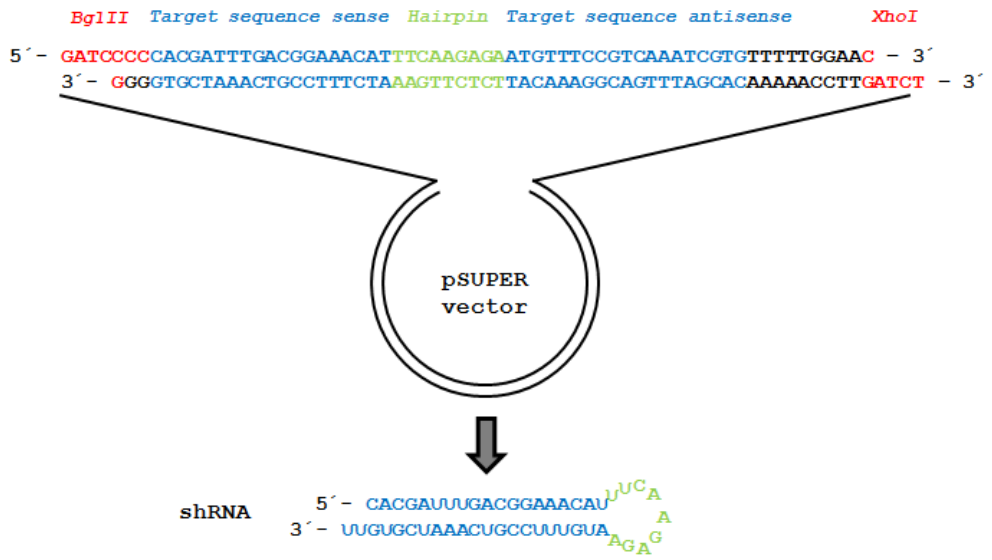

Figure 11: A design of shRNAs used for the generation of pSUPER.retro.puro expression constructs. *Each shRNA was designed as two complementary 60 nucleotides oligomers containing target sequence. Each oligomer contains 19 nucleotides* ***sense*** *and* ***antisense*** *target sequence (depicted in blue letters), 9 nucleotides* ***hairpin*** *(depicted in green letters),* ***shRNA transcription termination signal*** *(depicted in black letters) and 4 nucleotides overlaps on the 5' end mimicking a* ***BglII, and XhoI restriction sites*** *respectively (depicted in red letters) used for the ligation into the pSUPER.retro.puro vector.*

The whole volume of ligation reaction was then transformed to TOP 10F' competent cells (Invitrogen) according to the manufacturer's instructions and seeded onto the LB agar plates containing ampicillin (100 μg/ml). After growing, a single colony was picked up, grown in liquid LB medium with 100 μg/ml ampicillin and mini preparated using a Plasmid MINI preparation kit (Qiagen).

Isolated plasmid DNA was first pre-screened using a BglII digestion with a subsequent electrophoresis. The positive one was sequenced in the full length of insert using primer complementary to the pSUPER.retro.puro plasmid sequence (5'-GCATGTCGCTATGTGTTCTG–3').

3.1.2 DNA sequencing

For the sequencing reaction, 0.5 μg of template DNA, 2 μl of 5x sequencing buffer, 2 μl of Big Dye v3.1 master mix (Life Technologies), 3.2 pM of primer was cycled 25 times at 96°C – 5s; 55°C – 5s; 60°C 4 min with the initial denaturation at 96°C for 45s in 10 μl reaction volume. The PCR product was subsequently EDTA/NaAc/EtOH precipitated and dissolved in 20 μl of Hi-Di formamide (Life Technologies). An automatic ABI3130 (Life Technologies) sequencer was used for the analysis.

3.1.3 Tissue culture and transfection

A human adherent breast adenocarcinoma-derived stable cell line MCF-7 (ATCC#: HTB-22) was used for functional *in vitro* experiments. Cells were cultivated in Dulbecco-modified Eagles medium (DMEM; Invitrogen) supplemented with 10% fetal calf serum (FCS; Gibco) with addition of L-glutamine, penicillin, and streptomycin (100xGPS; Gibco) at 37°C in a humidified atmosphere of 5% CO_2. During the standard cultivation, medium was replaced every third day. Confluent cells were passaged using a trypsin/EDTA solution (Invitrogen) and split up into a new cultivation Petri dish in dilution 1/10.

The cells were transfected using a calcium-phosphate protocol [217]. Briefly, cells were seeded onto the 3 cm diameter Petri dish and grown under the standard cultivation conditions until 75% of subconfluency. One day before transfection, medium was replaced by the fresh one. Two hours before transfection, medium was replaced by medium with 5% FCS and without antibiotics. To increase the probability of incorporation of expression construct into the host's genome during the transfection, all used expression vectors were first linearized by NsbI. Ten μg of pure linearized DNA were mixed with 30 μl 2M $CaCl_2$ and up to 250 μl ddH_2O. This solution was slowly added to 250 μl of 2xHBS buffer (Sigma Aldrich) by a drop-wise manner. Obtained soft DNA precipitate was immediately applied on the cells and incubated for 5 hours. Then, cells were rinsed twice with PBS, once with HBS containing 15% glycerol and recovered under the standard cultivation conditions for 24 hours. After

recovery, cells were transferred into the new 6 cm diameter Petri dish. The single cell colonies were obtained following a selection by Hygromycin B 200 μg/ml (Invitrogen) for pcDNA3.1 based expression constructs, and puromycin 2 ng/ml (Invitrogen) for pSUPER.retro.puro based expression constructs, respectively. Single cell colonies were separately picked up and grown under the standard cultivation conditions.

The integration of the expression construct into the host's chromosomal DNA was checked by PCR using the gDNA template. The PCRs were performed with primers complementary to the corresponding sequence of pcDNA 3.1 or pSUPER vectors (5'-GTGTTGGAGGTCGCTGAGTAG-3' or 5'-TGAACCTCCTCGTTCGACCC-3', respectively) and sequences of *BRCA1* or interfering RNA (5'-GTGTTGGAGGTCGCTGAGTAG-3' or 5'-GCATGTCGCTATGTGTTCTG-3', respectively). For the 20 μl PCR reaction, 2 μg of gDNA, 0.5 mM of each primer and 0.5 U of TaKaRa La Taq polymerases were used. The PCR was performed in 30 cycles (98°C for 10s; 56°C for 10s; 68°C for 7.5 min) with initial denaturation at 94°C for 1 min and terminal elongation at 72°C for 10 min. The efficiency of the BRCA1 expression's modulation was scored by qPCR and western blotting.

For the preparation of combined clones with upregulated particular BRCA1 splicing variant with coincidental shRNA-mediated downregulation of endogenous wtBRCA1, the MCF-7 cells were first transfected by pSUPER constructs and selected stable clones were subsequently transfected by the pcDNA3.1 expression constructs. An empty pcDNA3.1 and pSUPER vectors were transfected to the MCF-7 cells as a control. To exclude the off-target effect of shRNA expression, the cells were transfected by a pSUPER construct containing an irrelevant shRNA targeting the mouse C/EBPγ [218]. To exclude the effect of integration of vector into the random position within the host's genome three different stable clones were selected from each expression construct.

3.1.4 RNA isolation and real-time (qPCR) analysis

Total RNA was isolated by RNeasy MINI kit (Qiagen). Reverse transcription was performed by SuperScript III Reverse Transcriptase (Invitrogen) according to the manufacturer's instructions.

For qRT-PCR analysis, 0.1 μg of cDNA, 0.5 μM of each primer and 5 μl of LightCycler 480 SYBR Green I Master mix were cycled 50 times at 95°C for 10 s, 70°C for 10 s and 72°C for 10 s. BRCA1-specific primers (5'-AGAGTGTCCCATCTGTCTGGAGTTG-3' and 5'-GGACACTGTGAAGGCCCTTTCTTC-3') targeting BRCA1 coding sequence (mRNA: 185-304 bp) and housekeeping genes β2-microglobulin (B2M; SuperArray) and glyceraldehyde-3-phosphate dehydrogenase (GAPDH; 5'-ATGTCTGGTAACGGCAATGCGG-3' and 5'-TGTCCCCTGTGGTGGACATAGC-3') were used. qRT-PCR results were analyzed by LightCycler software (Roche) and values of crossing points (CPs) and amplification efficiencies were evaluated for each reaction. A BRCA1 expression was normalized using on the GAPDH and B2M expression using the qREST-2005 software (Relative Expression Software Tool) 2008 ver. 2.0.7 (Corbett Research Pty. Ltd).

3.1.5 Protein isolation and western blot analysis

To isolate the total proteins, cells were rinsed once with ice-cold PBS and lysed directly on a culture dish by a RIPA buffer (50mM Tris; 150mM NaCl; 1% NP-40; 0.5% sodium deoxylsulphate; 0.1% SDS) containing a protease inhibitor cocktail (Complete MINI ptotease inhibitor cocktail; Roche) for 15 minutes on ice. The undissolved fragments were discarded by centrifugation and a protein concentration was measured using the BCA Protein Assay (Bio-Rad).

For a western blotting analysis, 30 μg of total protein of each sample was boiled for 5 min in 5x SDS sample buffer (BioRad), loaded onto precast 6% polyacrylamide gel (BioRad; for the BRCA1 analysis) or 10% polyacrylamide gel (BioRad; for the β-actin analysis) and separated in a 1xTris/glycine/SDS buffer (BioRad) under the constant voltage of 200V for 100 min. Separated proteins were transferred onto a nitrocellulose membrane (Amersham) using a semi dry MINI protean system (BioRad) in a 1xTris/glycine buffer (BioRad) with 20% methanol under the constant voltage of 100V for 120 min. The efficiency of transfer was swiftly checked by a non-specific Ponceau S staining solution (BioRad) and the membrane was blocked in 5% non–fat milk 2 hours at RT. For immunostaining, membranes with transferred proteins were incubated with primary antibody anti-BRCA1 (Calbiochem mouse mAbMS110, dilution 1:100); anti-β-actin (A300-491A; Bethyl rabbit polyclonal, dilution 1:2500) for 2 hours at RT, washed three times by TBSt buffer (0.05% Tween 20) for 5 min at RT and then incubated with horseradish peroxidase-conjugated antibodies anti-

mouse IgG-HRP (Sigma; A-0168, dilution 1:80 000); Anti-rabbit IgG-HRP (Sigma; A-545, dilution 1:160 000) for 2 hours at RT. After the final washes three times by TBSt buffer (0.25% tween 20) and three times by TBSt buffer (0.05% tween 20), the proteins were visualized using the Super Signal West Pico chemiluminescent substrate (Pierce). After developing of Kodak X-OMAT film (Kodak), UN-SCAN-IT gel ver. 6.1 (SilkScientific) was used for a relative quantification of BRCA1 bands using β-actin as a protein loading control.

3.2 Functional analysis of selected BRCA1 alternative splicing variants

3.2.1 Comet assay

Cells were grown in triplicates under the standard cultivation conditions to 75% sub-confluency and treated with a single dose of 1.5 Gy of γ-radiation (using ^{60}Co 1 Gy/min). Non-irradiated cells (marked here as 0 min) and irradiated cells collected in the particular times (15, 30, 60, and 120 min) post-irradiation (PI) were rinsed once with ice-cold PBS, released from the culture dish by scraper and diluted to the final concentration of $1x10^5$ cells/ml in ice-cold PBS. Ten μl of cell suspension was mixed with low melting agarose (Trevigen) pre-heated to 37°C, applied on a Trevigen comet assay slides (Trevigen) and let solidified for 30 min in dark on ice. Cells were subsequently permeabilized by soaking in ice-cold lysis buffer with 10% DMSO in dark for 1 hour. After lysis, the slides were rinsed three times in a fresh ice-cold lysis buffer and proceeded in a neutral comet assay for 20 minutes in a 1V/cm constant voltage. After electrophoresis, the slides were rinsed in ddH_2O, soaked in a 100% ethanol and air-dried. For visualization, the DNA was stained by a 10 μM SYBR Gold staining solution (Trevigen). After brief washing in PBS, VECTASHIELD medium (Vector Laboratories, Burlingame, CA, USA) was used for the final mounting of slides. Cells treated by 0.05% H_2O_2 for 30 s were used as a positive control. The slides were analyzed using BX41 fluorescent microscope (Olympus) equipped with ProgRes MF cool CCS camera (Jenoptik AG). Automated exposure, image quality control, and other procedures were performed using NIS-Elements software (Laboratory Imaging). At least 30 pictures were captured for each sample. The CometScore ver. 1.5 software (AutoComet) was used for the analysis of the mean tail moment.

3.2.2 Fluorescence immunohistochemistry and confocal microscopy of IRIF

Cell were seeded onto the microscope slides and incubated under the standard cultivation conditions for 12 hours before irradiation and consequent processing. A non-irradiated cells (marked here as a 0 min) and cells in the particular times (5, 30, 60, 120, 240 and 1440 min) after irradiation with 1.5 Gy of γ-rays (^{60}Co; 1.0 Gy/min) were washed two times in PBS for 2 min, fixed with 4% formaldehyde in PBS for 10 min at RT, washed three times in PBS, permeabilized with 0.2% Triton X100/PBS for 14 min, and washed three times for 5 min in PBS. Prior to incubation with primary antibody, the cells were blocked with 7% inactivated FCS+2% bovine serum albumin/PBS (Sigma-Aldrich) for 30 min at RT. To detect two different proteins in the same nuclei, the cells were subsequently incubated overnight at 4°C with primary antibodies from two different host animals [anti-phospho-H2AX(serine 139) from Upstate Biotechnology (Lake Placid, NY, dilution 1:500), and anti-53BP from Cell Signaling (dilution 1:500), and anti BRCA1, clone M4C7, from Millipore (MA, USA, dilution 1:500) respectively]. Secondary antibodies were affinity purified FITC conjugated donkey anti-mouse (dilution 1:100) and Cy3-conjugated donkey anti-rabbit (dilution 1:200) from Jackson Laboratory (West Grove, PA). The mixture of both antibodies was applied to each slide (after their pre-incubation with 5.5% donkey serum/PBS for 30 min at RT) and incubated for 1 hour in the dark at RT. This was followed by washing three times for 5 min in PBS. Cells were counterstained with 1 μM TOPRO-3 (Molecular Probes, Eugene, USA) in saline sodium citrate (SSC) prepared fresh from a stock solution. After brief washing in SSC, Vectashield medium (Vector Laboratories, Burlingame, CA, USA) was used for the final mounting of slides. An automated Leica DM RXA fluorescence microscope, equipped with a CSU10a Nipkow disc (Yokogawa, Japan) for confocal imaging, a CoolSnap HQ CCD-camera (Photometrix, Tucson, AZ, USA) and an Ar/Kr-laser (Innova 70C, Coherent, Palo Alto, CA) and an oil immersion Plan Fluotar objective (100×/NA1.3) was used for image acquisition (Fig. 12).

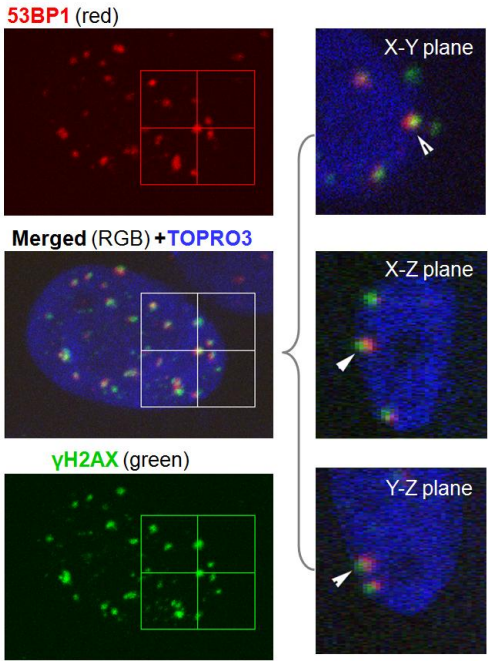

Figure 12: A preservation of the 3D structure of a nuclei analyzed by a high-resolution immuno-fluorescence confocal microscopy. *Intranuclear localization of γH2AX (**green**) and 53BP1 (**red**) signals and their mutual co-localization in all three planes is demonstrated at the maximal images (composed from 40 confocal slices taken with a z-step 0.2 μm; left panels) as well as individual confocal slices in all three planes (x-y, x-z and y-z; right panels). The positions of the planes are indicated at the maximal images by a white cross; the γH2AX/53BP1 focus located in the intersection of x-y, x-z and y-z planes is marked by an arrow at confocal slices (right panels). Nuclear chromatin was counterstained by TOPRO-3 (**artificially blue**).*

3.2.3 A mitomycin C sensitivity assay

Cell were seeded onto the E plate 96 (Roche) in a density of $3x10^4$ cells per well in triplicates and grown for 24 hours under standard cultivation conditions. Subsequently, mitomycin C (Sigma-Aldrich) was added to the final concentration of 0, 2; 4; 6 and 8 μg/ml and cells were grown for an additional 5 days with continual measuring of the cell index (CI; derived as a relative change in measured electrical impedance to represent cell status, for details see: *https://www.roche-applied-science.com/sis/xcelligence/index.jsp?*) using an xCELLigence RTCA analyzer (Roche). The RTCA software ver. 1.2 (Roche) was used for the analysis of cell's proliferation and dose response curves.

3.2.4 *In vitro* NHEJ assay

The NHEJ capacity was assayed by measuring the recovery of lucipherase activity in the cells co-transfected by the pGL-control (Promega) vector linearized by either HindIII (overall NHEJ) or EcoRI (precise NHEJ), and by the circular pRL-tk vector as an internal control [219]. The cells were grown in triplicate under the standard cultivation conditions and co-transfected by 0.5 μg of a pure linearized pGL-control vector together with 0.05 μg

of a pRL-tk vector using Lipofectamine 2000 (Invitrogen). The lucipherase activity was scored by the Dual lucipherase reporter assay (Promega) 48 hours after transfection. Cells were rinsed by PBS and lysed directly on the well using Cell lysis solution (Promega) for 15 minutes at RT. Cell suspension was spun down and 10 µl of total cell lysate were mixed with 10 µl of freshly-prepared Lucipherase assay solution A (Promega) and immediately measured on the GloMaxR 96 Luminometer (Promega) for 10 seconds with a starting temperature 23°C. Next, 10 µl of freshly prepared STOP and Glow solution (Promega) were added to the reaction mix in a reader 96 well plate and measured immediately using the same protocol. Non-transfected MCF-7 cells were used as a negative control. Activity of rescued pGL lucipherase activity was normalized to the pRL lucipherase activity. Cells treated with 2 mmol benzamide (Roche), a potent PARP-1 inhibitor, 48 hours prior to the transfection were used as a control of assay functionality.

The functionality of used assay was proved using a benzamide as a potent NHEJ inhibitor. Non-transfected MCF-7 cells treated with increasing concentration of benzamide exerted proportionally decreased NHEJ activity (Fig. 13). The most effective concentration was 2.5 mmol/l. Concentrations of benzamide higher than 2.5 mmol/l were lethal.

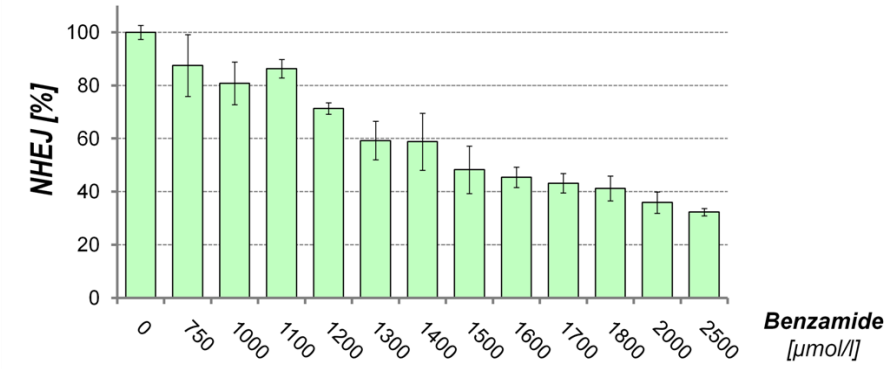

Figure 13: Inhibition of NHEJ by the benzamide. *The non-transfected control MCF-7 cells were grown in triplicates and treated by different concentrations of benzamide 48 hours prior a transfection by the pGL-control vector. The NHEJ activity was determined as described in the Material and Methods section. Benzamide as a potent inhibitor of PARP-1 proved the functionality of the in vitro NHEJ assay.*

3.2.5 Clonogenic assays

The clonogenic (colony survival) assay was used for the determination of clonal viability and radiation sensitivity of MCF-7 based clones with modified expression of BRCA1. Cells were cultivated under the standard cultivation conditions until 90% of subconfluency and then treated with a single dose of γ-radiation (0, 1 and 5 Gy; ^{60}Co 1 Gy/min). After the 2 hours of recovery, the cells were released from the cultivation dish surface using trypsin/EDTA solution, diluted in a cultivation medium and seeded onto the new 3 cm∅ Petri dish in duplicates in the exact amount (100 – 200 cells per dish). Cells were cultivated under the standard cultivation conditions for 10 days with replacement the cultivation medium every third day. After 10 days, the cells were stained using the crystal violet staining protocol (as described in *3.2.6. Proliferation assay*) and colonies containing at least 10 cells were counted manually in optical microscope. The absolute plating efficiency (PE) of particular clones for different doses of ionizing γ-radiation was counted as a number of colonies containing more than 10 cells, while the number of seeded cells was taken as a 100%. After the counting of number of colonies, the crystal violet was extracted and the absorbance was measured (as described in *3.11. Proliferation assay*). The surviving fraction (SF) of particular clones cells for different doses of ionizing γ-radiation was calculated as a relative absorbance to the control (non-transfected MCF-7 cells).

3.2.6 Proliferation assay

Clones expressing the particular BRCA1 alternative splicing variant with relevant controls were seeded onto the 24 well plate in the density $2x10^5$ cells/well in triplicates and grown under the standard cultivation conditions for 24 hours. Then were cells irradiated by a single dose (0, 1, 3 and 5 Gy) of γ-rays (^{60}Co; 1.0 Gy/min). In a day 0, 4, 5, 6 and 7 after the irradiation, the cells were rinsed once with PBS and fixed by 10% aqueous solution of formaldehyde for 30 min at 37°C, rinsed briefly by PBS and stained by a solution of 0.1% crystal violet in 10% ethanol for 30 min at 37°C. Stained cells were extensively rinsed with water and plates were dried. The dye was extracted with 1 ml of 10% acetic acid and an absorbance of solution was measured at λ = 590 nm. Staining an empty well without cells was used as blanks. Data were plot as a relative absorbance ratio to a day 0. To rule out the influence of BRCA1 upstream signaling to the possibly altered proliferation of the MCF-7 clones after the ionizing radiation-induced DNA damage, the cells were treated by the ATM inhibitor caffeine at concentration of 1 mmol/l for 48 hours prior to irradiation. The

population doubling time (G) of particular clones was calculated from the growth curves using the formula:

$$G = t*log2/(logN_t - logN_0)$$

Where t is the time period, N_t is the number of cells at the time t and N_0 is the initial number of cells within the time period t. The angular coefficient (k) of particular growth curves was calculated from a linear regression and an equation calculation using Excel spreadsheet (Microsoft).

3.2.7 Statistical analysis

A statistical analysis was done using the non-parametric ANOVA (Wilcoxon two sample test) using Excel spreadsheet. $P < 0.05$ was considered statistically significant. All data are presented as mean ± standard deviation.

4 RESULTS

4.1 A model system for functional analysis of BRCA1 alternative splicing variants

The pcDNA3.1 BRCA1Δ14-15 and pcDNA3.1 BRCA1Δ17-19 expression constructs were prepared by a PCR splicing approach with a direct ligation into the expression pcDNA3.1 Hygro vector (Fig. 14).

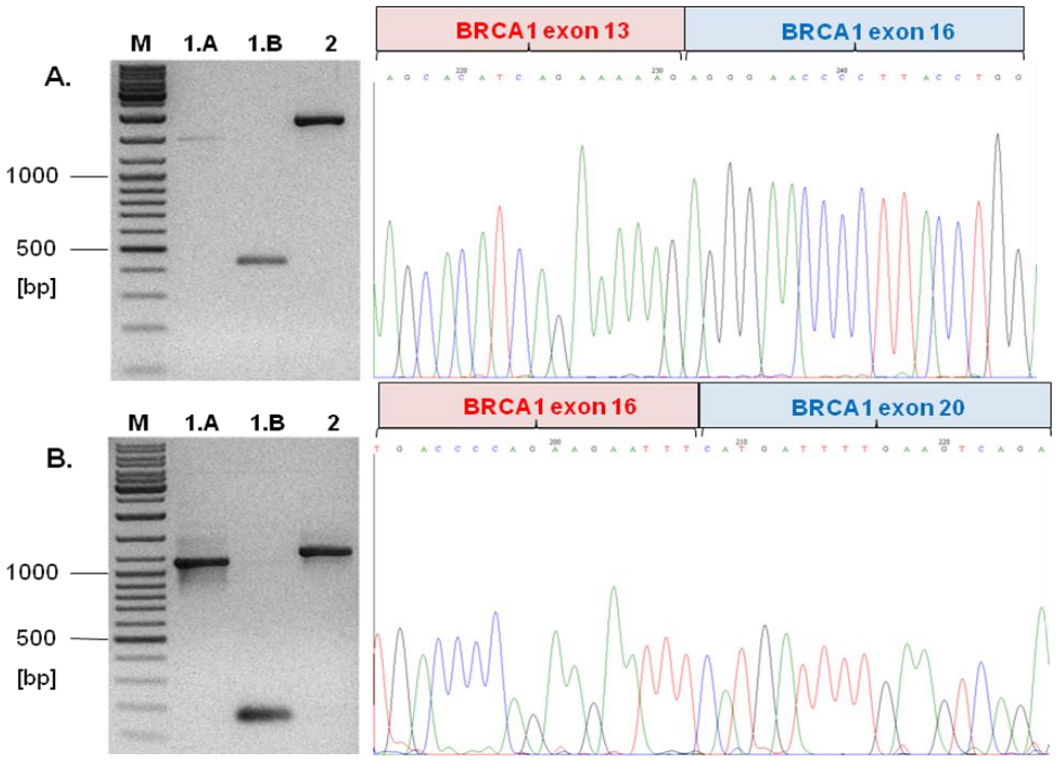

Figure 14: Construction of BRCA1 inserts using a PCR splicing approach. *The products of the first PCR (**1.A** and **1.B**) were linked together in the second PCR (**2**), digested using BamHI/XhoI and ligated into the pcDNA3.1 wtBRCA1 resulting in pcDNA3.1 BRCA1Δ14-15 (**A**), and pcDNA3.1 BRCA1Δ17-19 (**B**) expression constructs respectively.*

A stable human breast adenocarcinoma-derived cell line MCF-7 expressing BRCA1 +/+ was used as an *in vitro* model system. With respect to the further experimental purposes, clones with expression constructs fully integrated into the MCF-7's genome ensuring stable

expression of BRCA1 variants were prepared. The calcium-phosphate transfection with subsequent long term selection was chosen as reliable and reproducible method. Cells were first transfected by a pcDNA3.1 Hygro-based expression constructs enabling the overexpression of studied BRCA1 alternative splicing variants with endogenously expressed wtBRCA1. To assess the biological effect of studied BRCA1 alternative splicing variants (BRCA1Δ14-15 and BRCA1Δ17-19) solely, MCF-7 clones combining the expression of analyzed BRCA1 splicing constructs together with a shRNA-mediated downregulation of endogenous wtBRCA1 were prepared. A highly specific downregulation of expression of endogenous wtBRCA1 only was achieved by a human H1 promoter-driven expression of interfering shRNAs targeting the BRCA1 coding sequences lacked in the examined BRCA1 splicing variants. To rule out the nonspecific effect of transfection procedure and construct's integration into the host genome, three stable MCF-7 clones of each engineered expression construct were further examined. The stable MCF-7 clones expressing used shRNAs only, irrelevant shRNAs (targeted to mouse CEBPγ), empty pSUPER and pcDNA3.1 vectors, and non-transfected MCF-7 cells were used as controls for functional analyses.

The integration into the MCF-7 genome was proved by a PCR using gDNA as a template Fig. 15.A-B). Results of RT-PCR (Fig. 15.C), qPCR (Fig. 15.D-E) and WB analysis (Fig. 15.F-G) in the stably transfected clones in the two consecutive passages proved functionality of the model system and temporal stability of the modification of BRCA1 expression on both mRNA, and protein levels respectively. By the interfering shRNA, the expression of endogenous wtBRCA1 mRNA was downregulated up to 10% of its normal level (for sh5196; normalized to GAPDH). The total BRCA1 expression in the combined clones was 95% (in the case of BRCA1Δ14-15; normalized to the GAPDH), and 80% (in the case of BRCA1Δ17-19; normalized to the GAPDH) of the control MCF-7 cells BRCA1 expression level, respectively. The modification of BRCA1 expression on the mRNA level correlated directly with the results of quantitative WB (Fig. 15F). The small difference in a molecular weight between full-length BRCA1 and BRCA1Δ14-15 and BRCA1Δ17-19 (207.7 kDa vs.195.9 kDa and 199.6 kDa, respectively[4]) disabled to distinguish endogenous wtBRCA1 and expressed splicing variants on the protein level.

[4] Theoretical molecular weight calculated using Sequence Manipulation Suite (http://www.bioinformatics.org/sms2/).

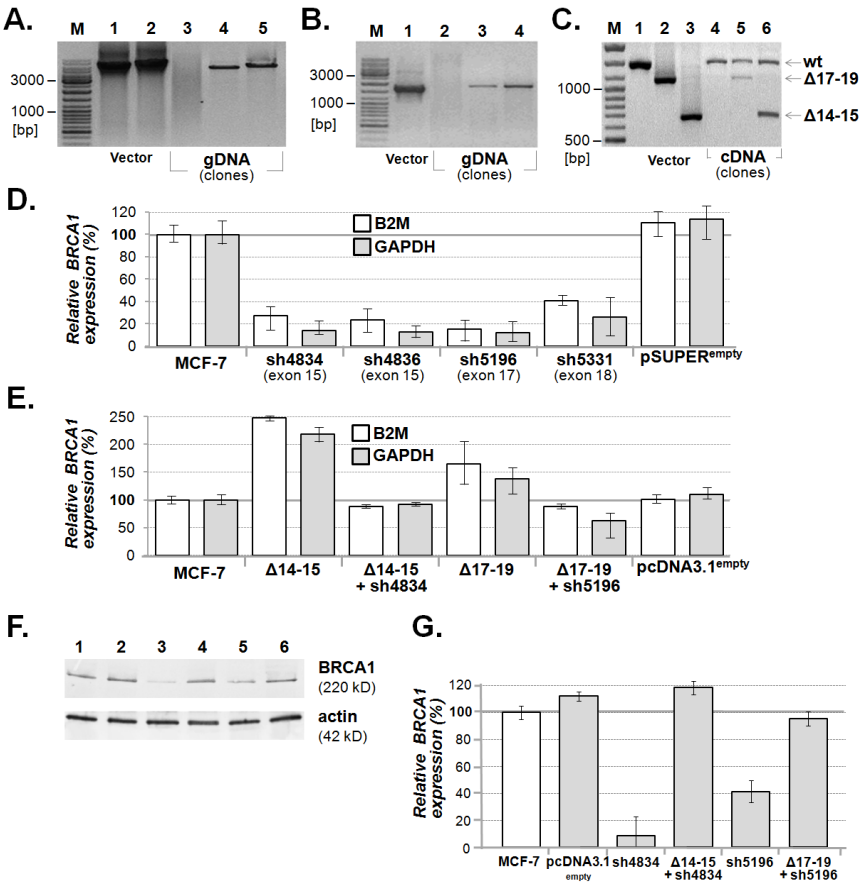

Figure 15: Modulation of a BRCA1 expression in model MCF-7 clones. *Using a two-step transfection and selection of single cell colonies, a set of stable MCF-7 clones with a modified expression of BRCA1 was prepared. The full integration of pcDNA3.1-based (**A**) and pSUPER-based (**B**) expression constructs into the MCF-7 genome was proven by PCR using a gDNA from particular clone as a template [**lanes: A**: (**1**). pcDNA3.1 BRCA1Δ14-15 (**2**) pcDNA3.1 BRCA1Δ17-19, (**3**) gDNA from non-transfected MCF-7 cells, (**4**) gDNA from MCF-7 clone transfected by the pcDNA3.1 BRCA1Δ14-15 and (**5**) pcDNA3.1 BRCA1Δ17-19 expression constructs]. [**lanes: B**: (**1**) pSUPER sh4834, (**2**) gDNA from non-transfected MCF-7 cells, (**3**) MCF-7 clone transfected by the pSUPER shRNA4834 and (**4**) pSUPER shRNA5196 expression constructs]. (**C**) The upregulated expression of the BRCA1Δ14-15 and BRCA1Δ17-19 alternative splicing variants alongside the endogenous wtBRCA1 was proved by rt-PCR on the RNA level [**lanes**: (**1**) pcDNA3.1 vector carrying full-length BRCA1 insert, (**2**) the BRCA1Δ14-15 and (**3**) BRCA1Δ17-19 variants, (**4**) cDNA prepared from non-transfected MCF-7 cells, (**5**) stable clone expressing the BRCA1Δ14-15 and (**6**) BRCA1Δ17-19 variants]. (**D, E**) A long-term modulation of the BRCA1 expression was checked by qPCR using the cDNA templates prepared from mRNAs isolated from particular clones in two different passages. The expression of BRCA1 on the mRNA level was quantified by qPCR using GAPDH and B2M as reference genes. (**D**) The endogenous wtBRCA1 was specifically downregulated by shRNAs up to <10% relative to control cells [pSUPER vector]. (**E**) Upregulation of the BRCA1Δ14-15 variant expressed in stable MCF-7 clones without (Δ14-15; Δ17-19) and with (Δ14-15+sh4834; Δ17-19+sh5196) coincidentally downregulated wtBRCA1 in comparison to non-transfected MCF-7 (= 100%) and MCF-7 transfected by an empty pcDNA3.1 vector. (**F**) The expression of BRCA1 on the protein level was quantified by WB using β-actin as a protein loading control. (**G**) The relative level of BRCA1 protein expression was scored using UN-SCAN-IT gel ver. 6.1 software.*

4.2 Functional analysis of BRCA1 alternative splicing variants

4.2.1 The BRCA1Δ14-15 and BRCA1Δ17-19 splicing variants slow down the overall DDSB repair

Both protein structural motifs, the SCD lacking in BRCA1Δ14-15, and first of tandem BRCT lacking in BRCA1Δ17-19, were shown to be important determinants of BRCA1 activity in the DNA repair process [220,16,221]. With regard to that, we first examined whether the expression of these BRCA1 alternative splicing variants influences the DNA repair capacity in MCF-7 cells. A time course of DNA damage level was directly scored by a comet assay after a single 1.5 Gy dose of γ-radiation (Fig. 16.B) [222].

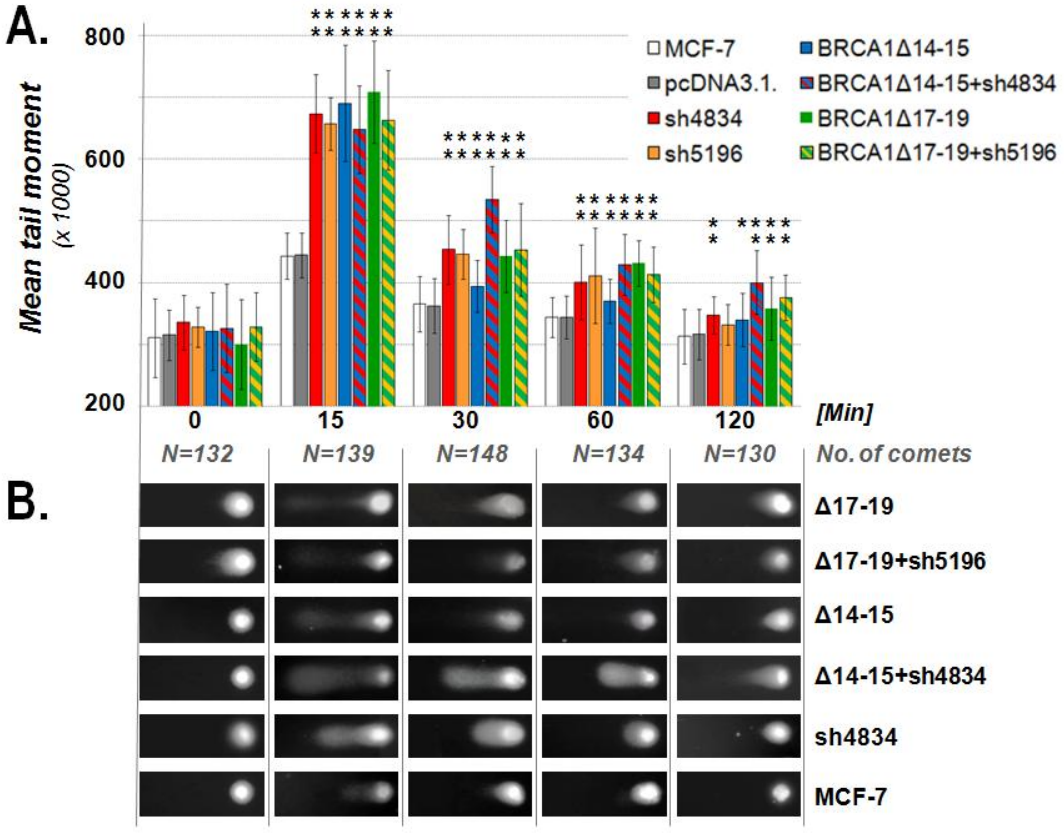

Figure 16: DNA damage time-course in clones with a modified BRCA1 expression after the γ-irradiation. *A neutral comet assay was used for the determination of DNA damage level. (**B**) For each analyzed clones were captured pictures of comets using a fluorescence microscopy in times 0; 15; 30; 60, and 120 minutes PI. (**A**) For a DDSB repair time course quantification, the comet mean tail moment was calculated using a CometScore ver. 1.5 software (AutoComet). Non-irradiated samples are represented as time 0. Data are mean ± S.D. *p<0.05, ** p<0.001 (Wilcoxon test).*

This dose of ionizing radiation was chosen considering the experimental procedure and used methods, as in MCF-7 cells, the 1 Gy of γ-radiation causes approximately 30 DDSB per nucleus. This amount is the most suitable for the reliable determination of DDSB repair capacity and kinetics [40]. Due to the time-consuming sample preparation, the firstly analyzed time was 15 min PI and further in 30, 60, and 120 minutes PI respectively. In all analyzed cells, the peak DNA damage was detected at the time of 15 minutes PI with significant differences in the rate of DNA damage between controls and clones with modified BRCA1 expression (Fig. 16.A). In control cells, the degree of the DNA damage decreased progressively over the further analyzed time period reaching the level comparable to the initial DNA damage rate in the time 120 min PI. In the clones with modified BRCA1 expression, the DNA repair velocity was slower though the differences in the degree of DNA damage between controls and clones with modified BRCA1 expression decreased during the examined time period. However, at the time of 120 min PI, the DNA damage rate was still significantly higher in all clones with modified BRCA1 expression compared with controls, except the clone expressing shRNA5196. There were not detected significant differences in the DNA repair time course between clones with downregulated expression of wtBRCA1 and clones with overexpressed BRCA1Δ14-15 and BRCA1Δ17-19 alternative splicing variants.

These results showed that both downregulation of wtBRCA1 or overexpression of BRCA1Δ14-15 or BRCA1Δ17-19 splicing variants slows down the DDSB repair particularly in the initial phase after the DNA damage. Moreover, the presence of either of examined BRCA1 splicing variants interferes with the activity of wtBRCA1 in a dominant-negative fashion.

4.2.2 Kinetics of IRIF formation is influenced by BRCA1Δ14-15 and BRCA1Δ17-19 splicing variants after ionizing radiation-induced DNA damage

Assuming the main role of BRCA1 as a central protein-interaction modulator in orchestration of the DNA damage response, we next examined whether the BRCA1Δ14-15 or BRCA1Δ17-19 splicing variants influence the kinetics of IRIF formation. For this purpose, we scored the *in vitro* co-localization of γH2AX with 53BP1 (Fig. 12) using the immunofluorescence confocal microscopy [223]. Compared to the neutral comet assay, this DNA damage assessment is more sensitive and allows us to exactly determine the level of endogenous DNA damage and the time course of DDSB repair on a molecular level (Fig.

17). Within seconds after the DNA damage, histone H2AX is phosphorylated at Ser 139 in about 2-Mbp region around the DDSBs, forming so called γH2AX foci that are generally considered as a specific and the sensitive markers of this type of DNA lesion. The 53BP1 protein was used for the visualization of IRIFs with regards to its unequivocal co-localization with γH2AX foci within a few minutes PI, irrespective of further DDSB repair pathway. Moreover, in comparison to BRCA1, the 53BP1 foci are more precisely distinguishable from the background. The number of γH2AX/53BP1 foci was determined in different times after the same single dose of 1.5 Gy of γ-radiation as in the previous experiment and in non-irradiated clones. As all analyzed clones originated from the identical MCF-7 line, it could be expected that the γ-irradiation induces an identical initial number of DDSBs.

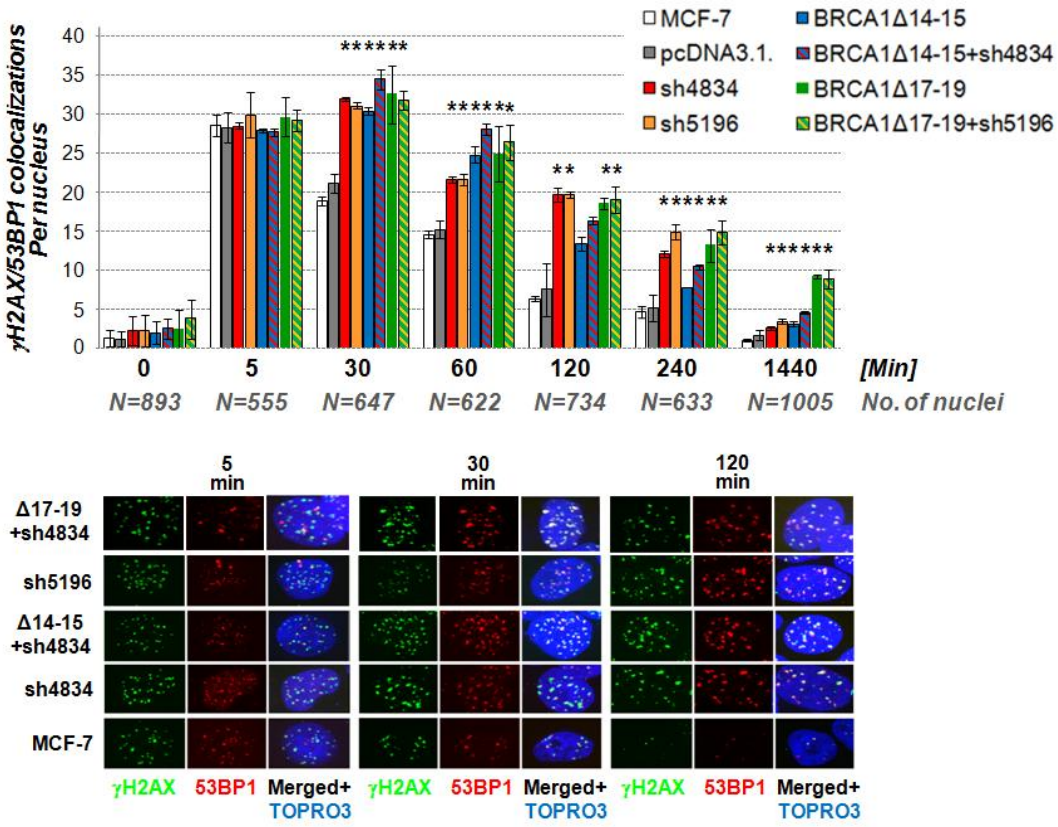

Figure 17: Time course of IRIF number. *The levels of DDSB were (**A**) determined by counting the number of the co-localizations of γH2AX (green) and 53BP1 (red) proteins characterizing an early response to DSB in spatiotemporal manner in times of 5, 30, 60, 120, 240, and 1440 minutes PI using high-resolution fluorescent confocal microscopy (**B**). Maximal images composed from 40 confocal optical slices taken with a z-step of 0.2 μm are shown. Total nuclear chromatin was counterstained by TOPRO-3 (artificially blue). Data are mean ± S.D., N = total number of analyzed comets in group. *p<0.05 (Wilcoxon test).*

Under the standard cultivation conditions, the rate of endogenous DNA damage was higher in clones with downregulated expression of wtBRCA1 (sh4834; sh5196) and in clones expressing the alternative splicing variants BRCA1Δ14-15 (Δ14-15 and Δ14-15+sh4834) or BRCA1Δ17-19 (Δ17-19 and Δ17-19+sh5196) variants (Fig. 17, time 0). This suggests that low expression of full-length BRCA1 as well as overexpression of BRCA1Δ14-15 or BRCA1Δ17-19 slightly increases the level of endogenous DNA damage and could thus contribute to the genome instability in model MCF-7 clones.

Following the γ-irradiation, the maximal number of γH2AX/53BP1 foci in controls was detected at the time of 5 minutes PI. A dissociation of γH2AX/53BP1 foci was apparent since that time as the number of foci progressively decreased over the entire analyzed time period (Fig. 16).

In MCF-7 clones expressing the BRCA1Δ14-15 (Δ14-15 and Δ14-15+sh4834) or BRCA1Δ17-19 variant (Δ17-19 and Δ17-19+sh5196) with coincidentally downregulated expression of wtBRCA1 (sh4834 and sh5196), the number of IRIFs further increased at the time beyond 5 minutes PI reaching the peak values at the time of 30 minutes PI (Fig. 17). In all clones with modified expression of BRCA1, the number of IRIF successively decreased since the time of 30 minutes PI, however, the initial delay (compared with control cells) was sustained throughout the overall analysis period. The slowest decomposition of γH2AX/53BP1 foci was registered in the clones expressing BRCA1Δ17-19 variant. The difference between the number of persisted IRIF in clones expressing BRCA1Δ17-19 variant, other clones with modified BRCA1 expression, and control cells was most apparent at 24 hours (1440 min) PI.

If the kinetics of IRIF formation was expressed as a percentual increase or decrease in their number relative to the number of IRIFs at the time 5 min PI (Fig. 18), the results will show that the majority (more than 80%) of the DNA lesions is repaired within first 120 minutes PI in control cells. The rest of the persisted IRIF was repaired within subsequent 1220 minutes. From the IRIF kinetics point of view, the DDSB repair can be thus subdivided into two main phases. i) The rapid one, represented by the fast dismantle of IRIF within the first 120 minutes PI, and ii) the slow one, represented by a deliberate decomposition of the rest of persisted IRIF (Fig. 16). The rapid phase of the DDSB was significantly harmed in all clones with BRCA1 modified expression as the number of IRIF increased after the 5 minutes PI, reaching its peak value at 30 minutes PI. In cells with overexpressed BRCA1 splicing variant BRCA1Δ14-15 (Δ14-15 and Δ14-15+sh4834), the kinetic of IRIF dismantle correspond to

the control cells after the 30 minutes PI. In cells with downregulated expression of wtBRCA1 (sh4834 and sh5196) kinetic of IRIF dismantle also correspond to the control cells after the 30 minutes PI, however, there was a secondary deceleration of IRIF dismantle notable between 60 to 120 minutes PI. In cells with overexpressed BRCA1 splicing variant BRCA1Δ17-19 variant (Δ17-19 and Δ17-19+sh5196), the kinetics of IRIF decomposition was slowest without any different phases apparent in control cells.

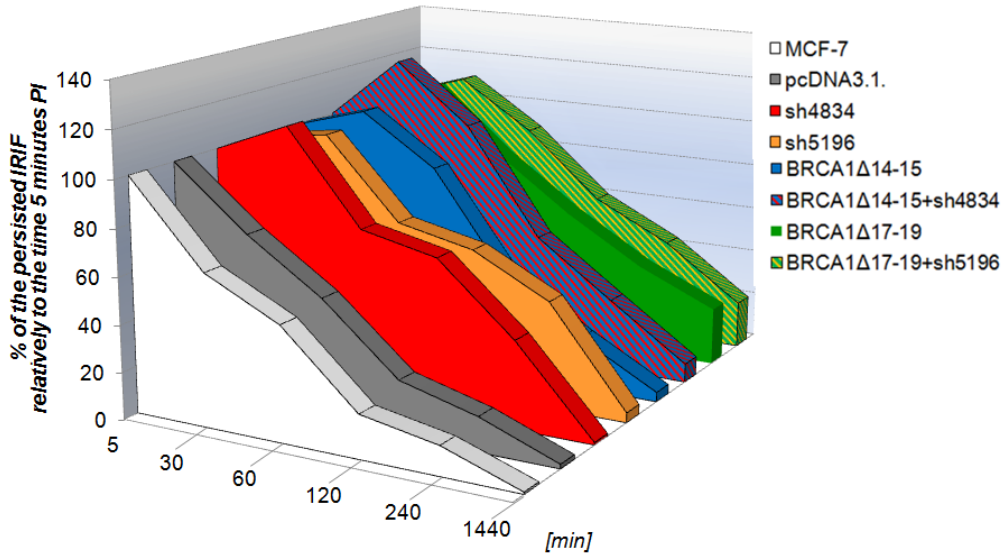

Figure 18: The kinetics of γ-radiation induced DNA damage. *The kinetics of DDSB was counted as a* ***percentual (%)*** *decrease/increase of the number of γH2AX/53BP1 co-localizations relative to the number of IRIF in the time of 5 minutes PI. In the controls non-transfected MCF-7 cells and cells transfected by an empty pcDNA3.1 vector there are apparent two phases of IRIF dismantle, the rapid one in the first 120 minutes PI and the slow one, from 120 to 1440 minutes PI. The modification of BRCA1 expression significantly altered the first rapid phase of DDSB, while the second one is comparable to controls.*

These results show that either downregulation of wtBRCA1 or overexpression of any of studied BRCA1 splicing variants impairs the kinetics of formation of IRIF compared with controls. In either of BRCA1Δ14-15 or BRCA1Δ17-19 splicing variant, the effect on slower IRIF formation was independent on the presence of wtBRCA1 indicating that neither of analyzed splicing variants is able to functionally substitute for wtBRCA1 in the process of the γH2AX/53BP1-containing DNA repair protein complexes formation. In concord with the

previous comet assays, the most obvious difference in the DDSB level between control and clones with modified expression of BRCA1 appears at the time 30 minutes PI. The kinetics of IRIF decomposition was significantly decreased during the first rapid phase (within the first 120 minutes PI) in the clones with modified expression of BRCA1, while the second phase was comparable to the controls. The most prominent impairment of IRIF decomposition was seen in BRCA1Δ17-19 variant suggesting the ultimate importance of BRCA1 BRCT domain-mediated protein/protein interaction for DDSB repair. Finally, our results support the evidence about the importance of BRCA1 on the process of IRIF formation during both initial as well as delayed phases of DDSB repair.

4.2.3 The BRCA1Δ14-15 and BRCA1Δ17-19 splicing variants selectively change the sensitivity of cells to mitomycin C

It has been documented, that BRCA1 protein directly participates on the process of HR. Mitomycin C causes DNA interstrand covalent cross-links repaired exclusively by HR. Thus, the sensitivity of cells to mitomycin C treatment indirectly reflects the HR capacity. With respect to the previous results, we further examined the response of MCF-7 clones with a modified expression of BRCA1 to the different concentrations of mitomycin C on the proliferation level (Fig. 19).

Based on the results of growth curves and the EC-50 calculated from a dose response curve (Tab. 4), we concluded that clones with a shRNA-downregulated expression of wtBRCA1 were the most sensitive to mitomycin C as the lowest used mitomycin C concentration (2 μg/ml) was closed to lethal. Significantly increased sensitivity to mitomycin C was also observed in cells expressing the BRCA1Δ17-19 splicing variant alone or together with wtBRCA1. On the contrary, the sensitivity of clones expressing the BRCA1Δ14-15 splicing variant alone or together with wtBRCA1 was comparable with controls.

Table 4: *The effective concentration (EC-50) of mitomycin C for MCF-7 clones with modified expression of BRCA1. The EC-50 was calculated at a time point of 64 hours from the seeding of cells to the plate as a cell index at a time point versus concentration. Data are means from triplets ± S.D.*

Clone	MCF-7	pcDNA3.1	shRNA 4834	shRNA 5196	Δ14-15 +sh4834	Δ14+15	Δ17-19	Δ17-19 +sh5196
EC-50 [μg/ml]	6.18 ±0.18	6.06 ±0.23	2.88 ±0.11	2.89 ±0.27	6.21 ±0.43	5.85 ±0.55	4.02 ±0.71	3.60 ±0.2

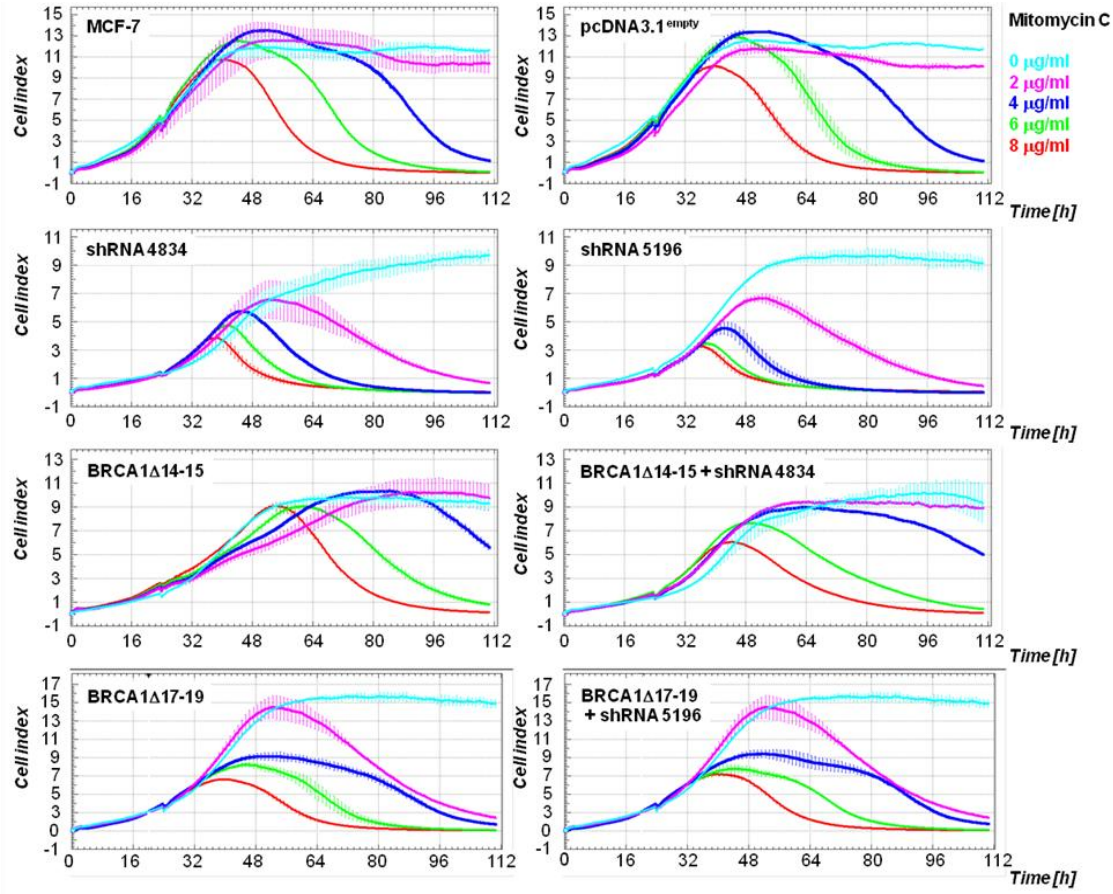

Figure 19: The sensitivity of MCF-7 clones with modified expression of BRCA1 to the mitomycin C. *Cells were cultivated for 5 days in the medium with different concentrations of mitomycin C (0, 2, 4, 6, and 8 µg/ml) with continual measurement of proliferation activity expressed here as a cell index (CI) using xCELLigence RTCA analyzer. The CI was normalized to the time of addition of mitomycin C. Clones with shRNA-mediated downregulation displayed expected hypersensitivity to mitomycin C. The sensitivity of clones with upregulated expression of BRCA1Δ17-19 was increased in comparison with controls, while the sensitivity of cells expressing the BRCA1Δ14-15 alternative splicing variant were comparable to non-transfected MCF-7 and controls transfected with an empty expression vector. Data are mean ± S.D.*

These results are consistent with previously published findings [224] that a downregulation of wtBRCA1 impairs the HR pathway and causes hypersensitivity to the DNA cross-linking agents. A similar phenotype exerts the cells expressing variant BRCA1Δ17-19 lacking first BRCT domain. This suggests that this variant significantly impairs HR, however, the exposure of the BRCA1Δ17-19 clones to mitomycin C was not as detrimental as in the case of complete downregulation of wtBRCA1. On the other hand, the BRCA1Δ14-15 splicing variant did not influence mitomycin C sensitivity. This suggests that unlike the depletion of wtBRCA1, or overexpression of the BRCA1Δ17-19, the BRCA1Δ14-15 alternative splicing

variant does not substantially impair the HR and indicates that loss of phosphorylation targets coded by exons 14 and 15 is dispensable for BRCA1-mediated HR repair.

4.2.4 The activity of NHEJ is decreased in clones with modified expression of BRCA1

Negative effect of BRCA1 inactivation on capacity and fidelity of DDSB repair has been described in both pathways - HR and NHEJ [224,73,81]. Hence, after finding that the cells expressing BRCA1 alternative splicing variants have decreased DNA repair capacity, however, exert differential sensitivity to the DNA cross-linking, we further analyzed the influence of the analyze BRCA1 alternative splicing variants on NHEJ. We used the indirect *in vitro* assay based on measurement of the lucipherase activity recovery from pGL-control expression vector linearized prior to its transfection to model clones. The unique HindIII and EcoRI restriction sites lay within the promoter and lucipherase coding sequence, respectively. The overall NHEJ activity is represented by joining of free DNA ends in HindIII-linearized vector as the expression of lucipherase is conditioned by vector recircularization regardless of possible loss of several bases in lucipherase promoter region during imprecise NHEJ. On the contrary, only precise joining of EcoRI-linearized vector by precise NHEJ ensures the expression of functional lucipherase as loss of several bases during imprecise NHEJ results in introduction of frame-shifting mutation with synthesis of truncated nonfunctional lucipherase.

The activity of both overall and precise NHEJ was significantly lower in all examined clones with downregulated expression of wtBRCA1, and expression of BRCA1Δ14-15 or BRCA1Δ17-19 splicing variants compared with controls (Fig. 20).

Though the activity of precise NHEJ was reduced in clones with modified expression of BRCA1, the decrease was proportional as the ratio of overall to precise NHEJ was not significantly distinct from controls. In all clones the precise NHEJ constituted from 20% (for shRNA4834, BRCA1Δ14-15, MCF-7 and pcDNA3.1^{empty};) to 25% (for shRNA 5196 and BRCA1Δ14+15 +shRNA 4834) of the overall NHEJ activity. The only exception constituted clones expressing the BRCA1Δ17-19 splicing variants with or without coincidentally downregulated endogenous wtBRCA1. The precise NHEJ accounted only 10% of overall NHEJ activity and was thus decreased in comparison with controls and other analyzed clones (Tab. 5).

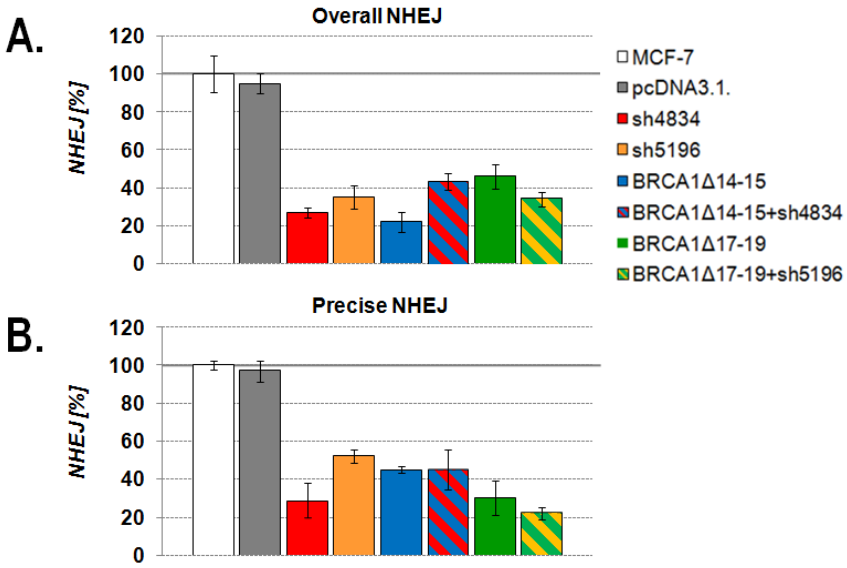

Figure 20: NHEJ activity in clones with a modified expression of BRCA1. *The particular clones and relevant controls were co-transfected by a linearized pGL-control vector and a circular pRL-tk vector. Forty-eight hours after transfection, the rescued activity of glow worm (pGL) lucipherase was measured by luminometer in triplicates using the dual lucipherase assay kit. The measured pGL lucipherase activity was normalized to the activity of control pRL-tk lucipherase. The lucipherase activity rescued from the EcoRI linearized pGL-control vector (**A.**) reflects the **precise NHEJ**, while that from the HindIII linearized pGL-control vector (**B.**) reflects the **overall NHEJ**. The experiment was repeated three times. Data are mean ± S.D.*

Table 5*: The percentual ratio of precise to overall NHEJ activity in MCF-7 cells. The overall NHEJ activity is taken as a 100%. Data are mean ± S.D.*

Clone	Precise to overall NHEJ percentual ratio (%) ± S.D.
MCF-7	18.55 ± 1.21
pcDNA3.1^{empty}	19.77 ± 0.97
shRNA 4834	19.66 ± 3.12
shRNA 5196	27.65 ± 6.79
BRCA1Δ14-15	27.87 ±4.67
BRCA1Δ14-15 + shRNA 4834	19.26 ± 2.37
BRCA1Δ17-19	12.22 ± 2.61
BRCA1Δ17-19 + shRNA 5196	11.91 ± 2.01

These results indicate that expression of all of examined BRCA1 splicing variants has dominantly-negative effect on the activity and fidelity of NHEJ comparable to the shRNA-mediated downregulation of wtBRCA1.

4.2.5 Overexpression of the BRCA1Δ14-15 or BRCA1Δ17-19 alternative splicing variants influences the viability and radiation sensitivity of MCF-7 cells.

After finding that BRCA1 alternative splicing variants decrease the efficiency of DDSB repair, we further examined whether modifications of the BRCA1 expression can influence vital and growth characteristics of MCF-7-based stable clones. A clonogenic assay was used to evaluate the possible effect of the BRCA1Δ14-15 or BRCA1Δ17-19 alternative splicing variants on the viability and radio-sensitivity of MCF-7 clones. The clonogenic assay has become the most widely accepted technique in radiation biology for an assessment of the differences in reproductive viability (capacity of cells to produce progeny; i.e. a single cell to form a colony of 50 or more cells expressed by the plating efficiency) and for an evaluation of the radiation sensitivity of different cell lines expressed as a relative surviving fraction. Cells of clones with modified BRCA1 expression were treated by a single dose of ionizing γ-radiation (1 and 5 Gy) and seeded in a dilution ensuring the formation of single cell colonies. After 10 days of cultivation, the plating efficiency (PE) and surviving fraction (SF) of cells were determined by a crystal violet staining. In this assay, the plating efficiency (number of colonies containing more than 10 cells) reflects the viability of particular clones under the standard conditions and upon γ-radiation DNA damage, while the average number of cells per colony is an indirect marker of the cell proliferation and radiation sensitivity.

Under the standard cultivation conditions, the highest plating efficiency was scored in the control non-transfected MCF-7 cells and in the cells transfected by an empty expression vector (tab. 6). Compared with that, the plating efficiency of clones with stably modified expression was generally lower, though there were relatively high differences between different clones of one particular expression construct. Cells expressing the BRCA1Δ14-15 alternative splicing variant had the lowest plating efficiency in comparison with other analyzed clones (Tab. 6). Upon ionizing radiation induced DNA damage, the clonal viability (expressed as PE) decreased non-proportionally in all analyzed clones and controls.

The MCF-7 clones with stably downregulated expression of endogenous BRCA1 (sh4834 and sh5196) had the lowest PE in both used γ-radiation doses as well as the highest decrease

of PE in relation to the standard cultivation conditions [5 Gy PE: sh4834 = 7.9% (44% of the PE in standard cultivation conditions) and sh5196 = 5% (31% of the PE in standard cultivation conditions)]. The decrease of PE of the cells expressing the BRCA1Δ14-15 was comparable with controls. On the contrary, the PE of BRCA1Δ17-19 cells treated with γ-radiation was highest and the decrease in its rate lowest from all analyzed clones and controls.

Table 6: The plating efficiency. *The plating efficiency of the MCF-7 clones with stable downregulated expression of endogenous wtBRCA1 (sh4834 and sh5196), clones expressing the BRCA1Δ14-15 (BRCA1Δ14-15 and BRCA1Δ14-15+sh4834) and BRCA1Δ17-19 (BRCA1Δ17-19 and BRCA1Δ17-19+sh5196) alternative splicing variants under the standard cultivation conditions (0 Gy) and upon ionizing γ-radiation (1 and 5 Gy) induced DNA damage. Data are mean from three independent experiments ± S.D.*

Plating efficiency (%)			
Clone	**0 Gy**	**1 Gy**	**5 Gy**
MCF-7	19.06 ± 0.93	16.87 ± 3.75	10.93 ± 0.31
pcDNA3.1 empty	23 ± 2	20.5 ± 0.5	12 ± 1
sh4834	17.91 ± 0.41	15.41 ± 1.25	7.91 ± 0.41
sh5196	16 ± 1.33	15.66 ± 1.66	5 ± 0.33
BRCA1Δ14-15	15.66 ± 0.33	16 ± 1.33	9 ± 1
BRCA1Δ14-15+sh4834	15.5 ± 2	16.5 ± 0	6.75 ± 1.75
BRCA1Δ17-19	18.63 ± 0.9	17.27 ± 0.45	12.04 ± 0.68
BRCA1Δ17-19+sh5196	20.88 ± 1.47	18.52 ± 0.88	14.41 ± 1.47

Results of SF were in consistence with that of PE for all analyzed clones and controls which responded to ionizing radiation-induced DNA damage by the decrease in the SF of cells (Fig. 21). However, the relative SF upon γ-radiation treatment was highest in clones expressing the BRCA1Δ17-19 alternative splicing variant (BRCA1Δ17-19 and BRCA1Δ17-19+sh5196) and lowest in the clones with stably downregulated expression of endogenous wtBRCA1 (sh4834 and sh5196). The relative SF of cells with upregulated expression of BRCA1Δ14-15 alternative splicing was comparable with controls after the γ-radiation treatment.

These results showed that downregulation of endogenous wtBRCA1 significantly decrease the clonal viability while increasing the radiation sensitivity of MCF-7 cells. The overexpression of the BRCA1Δ17-19 alternative splicing variant increases the radioresistance of MCF-7 clones on both PE and SF levels, while the overexpression of the BRCA1Δ14-15 alternative splicing variants leads to slight increase in radio-sensitivity of

MCF-7 cells. These results indicates, that expression of distinct BRCA1 alternative splicing variants can differentially influence the viability and radio-sensitivity of MCF-7 cells under the DNA damaging conditions.

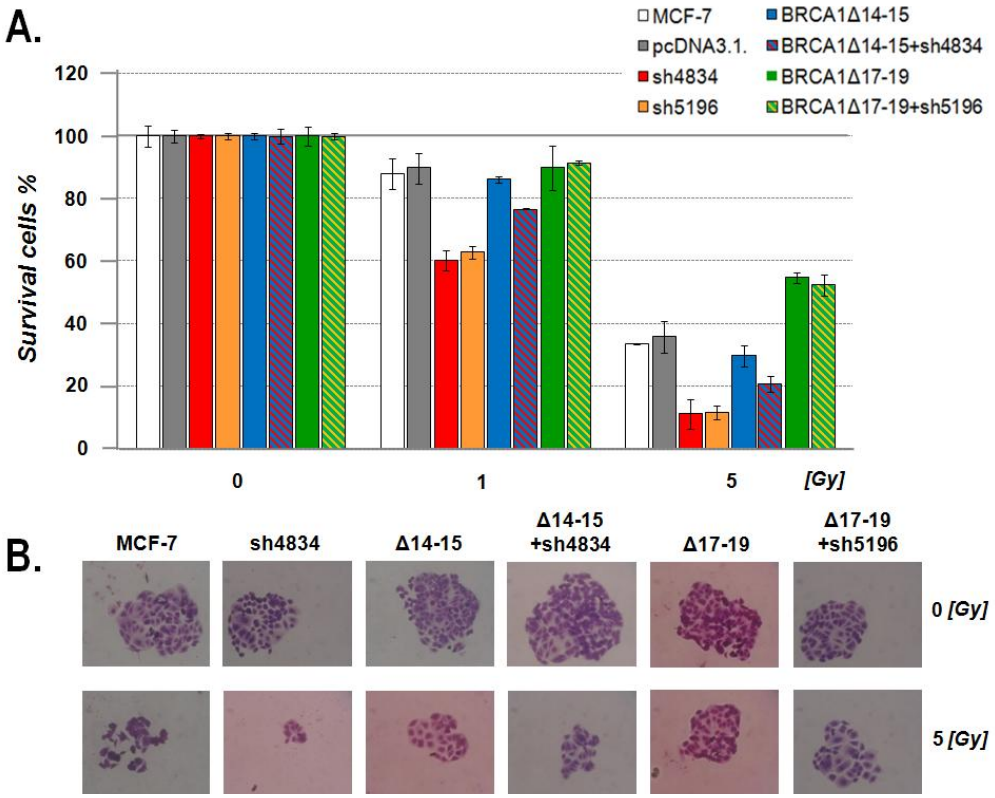

Figure 21: The surviving fraction (SF) of MCF-7-based clones with stably modified expression of BRCA1. *Cells were irradiated by a single dose of ionizing γ-radiation (0, 1 and 5 Gy), diluted to a high rate and seeded onto a new cultivations dish. After 10 days of cultivation the cells surviving fraction (**A**) was determined were stained using crystal violet (**B**) staining and measurement of absorbance. For assessment of radiation sensitivity of particular clones was used a relative surviving fraction normalized to the non-irradiated cells (0 Gy was considered as a 100%). Data are mean ± S.D.*

4.2.6 Overexpression of the BRCA1Δ14-15 or BRCA1Δ17-19 alternative splicing variants influences the proliferation of MCF-7 cells.

After the finding that modification of BRCA1 expression can influence the viability of MCF-7 clones, we further directly examined the proliferation activity of clones under the standard cultivation conditions and upon the different rate of γ-radiation-induced DNA damage (0, 1, 3 and 5 Gy) by an independent assay. To prove that the possible change in the proliferation activity is attributed to BRCA1 and its downstream but not upstream signaling,

the cells were cultivated with caffeine, a potent inhibitor of the BRCA1 upstream activator ATM, prior to irradiation in a parallel experiment.

The population doubling times (G) for particular clones were calculated from the growth curves obtained after seven days cultivation under the standard conditions. Obtained results were inconsistent due to apparent differences among singular analyzed clones of the particular expression construct (Tab. 7). These differences were most probably generated by a transfection process or by the exact position of integration of the expression construct within the MCF-7 genome.

Table 7: Population doubling time. *Population doubling time (G) of selected MCF-7 clones with stably integrated expression construct for overexpression (BRCA1Δ14-15) or downregulation (sh4834) of BRCA1 and the control empty vector (pcDNA3.1 empty). Population doubling time was calculated for three different clones of one particular expression construct (marked here by I;II and III numeral) using a growth curve data of cell population cultivated under the standard cultivation conditions for 7 days.*

Clone	MCF-7	pcDNA3.1			Sh4834			BRCA1Δ14-15		
	I.	I.	II.	III.	I.	II.	III.	I.	II.	III.
G [h]	38	38	40	36	37	33	39	38	40	36

However, the growth curves of clones with modified expression of BRCA1 irradiated by a single dose of ionizing radiation showed different proliferation tendencies in comparison with controls. As supposed from previous experiment, the control non-transfected MCF-7 cells responded to the irradiation by the decrease in a proliferation rate proportionally to the γ-radiation dose. The slope of growth curves (Fig. 22) and their angular coefficients (Tab. 8) of control MCF-7 cells showed that after the initial proliferation deceleration (caused by the DNA damage), the cells grew with the proliferation rate comparable to the non-irradiated ones. Compared to that, clones with downregulated expression of endogenous wtBRCA1 (sh4834 and sh5196) and cells expressing the BRCA1Δ14-15 alternative splicing variant (BRCA1Δ14-15 and BRCA1Δ14-15+sh4834) were more sensitive to the ionizing radiation showing markedly decreased proliferation rate during whole time period. On the contrary, cells expressing the BRCA1Δ17-19 alternative splicing variant (BRCA1Δ17-19 and BRCA1Δ17-19+sh5196) exerted an increased radio-resistance.

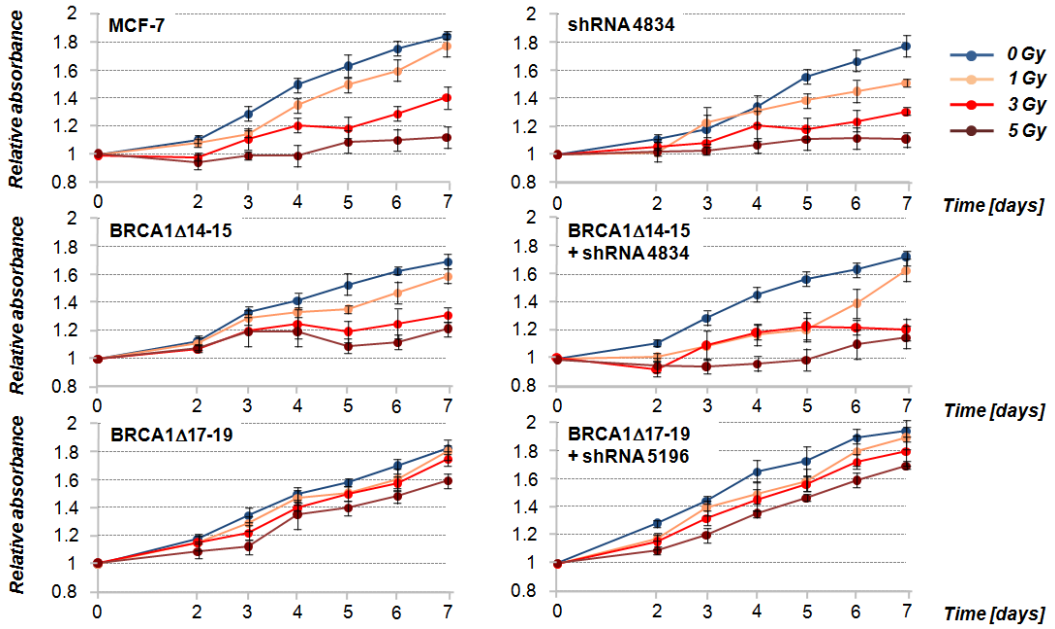

***Figure 22*: Proliferation of MCF-7 clones with stably modified expression of BRCA1 under the standard cultivation conditions and upon γ-radiation induced DNA damage.** *Cells were seeded in triplicates on the 24 well plates in the same number, treated by the single dose of ionizing γ-radiation (0; 1; 3 and 5 Gy) and cultivated for 7 days. Growth curves were determined by the crystal violet staining. Data are plotted as a relative absorbance normalized to the day 0. Data are mean ± S.D.*

Table 8: The angular coefficients of MCF-7 clones. *The angular coefficient (k) for particular growth curves of analyzed MCF-7 clones with modified expression of BRCA1 under the standard cultivation conditions (0 Gy) and upon γ-radiation induced DNA damage (1, 3 and 5 Gy). The angular coefficients were calculated from the exponential phase of cell growth using excel linear regression and equation calculation.*

Dose (Gy)	Angular coefficients (k)							
	MCF-7	pcDNA3.1	sh4834	sh5196	Δ14-15	Δ14-15 +sh4834	Δ17-19	Δ17-19 +sh5196
0	0.164	0.181	0.148	0.155	0.120	0.132	0.126	0.151
1	0.139	0.121	0.103	0.120	0.077	0.088	0.110	0.144
3	0.069	0.070	0.047	0.061	0.034	0.073	0.112	0.138
5	0.042	0.038	0.027	0.029	0.010	0.034	0.106	0.125

The results of parallel experiment with the same set of clones from the identical passage, cultivated under the same conditions but treated with the caffeine showed, that inhibition of ATM causes hypersensitivity of cells to the DDSB with a total abrogation of proliferating

activity. The proliferation tendencies were comparable within all analyzed clones and control cells irrespectively to the BRCA1 expression modification (Fig. 23).

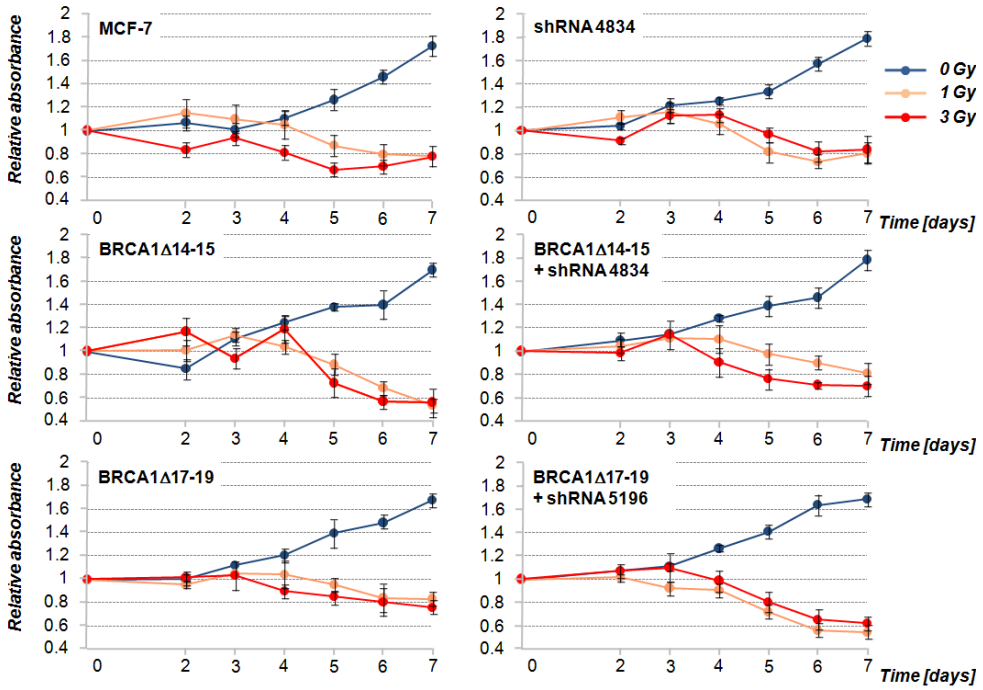

Figure 23: Proliferation of MCF-7 clones with inhibited activity of ATM *Proliferation of MCF-7 clones with stably modified expression of BRCA1 with caffeine-inhibited ATM kinase under the standard cultivation conditions and upon γ-radiation induced DNA damage. Forty eight hours before seeding onto the 24 well plates the cells were cultivated in medium containing 1mmol/l caffeine as a potent inhibitor of ATM activity. Cells were seeded from the same passage like in the parallel experiment, irradiated by a single dose of γ-radiation (0; 1 and 5 Gy) and stained by crystal violet for the growth curve determination. Data are plotted as a relative absorbance normalized to the day 0. Data are mean ± S.D.*

Overall results of proliferation assays, consistent with the result of clonogenic assay, showed that modulation of BRCA1 expression can differently influence the proliferation of MCF-7 cells upon the ionizing radiation-induced DNA damage. The altered proliferation capacity of particular clones was independent on the presence of the endogenous wtBRCA1 which indicates the dominant effect of BRCA1Δ14-15 and BRCA1Δ17-19 alternative splicing variants. Moreover, the observed shift in the proliferation rate in MCF-7 clones was completely abolished by a caffeine-mediated ATM inhibition and is thus not caused by the superordinate DDSB signaling pathway, but it is most likely the specific response to modified expression of BRCA1.

5 DISCUSSION

Despite that *BRCA1* has been described nearly 20 years ago and the unequivocal importance of BRCA1 in mutations in this gene for breast and ovarian cancer susceptibility has been documented by thousands of published papers, there is a lack in current knowledge about the biological relevance of BRCA1 sequence variants naturally produced by the alternative pre-mRNA splicing processes. In this study, we focused on a detail characterization of the effect of BRCA1Δ14-15 and BRCA1Δ17-19 alternative splicing variants on the DDSB repair. Both variants were selected for functional analyzes due to their repeated ascertainment during the screening program of high-risk breast cancer individuals. Both variants retain the original BRCA1 reading frame while lacking several short N-terminal exons coding for portions of structural domains – the serine-containing domain (SCD) in BRCA1Δ14-15, and first BRCT domain in BRCA1Δ17-19. Both these protein motifs were previously described as important determinants of BRCA1 function within DDSB repair pathways. Translation of these sequence variants can lead to the production of protein with altered biological properties with a relevant impact on the BRCA1-mediated processes.

In our model system the BRCA1Δ14-15 and BRCA1Δ17-19 variants were overexpressed in a breast adenocarcinoma-derived $BRCA1^{+/+}$ MCF-7 cell line with/without subsequent RNAi-mediated downregulation of endogenous wtBRCA1. A stable incorporation of pcDNA3.1-based constructs with BRCA1Δ14-15 and BRCA1Δ17-19 into the MCF-7 genome resulted in the expression level comparable to the expression level of endogenous wtBRCA1. Using the sequence-specific shRNAs, we downregulated the endogenous wtBRCA1 up to 7% of its normal expression rate at mRNA level. Thus, the expression of endogenous wtBRCA1 in combined stable clones was proportionally replaced by the expression of analyzed splicing variants. However, all results of functional analyzes must be interpreted with respect to the limits of used model system.

Our results showed that depletion of wtBRCA1 in MCF-7 cells slightly increased the level of endogenous DDSBs, decelerated the initial IRIF assembling after the γ-radiation-induced DNA damage, slowed down the IRIF disassembling, and prolonged their persistence. A retarded formation of γH2AX/53BP1-containing IRIF correlated directly with slower DDSB repair. Moreover, the cells with downregulated expression of wtBRCA1 were increasingly radiosensitive and less viable in comparison with controls. The similar, but not same,

phenotypic pattern exerted the cells with overexpressed BRCA1Δ14-15 or BRCA1Δ17-19 alternative splicing variant.

Various experiments with silencing the expression of particular members of HR and NHEJ pathways have shown that NHEJ takes place faster than HR [45]. NHEJ is also a prevailing DNA repair mechanism within the period of first four hours after a genotoxic DNA insult [44]. On the other hand, HR is used for DDSB repair in specific chromatin regions, IRIF of homology-directed DNA repair typically occur with a delay, and persist for a longer time period [46,225]. The γH2AX and 53BP1 proteins are involved in both HR and NHEJ pathways. A time course of their co-localization after the γ-radiation-induced DNA damage suggested that downregulation of endogenous wtBRCA1 or overexpression of BRCA1Δ14-15 or BRCA1Δ17-19 negatively influences, in particular, the initial rapid phase of DDSB repair. Moreover, cells with overexpressed BRCA1Δ17-19 exhibited significantly prolonged persistence of γH2AX/53BP1 IRIF indicating additional functional block in the later phases of a DDSB repair response pathway. In accordance with the importance of BRCA1 protein in HR pathway, the cells with downregulated expression of endogenous wtBRCA1 were hypersensitive to the DNA cross-linking agent mitomycin C. Surprisingly, the cells expressing the BRCA1Δ14-15 alternative splicing variant displayed no difference in the sensitivity to mitomycin C compared to the non-transfected MCF-7 controls. On the contrary the cells expressing BRCA1Δ17-19 were more sensitive to mitomycin C in comparison with controls. This suggests that unlike to BRCA1Δ17-19, the presence of BRCA1Δ14-15 protein isoform does not totally corrupt the activity of HR. Additionally, the results of direct *in vitro* assay proved, that activity of NHEJ was generally decreased in all MCF-7 clones with depleted wtBRCA1 and in clones expressing the BRCA1Δ14-15 and BRCA1Δ17-19 alternative splicing variants. Moreover, the expression of BRCA1Δ17-19 variant impaired the precise NHEJ pathway to a higher degree in comparison with other analyzed clones. All together, the altered structures of the BRCA1Δ14-15 and BRCA1Δ17-19 differentially influence the biological activity of BRCA1 protein in the process of DDSB repair. As this effect was not dependent on the presence of wtBRCA1, we assume that BRCA1Δ14-15 and BRCA1Δ17-19 exert the dominantly-negative effect on the BRCA1-mediated processes in the DDSB repair.

The DDSB repair in eukaryotic cells is secured by two main pathways, a precise but relatively slow and complicated homologous recombination and rapid and relatively simple non-homologous end joining which is generally accepted as an error prone mechanism. The preferential usage of each of these pathways is determined by the cell cycle phase and by the

anatomy of DDSB itself. NHEJ is the DDSB repair pathway of first choice during the G1 and early S phases of the cell cycle, while the HR can only be effectively used during the S and G2 phases of a cell cycle, when sister chromatids are available for a homologous exchange. Besides that, DDSB introduced in the mildly condensed euchromatin are preferentially repaired by the NHEJ mechanism. DDSB generated in tightly packed heterochromatin or those in euchromatin which failed to be repaired by NHEJ are switched to homology-directed repair. Thus both pathways rather cooperate then compete for repair of the DNA lesions and constitute the double-secured mechanism capable to effectively maintain genomic integrity and cellular viability by balanced fast (but erroneous) and slow (but precise) DDSB processing, respectively [226]. The decision-making element governing the preferential usage of either form of these two DNA repair mechanisms has not been fully understood yet. It has been proposed that these two pathways at least to some degree compete with each other during the initial sensing phase and that the strand resection is one of the main factors governing the usage of these two possible repair mechanisms [36]. While classic NHEJ does not require additional processing of the free DNA ends in the break site, a microhomology is required for the precise NHEJ, and the long RPA-coated ssDNA regions are necessary for HR. Besides that, there probably exist active switches between both pathways during the processing of DNA lesions enabling to completely fulfill the repair of those DDSB which failed to undergo the process of first choice under some circumstances.

It has been documented, that BRCA1 protein depletion has unexceptionably detrimental effect on the DNA repair [83]. The BRCA1 protein was initially identified as a mediator of the apical signaling in a homology-directed repair of DDSB. Later it has been proposed that BRCA1 may participate also in the NHEJ pathway [219]. Regarding that, it could be assumed that inactivating mutations in the BRCA1 gene affect both DNA repair pathways in a similar manner. However, specific analyses of the BRCA1's role in DNA repair pathways raised several seemingly contradictory results. While Jasin et al. showed that BRCA1-deficient cells have heavily impaired homology-directed DNA repair, highly instable genome, and increased sensitivity to mitomycin-C compared to wtBRCA1-expressing cells [224], Dever et al. documented, that a mutation in the BRCA1 BRCT domain leads to a hyperrecombination [73]. Further, Jasin et al. described that BRCA1-/- cell line has reduced homology-directed DNA repair, while NHEJ is slightly elevated at the same time as a compensatory mechanism for decreased DNA repair capacity [83]. Contrary to that, Wang et al. proved that, BRCA1 knock-down compromise the accuracy of NHEJ [219]. The results of our study showed that a relatively subtle change in the BRCA1Δ14-15 and BRCA1Δ17-

19 mRNA structures lead to the production of BRCA1 protein isoforms which decrease the overall capacity of DDSB repair in a dominant-negative manner in a MCF-7 cells, however, the mechanism is different for both analyzed alternative splicing variants.

We hypothesized, that the overexpression of the BRCA1Δ14-15 variant leads to preferential usage of homology-directed DDSB repair in MCF-7 cells while the expression of BRCA1Δ17-19 compromise both the NHEJ and HR with substantial impact on precise NHEJ and final steps of HR (fig. 24).

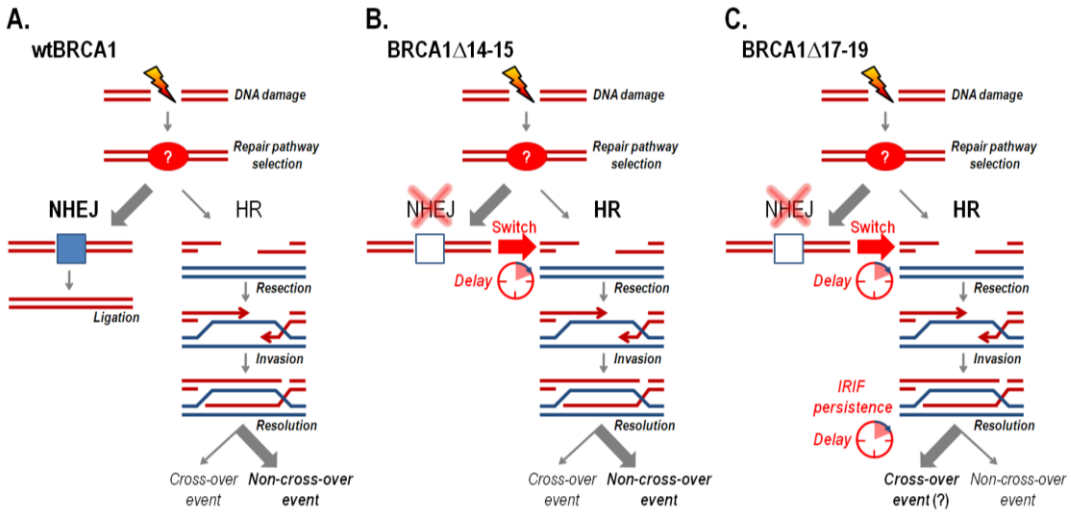

Figure 24: BRCA1 alternative splicing variants differentially impair the DDSB repair. A *When wtBRCA1 is presented, the NHEJ is preferred DDSB repair pathway within the population on non-synchronized cells leading to rapid ligation of broken DNA ends. This is exhibited by rapid decrease in the IRIF number within first two hours PI. Only a minority of DDSBs are proceeded by the HR mechanism ending with IRIF resolution without additional cross-over events leading to restoring the same chromatin conditions. This is exhibited by the same or even lower number of IRIF 24 hours PI in comparison with endogenous level of DDSB.* ***B****. The overexpression of BRCA1Δ14-15 impairs the NHEJ pathway at the early phase after the initial decision-making step in DDSB repair. Due to the redundancy of DDSB repair mechanism, a functional switch can shift DDSB from the initially-directed rapid NHEJ to a slower HR. This time-consuming switch causes an accumulation of IRIF within 30 minutes PI. Further DDSB processing by fully-active HR results in a complete but delayed repair.* ***C****. The overexpression of BRCA1Δ17-19 impairs a NHEJ pathway in a same manner as in the case of BRCA1Δ14-15. A successive decrease of IRIF number indicates that HR is active. However, an increased number of IRIF persisting for 24 hours PI indicates the additional block in a final resolution of IRIF causing (probably) a hyperrecombination exhibited as the increased sensitivity to mitomycin C.*

In our study, we worked with non-synchronized population of cells where most cells were resting in G1 cell cycle phase. Thus, it can be assumed that the majority of DDSB repair after irradiation by the ionizing γ-radiation relayed on the NHEJ pathway. A block of NHEJ pathway caused by either downregulation of wtBRCA1, or overexpression of BRCA1Δ14-15 or BRCA1Δ17-19 leads to the functional switch to alternative DDSB repair pathway. This causes that DDSB initially determined to undergo NHEJ must be redirected to HR. Homology-directed repair of DDSB is relatively slow process comparing to the NHEJ. Assuming that,"confusion" in the initial decision-making process leads to an accumulation of stalled NHEJ IRIF until triggering of HR. This produces a delay observed during the initial formation of IRIF within 30 minutes PI in our model cells.

The expression of BRCA1Δ14-15 does not change the sensitivity to mitomycin C which indicates that HR is sufficiently active to deal with radiation-induced DNA damage. This is supported by the finding that the number of IRIF at the time 24 hours PI is comparable to the initial endogenous DNA damage level in cells expressing the BRCA1Δ14-15 alternative splicing variant. On the other hand, the expression of BRCA1Δ17-19 increases sensitivity to mitomycin C which indicates that HR is impaired. Because the number of IRIF progressively decreased during the time PI we hypothesize that the problem relies to the later phases of HR, probably during the final dismantle of IRIF. This is in consistence with previously described finding that the inability to finalize HR properly leads to hyperrecombination and hypersensitivity to DNA cross linking agents [227,228].

Assuming the major and generally accepted function of BRCA1 as a protein-protein interaction modulator and mediator of the initial DDSB signal, the BRCA1 protein must be physically localized at the site of DDSB to exert its participation on the DNA repair process. The localization of BRCA1 to the site of DDSB is mediated mainly by a formation of the BRCA1-containing complexes. Failure to integrate into the relevant BRCA1 complex can cause a spatio-temporal mislocalization of BRCA1 and thus decrease a processing rate of the DDSB repair [74,229]. Once physically present at the site of requirement, the BRCA1-mediated tethering of chromatin- and DNA-remodeling protein factors determines further processing of damaged DNA regions and thus participate in the initial decision-making process of preferential usage of either of two main DNA repair pathways [230,231]. Thus, a shift in a BRCA1 binding capacity can lead to inability to interact with a "proper" factor and can harm the DDSB repair progress.

Phosphorylation of DNA repair-modulator protein CtIP by CDKs during S and G2 phase enables its phospho-specific interaction with BRCA1. Resulting complex, together with additional nucleases and helicases, then promote a strand resection generating the long ssDNA regions indispensable for the HR [232]. In a subtle balance with BRCA1-CtIP-promoted end resection is the assembly of BRCA1-RAP80 complex to ubiquitin-modified chromatin near the break site which blocks the CtIP activity and thus prevents the strand resection [233]. Additionally, BRCA1 binds to the MRN complex presented together with Ku proteins at the site of DDSB. MRN complex possess an exonuclease activity which can be stimulated by BRCA1 and hence BRCA1 may switch the balance among direct ligation by NHEJ, subtle end-processing of asymmetrical breaks that leads to precise NHEJ ligation, or large CtIP-mediated end resection resulting in HR.

Recently, it has been described that BRCA1 is an important factor ensuring the proper and well-timed IRIF dismantle preventing the undesirable crossing-over events. Though the mechanism is not fully understood yet, it is known that both RING finger and BRCT protein-interaction motifs of BRCA1 are indispensable for this process [234]. In consistence with this hypothesis is a finding that cells expressing the BRCA1 with mutation in BRCT domain exert hyperrecombination and genomic instability [73]. Thus, the formation of specific BRCA1-containing complexes seems to be a clue to the BRCA1 function in a DNA repair. Structural changes in the BRCA1 protein-interaction modules can influence its binding capacity. Moreover, the majority of protein-protein interactions in the process of DNA repair take place in the phosphorylation- or ubiquitin-dependent manner. Upon a DNA damage, a specific BRCA1 serine residues are phosphorylated by upstream kinases, which could in turn regulate the BRCA1 binding specificity [221]. The phosphorylation status was shown to be an important factor influencing the BRCA1 intracellular localization and trafficking [17]. The availability of the BRCA1 protein at the site of its requirement can thus influence the formation of specific complexes. The exons 14 and 15 deleted in analyzed variant BRCA1Δ14-15 contain six serine residues known to be targets of ATM upon DNA damage stimulation. This indicates, that phosphorylation of these serine residues is a part of DNA damage-induced reaction network which governs the activity of BRCA1 to the exact place in the DNA repair pathway. Thus, the BRCA1Δ14-15 variant, lacking the substantial part of SCD, results in formation of protein isoform with impaired sensitivity to the DNA damage up-stream signaling resulting in impaired DDSB repair as indicated by our results. Similarly to that, BRCA1Δ17-19, lacking the substantial part of first BRCT domain, has probably altered protein-binding capacity. So, even properly localized BRCA1Δ17-19 cannot elicit the

relevant protein-protein interactions and blocks the step which is dependent on this interaction in a dominant-negative manner. The DDSB were repaired even in cells with the downregulated BRCA1 to a low level. This indicates that BRCA1 is not absolutely indispensable for the process of DNA repair and rather enhances then enables this process in general. However, a delayed processing of potentially highly dangerous DNA lesions can contribute to a genomic instability. An increased number of endogenous IRIF testify for this assumption.

Our results further indicate the potential of BRCA1 alternative splicing variants to differentially influence the proliferative properties of MCF-7 cells. The downregulation of endogenous wtBRCA1 sensitized the MCF-7 cells to the ionizing radiation, decreased their clonogenic potential upon DNA-damaging conditions. The overexpression of BRCA1 splicing variants, however, had a different impact on the proliferative activity in MCF-7 cells. While the overexpression of BRCA1Δ14-15 leaded to the similar response to ionizing radiation at a proliferative level as the depletion of endogenous wtBRCA1, the overexpression of BRCA1Δ17-19 caused increased radioresistance of MCF-7 clones.

BRCA1 is unique in its broad activities in a maintenance of genomic integrity. Beside the direct involvement in the DDSB repair, BRCA1 participate in the DNA damage-induced check point pathway. It has been documented that the depletion of BRCA1 (and partially also haploinsufficiency) leads to the increased ability of the clonal growth in primary mammary epithelial cells [235,236]. This was specifically linked to the impaired differentiation but enhanced proliferation. The observed phenotype of the cells was rescued by the expression of either wtBRCA1 or mutant at the Rad50-binding domain (localized at the N-terminal part of the BRCA1 protein) but not by the expression of mutant in BRCT domain suggesting the critical role of BRCA1 BRCT domains within this process. Our results are in consistence with these findings, as we show that cells expressing the BRCA1Δ17-19 alternative splicing variant possess higher proliferative potential upon DNA damaging conditions while the cells expressing the BRCA1Δ14-15 alternative splicing variant resemble the phenotype of the control non-transfected cells.

The precise mechanism of BRCA1-participation on the proliferative activity has not been unraveled, yet. However, it can be affected by the involvement of BRCA1 in regulation of transcription. Beside the known direct interaction of BRCA1 with transcription factors [237], BRCA1 can C-terminally bind the RNA polymerase II and thus participate in transcription machinery regulation [90]. A change in the BRCA1 protein structure can thus influence the

activity of BRCA1 within the genome surveillance complex. This was documented on the BRCA1-IRIS isoform which has the potential to abrogate the DNA damage-induced p38MAPK/p53 signalization and thus promotes the proliferation [211].

The alternative splicing is a mechanism capable to produce a protein isoforms with markedly different biological properties from a single primary pre-mRNA transcript. Therefore, alternative splicing is thus responsible for a great genetic diversity [238]. We hypothesize that the overall biological activity of a certain gene's product is determined by the actual pool of its particular protein isoforms generated by the alternative (or aberrant) pre-mRNA splicing. The BRCA1 has a several common alternative splicing variants occurring frequently together with the main full-length product [239]. Their mRNA concentrations are at least partially dependent on the cell cycle phase suggesting their natural regulatory function within the global BRCA1 expression profile [206]. The relevance of BRCA1 splicing variants on the cellular processes has been demonstrated in the studies of BRCA1 variant lacking the exon 10 where was shown that BRCA1Δ10 failed to deliver the Rad51 recombinase to the site of DDSBs resulting in a severed HR and the genome instability [208,83]. Additionally, another BRCA1 alternative splicing variant BRCA1-IRIS lacking the C-terminal part of the protein exhibits pro-oncogenic properties and influences the cellular proliferation in opposite fashion to wtBRCA1.

In our current functional analysis we have shown, that overexpression of the BRCA1Δ14-15 and BRCA1Δ17-19 alternative splicing variants, ascertained during the screening of high risk breast cancer individuals, increases the level of endogenous DDSB and decreases the overall DDSB repair capacity by impairment of NHEJ pathway in MCF-7 cells. It seems that the occurrence of BRCA1 alternative splicing variants is rather frequent than rare, though the exact tissue specificity, quantity of particular alternative splicing variants, and their dynamics upon DNA-damaging events is not known yet. We hypothesize that the overall biological activity of a certain gene's product is determined by the actual pool of its particular protein isoforms generated by the alternative (or aberrant) pre-mRNA splicing. Therefore, besides to the inactivating mutation, great genomic rearrangements, loss of heterozygosity, hypermethylation of promoter sequence, the production of cancer-specific alternative splicing variants with dominantly negative effect on wtBRCA1-mediated cellular activities could represent another possible mechanisms for wtBRCA1 inactivation. This hypothesis, together with the results of our current work implies the importance of BRCA1 alternative splicing in the maintenance of genomic integrity and malignant transformation.

Except to their involvement in tumorigenesis, alternative splicing variants of BRCA1 could represent a possible prognostic factor for several solid cancers. Currently, selective PARP-1 inhibitors have been introduced into the clinical practice as a targeted and tailored therapy for cancer treatment in individuals carrying a pathogenic mutation in BRCA1/2 gene. This therapy, based on concept of synthetic lethality, affects NHEJ pathway (at the level of PARP-1 signalling) in cancer cells exhibiting a broad defect of HR due to the lost of the wtBRCA1 (or BRCA2) protein [240,241]. This therapy is currently (and logically) restricted to the BRCA1/2 mutation carriers, however, it has been also considered to be used in a cancer treatment in carriers of mutations in other breast/ovarian-cancer predisposing genes coding for proteins involved in DNA repair. Thus, the dominant-negatively-acting alternative splicing variants of BRCA1 may represent a possible target for their potential clinical utilization.

6 CONCLUSIONS

The BRCA1 alternative splicing variants have been repeatedly ascertained during the ongoing screening of high breast cancer risk individuals. Their relatively frequent occurrence and discrete changes in structurally and functionally important BRCA1 protein domains suggest a different biological activity to the full-length BRCA1 isoform. This work is primarily focused on the establishment of a model system that will allow to functionally characterize sequence variants of *BRCA1* gene, described during the population specific screening of high breast and/or ovarian risk individuals in Czech Republic, and to assess their possible relevance in the process of malignant transformation. Regarding to the working hypothesis (described in the chapter 2) we summarize the crucial results of the functional *in vitro* analysis of the BRCA1 alternative splicing variants:

- Assuming the limits of cancer cell line, stable transfection and expression modification, the MCF-7-based clones combining the PCR splicing approach and stable overexpression of studied BRCA1 sequence variants with coincidental RNAi-mediated downregulation of endogenous wtBRCA1, constitutes a **reliable model system for the functional *in vitro* analysis**.

- **Overexpression of BRCA1 Δ14-15 or Δ17-19 increases the degree of endogenous DNA damage and decreases the overall DDSB repair capacity**. This effect does not depend on the presence of endogenous wtBRCA1 and exerts phenotypic signs comparable to RNAi-mediated depletion of endogenous wtBRCA1in MCF-7 cells.

- **Overexpression of BRCA1 Δ14-15 or Δ17-19 decelerates the assembly of γ-radiation-induced γH2AX/53BP1 foci at the initial phases of DDSB repair and prolonged their persistence**.

- Stable clones expressing BRCA1 Δ17-19 and clones with downregulated expression of endogenous wtBRCA1, but not clones with overexpressed BRCA1 Δ14-15 exert hypersensitivity to mitomycin C. This result shows that **BRCA1 Δ17-19 and BRCA1 Δ14-15 differentially impair HR**. Both **alternative splicing variants** as well as downregulation of endogenous wtBRCA1 significantly **decrease overall NHEJ capacity**.

- **The overexpression of BRCA1 Δ14-15 or Δ17-19 increases the viability and clonogenic potential of MCF-7 cells**.

- The downregulation of endogenous wtBRCA1 and upregulation of BRCA1 Δ14-15 causes the radiation sensitivity while the upregulation of BRCA1 Δ17-19 cause a radiation resistance of MCF-7 cells.

The results of our study indicate, that the BRCA1 alternative splicing variants Δ14-15 and Δ17-19 are not able to functionally replace the full-length BRCA1 in a γ-radiation induced DDSB repair process in MCF-7 cells. Both variants exert a dominantly-negative effect on the DDSB repair, cell viability and clonogenic potential. The overall decrease of DDSB repair capacity caused by the overexpression of BRCA1 Δ14-15 or Δ17-19 could be a factor negatively influencing the genomic stability. This together with disregulated proliferation of MCF-7-based clones could contribute to the malignant transformation.

Hence, studied BRCA1 alternative splicing variants could potentially negatively influence the BRCA1 tumor suppressive activity indicating that alternative pre-mRNA splicing may represent an important regulatory pathway contributing to malignant transformation.

7 LIST OF ABBREVIATIONS

Abbreviation	Full name
Akt	V-akt murine thymoma viral oncogene homolog 1 (Protein kinase B)
ATM	Ataxia-telangiectasia mutated gene
ATR	Ataxia-telangiectasia and Rad3-related
BACH1	Basic leucine zipper transcription factor 1 (BTB and CNC homology 1)
BARD1	BRCA1-associated ring domain 1
BC	Breast cancer
BRAP1	BRCA1-associated protein 1
BRCA1/2	Breast Cancer 1/2 Gene
BRCC36	BRCA1/BRCA2-containing complex subunit36
BRCT	BRCA1 C-terminal (domain)
B2M	β-2-microglobulin
CCD	Coiled-coil domain
Cdc25	Cell division cycle 25
CDK1	Cyclin-dependent kinase 1
C/EBPγ	CCAAT/enhancer-binding protein gamma
CI	Cell index
CP	Crossing point
CRM	Required for chromosome region maintenance 1 (exportin 1)
CtIP	C-terminal interaction protein
DBD	DNA binding domain
DDSB	DNA double strand break
DMEM	Dulbeccco's modified Eagle medium
DNA-PK$_{CS}$	Protein kinase DNA-activated catalytic subunit
dsDNA	Double stranded DNA
ssDNA	Single stranded DNA
EDTA	Ethylendiamine tetraacetate
EJC	Exon junction complex
ERα	Estrogen receptor alpha
ESE	Exonic splicing enhancer
ESS	Exonic splicing silencer
EtOH	Ethyl alcohol
FCS	Fetal calf serum
FHA	Forkhead-associated domain
GADD45	Growth arrest-and DNA damage-inducible gene 45
HBS	HEPES-buffered saline
H2AX	H2A histone family member X
HDAC	Histone deacetylase
hnRNP	Heterogeneous ribonucleoprotein
HR	Homologous recombination
H-Ras	Harvey rat sarcoma viral oncogene homolog
CHK1/2	Checkpoint kinase 1/2
IRIF	Ionizing radiation induced foci
IRIS	in-frame reading of BRCA1 intron 10 splice variant
ISE	Intronic splicing enhancer
ISS	Intronic splicing silencer
JNK	c-JUN kinase 1 (MAPK8)
kbp	Kilo base pairs
Ku 80	X-ray repair, complementing defective, in Chinese hamster 5
LB agar	Luria-Bertani agar (medium)

(medium)	
LigIV	DNA Ligase IV
MAPK	Mitogene-activated protein kinase
MDC1	Mediator of DNA damage checkpoint protein 1
MRE11	Meiotic recombination 11
MRN	MRE11-Rad50-Nbs1 complex
NaAC	sodium acetate
Nbs1	Nibrin
NES	Nuclear export sequence/signal
NHEJ	Non-homologous end joining
NLS	Nuclear localization signal
NMD	Nonsense-mediated decay
ORF	Open reading frame
P21^{waf1}	P21 wildtype p53-activated fragment 1 (CDKN1A)
PALB2	partner and localizer of BRCA2
PBGD	Porphobilinogen deaminase
PBS	Phosphate-buffered saline
PE	Plating efficiency
PI	Post irradiation
PTB	Polypyrimidine tract binding protein
qPCR	Quantitative real-time PCR
Rad51	Recombination protein A
Rap80	Receptor-associated protein 80
RNA polII	RNA polymerase II
RING	Really interesting new gene (domain)
RNAi	RNA interference
RNF8	Ring finger protein 8
RPA	Replication protein A
RRM	RNA recognition motif
RT	Room temperature
RTCA	Real-time cell analyzer
RT-PCR	PCR with reverse transcription
SCD	Serine-containing domain
SF	Surviving fraction
shRNA	Short-hairpin RNA
snRNP	Small nuclear ribonucleoprotein
SR	Serine-arginine rich domain/protein
SSA	Single strand annealing
TBSt	Tris-buffered saline Tween containing
STAT1	Signal transducer and activator of transcription 1
TopBP1	DNA topoisomerase II-binding protein 1
U1-6	Ubiquitin interaction motif
UIM	Ubiquitin interaction motif
UTR	Untranslated region
U2AF	Upstream 2 activation factor
WB	Western blotting
WIP1	Wildtype p53-induced phosphatase 1 (PPM1D)
WRN	Werner syndrome gene (RECQL2 helicase)
XRCC1,4,5,6	X-ray repair, complementing defective, in Chinese hamster 1, 4, 5 (Ku80), 6 (Ku70)
ZBRK1	Zinc finger and BRCA1-interacting protein with a KRAB domain 1
53BP1	Tumor protein p53 binding protein 1

8 LIST OF FIGURES

9 LIST OF TABLES

10 REFERENCES

1. Y.Miki, J.Swensen, D.Shattuck-Eidens, P.A.Futreal, K.Harshman, S.Tavtigian, Q.Liu, C.Cochran, L.M.Bennett, W.Ding, ., Science. 266 (1994) 66-71.
2. T.M.Smith, M.K.Lee, C.I.Szabo, N.Jerome, M.McEuen, M.Taylor, L.Hood, M.C.King, Genome Res. 6 (1996) 1029-1049.
3. N.Puget, S.Gad, L.Perrin-Vidoz, O.M.Sinilnikova, D.Stoppa-Lyonnet, G.M.Lenoir, S.Mazoyer, Am. J. Hum. Genet. 70 (2002) 858-865.
4. C.F.Xu, M.A.Brown, J.A.Chambers, B.Griffiths, H.Nicolai, E.Solomon, Hum. Mol. Genet. 4 (1995) 2259-2264.
5. K.Sobczak, W.J.Krzyzosiak, J. Biol. Chem. 277 (2002) 17349-17358.
6. W.M.Elshamy, D.M.Livingston, Nat. Cell Biol. 6 (2004) 954-967.
7. P.S.Brzovic, P.Rajagopal, D.W.Hoyt, M.C.King, R.E.Klevit, Nat. Struct. Biol. 8 (2001) 833-837.
8. R.S.Williams, R.Green, J.N.Glover, Nat. Struct. Biol. 8 (2001) 838-842.
9. R.J.Deshaies, C.A.Joazeiro, Annu. Rev. Biochem. 78:399-434. (2009) 399-434.
10. Y.Xia, G.M.Pao, H.W.Chen, I.M.Verma, T.Hunter, J. Biol. Chem. 278 (2003) 5255-5263.
11. J.A.Rodriguez, B.R.Henderson, J. Biol. Chem. 275 (2000) 38589-38596.
12. M.Fabbro, S.Schuechner, W.W.Au, B.R.Henderson, Exp. Cell Res. 298 (2004) 661-673.
13. B.R.Henderson, Bioessays. 27 (2005) 884-893.
14. R.Naseem, A.Sturdy, D.Finch, T.Jowitt, M.Webb, Biochem. J. 395 (2006) 529-535.
15. T.T.Paull, D.Cortez, B.Bowers, S.J.Elledge, M.Gellert, Proc. Natl. Acad. Sci. U. S. A. 98 (2001) 6086-6091.
16. T.Ouchi, Cancer Biol. Ther. 5 (2006) 470-475.
17. S.Okada, T.Ouchi, J. Biol. Chem. 278 (2003) 2015-2020.
18. M.Gatei, B.B.Zhou, K.Hobson, S.Scott, D.Young, K.K.Khanna, J. Biol. Chem. 276 (2001) 17276-17280.
19. Y.F.Hu, T.Miyake, Q.Ye, R.Li, J. Biol. Chem. 275 (2000) 40910-40915.
20. F.Zhang, Q.Fan, K.Ren, P.R.Andreassen, Mol. Cancer Res. 7 (2009) 1110-1118.
21. I.A.Manke, D.M.Lowery, A.Nguyen, M.B.Yaffe, Science. 302 (2003) 636-639.
22. O.J.Gaiser, L.J.Ball, P.Schmieder, D.Leitner, H.Strauss, M.Wahl, R.Kuhne, H.Oschkinat, U.Heinemann, Biochemistry. 43 (2004) 15983-15995.
23. W.W.Au, B.R.Henderson, Cell Signal. 19 (2007) 1879-1892.

24. N.Mailand, S.Bekker-Jensen, H.Faustrup, F.Melander, J.Bartek, C.Lukas, J.Lukas, Cell. 131 (2007) 887-900.

25. L.Wei, L.Lan, Z.Hong, A.Yasui, C.Ishioka, N.Chiba, Mol. Cell Biol. 28 (2008) 7380-7393.

26. M.Fabbro, J.A.Rodriguez, R.Baer, B.R.Henderson, J. Biol. Chem. 277 (2002) 21315-21324.

27. A.C.Nelson, J.T.Holt, Radiat. Res. 174 (2010) 1-13.

28. N.Chiba, J.D.Parvin, J. Biol. Chem. %19;276 (2001) 38549-38554.

29. M.V.Bennetzen, D.H.Larsen, J.Bunkenborg, J.Bartek, J.Lukas, J.S.Andersen, Mol. Cell Proteomics. 9 (2010) 1314-1323.

30. R.A.Greenberg, B.Sobhian, S.Pathania, S.B.Cantor, Y.Nakatani, D.M.Livingston, Genes Dev. 20 (2006) 34-46.

31. R.Roy, J.Chun, S.N.Powell, Nat. Rev. Cancer. 12 (2011) 68-78.

32. D.T.Bau, Y.C.Mau, C.Y.Shen, Cancer Lett. 240 (2006) 1-8.

33. H.Zhang, K.Somasundaram, Y.Peng, H.Tian, H.Zhang, D.Bi, B.L.Weber, W.S.El Deiry, Oncogene. 16 (1998) 1713-1721.

34. N.Chiba, J.D.Parvin, Cancer Res. 62 (2002) 4222-4228.

35. M.J.Munoz, M.S.Perez Santangelo, M.P.Paronetto, M.M.de la, F.Pelisch, S.Boireau, K.Glover-Cutter, C.Ben Dov, M.Blaustein, J.J.Lozano, G.Bird, D.Bentley, E.Bertrand, A.R.Kornblihtt, Cell. 137 (2009) 708-720.

36. C.X.Deng, Nucleic Acids Res. 34 (2006) 1416-1426.

37. A.Asaithamby, B.Hu, D.J.Chen, Proc. Natl. Acad. Sci. U. S. A. 108 (2011) 8293-8298.

38. J.Chaudhuri, U.Basu, A.Zarrin, C.Yan, S.Franco, T.Perlot, B.Vuong, J.Wang, R.T.Phan, A.Datta, J.Manis, F.W.Alt, Adv. Immunol. 94:157-214. (2007) 157-214.

39. S.Keeney, M.J.Neale, Biochem. Soc. Trans. 34 (2006) 523-525.

40. M.M.Vilenchik, A.G.Knudson, Proc. Natl. Acad. Sci. U. S. A. 100 (2003) 12871-12876.

41. C.Acilan, D.M.Potter, W.S.Saunders, Genes Chromosomes. Cancer. 46 (2007) 522-531.

42. E.Sonoda, H.Hochegger, A.Saberi, Y.Taniguchi, S.Takeda, DNA Repair (Amst). 5 (2006) 1021-1029.

43. M.Lobrich, B.Rydberg, P.K.Cooper, Proc. Natl. Acad. Sci. U. S. A. %19;92 (1995) 12050-12054.

44. P.A.Jeggo, V.Geuting, M.Lobrich, Radiother. Oncol. 101 (2011) 7-12.

45. A.Shibata, S.Conrad, J.Birraux, V.Geuting, O.Barton, A.Ismail, A.Kakarougkas, K.Meek, G.Taucher-Scholz, M.Lobrich, P.A.Jeggo, EMBO J. 30 (2011) 1079-1092.

46. A.A.Goodarzi, P.Jeggo, M.Lobrich, DNA Repair (Amst). 9 (2010) 1273-1282.

47. M.Falk, E.Lukasova, S.Kozubek, Biochim. Biophys. Acta. 1783 (2008) 2398-2414.

48. A.T.Natarajan, A.Berni, K.M.Marimuthu, F.Palitti, Mutat. Res. 642 (2008) 80-85.

49. J.Essers, H.van Steeg, J.de Wit, S.M.Swagemakers, M.Vermeij, J.H.Hoeijmakers, R.Kanaar, EMBO J. 19 (2000) 1703-1710.

50. M.Takata, M.S.Sasaki, E.Sonoda, C.Morrison, M.Hashimoto, H.Utsumi, Y.Yamaguchi-Iwai, A.Shinohara, S.Takeda, EMBO J. 17 (1998) 5497-5508.

51. E.M.Kass, M.Jasin, FEBS Lett. 584 (2010) 3703-3708.

52. C.Richardson, M.Jasin, Mol. Cell Biol. 20 (2000) 9068-9075.

53. C.Allen, A.Kurimasa, M.A.Brenneman, D.J.Chen, J.A.Nickoloff, Proc. Natl. Acad. Sci. U. S. A. %19;99 (2002) 3758-3763.

54. R.S.Williams, J.S.Williams, J.A.Tainer, Biochem. Cell Biol. 85 (2007) 509-520.

55. N.Assenmacher, K.P.Hopfner, Chromosoma. 113 (2004) 157-166.

56. K.P.Hopfner, A.Karcher, L.Craig, T.T.Woo, J.P.Carney, J.A.Tainer, Cell. 105 (2001) 473-485.

57. K.P.Hopfner, L.Craig, G.Moncalian, R.A.Zinkel, T.Usui, B.A.Owen, A.Karcher, B.Henderson, J.L.Bodmer, C.T.McMurray, J.P.Carney, J.H.Petrini, J.A.Tainer, Nature. 418 (2002) 562-566.

58. E.Berkovich, R.J.Monnat, Jr., M.B.Kastan, Nat. Cell Biol. 9 (2007) 683-690.

59. E.Unal, A.Arbel-Eden, U.Sattler, R.Shroff, M.Lichten, J.E.Haber, D.Koshland, Mol. Cell. 16 (2004) 991-1002.

60. Z.Lou, K.Minter-Dykhouse, S.Franco, M.Gostissa, M.A.Rivera, A.Celeste, J.P.Manis, J.van Deursen, A.Nussenzweig, T.T.Paull, F.W.Alt, J.Chen, Mol. Cell. %20;21 (2006) 187-200.

61. C.Strauss, T.Halevy, M.Macarov, L.Argaman, M.Goldberg, DNA Repair (Amst). 10 (2011) 806-814.

62. J.R.Walker, R.A.Corpina, J.Goldberg, Nature. 412 (2001) 607-614.

63. S.Yoo, W.S.Dynan, Nucleic Acids Res. 27 (1999) 4679-4686.

64. K.Valerie, L.F.Povirk, Oncogene. 22 (2003) 5792-5812.

65. M.Shrivastav, L.P.De Haro, J.A.Nickoloff, Cell Res. 18 (2008) 134-147.

66. M.Shrivastav, C.A.Miller, L.P.De Haro, S.T.Durant, B.P.Chen, D.J.Chen, J.A.Nickoloff, DNA Repair (Amst). 8 (2009) 920-929.

67. S.E.Peterson, Y.Li, B.T.Chait, M.E.Gottesman, R.Baer, J.Gautier, J. Cell Biol. 194 (2011) 705-720.

68. C.Strauss, M.Goldberg, Cell Cycle. 10 (2011) 2850-2857.

69. A.J.Morrison, X.Shen, Nat. Rev. Mol. Cell Biol. 10 (2009) 373-384.

70. G.T.Lok, S.M.Sy, S.S.Dong, Y.P.Ching, S.W.Tsao, T.M.Thomson, M.S.Huen, Nucleic Acids Res. 40 (2012) 196-205.

71. S.M.Sy, M.S.Huen, J.Chen, Proc. Natl. Acad. Sci. U. S. A. 106 (2009) 7155-7160.

72. B.Wang, Cell Biosci. 2 (2012) 6-

73. S.M.Dever, S.E.Golding, E.Rosenberg, B.R.Adams, M.O.Idowu, J.M.Quillin, N.Valerie, B.Xu, L.F.Povirk, K.Valerie, Aging (Albany. NY). 3 (2011) 515-532.

74. L.Chen, C.J.Nievera, A.Y.Lee, X.Wu, J. Biol. Chem. 283 (2008) 7713-7720.

75. M.K.Shivji, S.R.Mukund, E.Rajendra, S.Chen, J.M.Short, J.Savill, D.Klenerman, A.R.Venkitaraman, Proc. Natl. Acad. Sci. U. S. A. 106 (2009) 13254-13259.

76. C.Chabalier-Taste, C.Racca, C.Dozier, F.Larminat, Biochim. Biophys. Acta. 1783 (2008) 2223-2233.

77. G.Adelmant, A.S.Calkins, B.K.Garg, J.D.Card, M.Askenazi, A.Miron, B.Sobhian, Y.Zhang, Y.Nakatani, P.A.Silver, J.D.Iglehart, J.A.Marto, J.B.Lazaro, Mol. Cell Proteomics. (2012)

78. J.Drouet, P.Frit, C.Delteil, J.P.de Villartay, B.Salles, P.Calsou, J. Biol. Chem. 281 (2006) 27784-27793.

79. J.Drouet, C.Delteil, J.Lefrancois, P.Concannon, B.Salles, P.Calsou, J. Biol. Chem. 280 (2005) 7060-7069.

80. J.Zhuang, G.Jiang, H.Willers, F.Xia, J. Biol. Chem. 284 (2009) 30565-30573.

81. Q.Zhong, T.G.Boyer, P.L.Chen, W.H.Lee, Cancer Res. 62 (2002) 3966-3970.

82. D.T.Bau, Y.P.Fu, S.T.Chen, T.C.Cheng, J.C.Yu, P.E.Wu, C.Y.Shen, Cancer Res. 64 (2004) 5013-5019.

83. M.E.Moynahan, J.W.Chiu, B.H.Koller, M.Jasin, Mol. Cell. 4 (1999) 511-518.

84. A.Bothmer, D.F.Robbiani, M.Di Virgilio, S.F.Bunting, I.A.Klein, N.Feldhahn, J.Barlow, H.T.Chen, D.Bosque, E.Callen, A.Nussenzweig, M.C.Nussenzweig, Mol. Cell. 42 (2011) 319-329.

85. C.Baldeyron, E.Jacquemin, J.Smith, C.Jacquemont, O.De, I, S.Gad, J.Feunteun, D.Stoppa-Lyonnet, D.Papadopoulo, Oncogene. 21 (2002) 1401-1410.

86. J.J.Gorski, K.I.Savage, J.M.Mulligan, S.S.McDade, J.K.Blayney, Z.Ge, D.P.Harkin, Nucleic Acids Res. 39 (2011) 9536-9548.

87. A.N.Monteiro, A.August, H.Hanafusa, Proc. Natl. Acad. Sci. U. S. A. 93 (1996) 13595-13599.

88. F.Hayes, C.Cayanan, D.Barilla, A.N.Monteiro, Cancer Res. 60 (2000) 2411-2418.

89. S.A.Krum, G.A.Miranda, C.Lin, T.F.Lane, J. Biol. Chem. 278 (2003) 52012-52020.

90. T.F.Lane, Cancer Biol. Ther. 3 (2004) 528-533.

91. R.Scully, J.Chen, R.L.Ochs, K.Keegan, M.Hoekstra, J.Feunteun, D.M.Livingston, Cell. 90 (1997) 425-435.

92. J.S.Lee, K.M.Collins, A.L.Brown, C.H.Lee, J.H.Chung, Nature. 404 (2000) 201-204.

93. H.Kawai, H.Li, P.Chun, S.Avraham, H.K.Avraham, Oncogene. 21 (2002) 7730-7739.

94. Y.Zhang, S.Fan, Q.Meng, Y.Ma, P.Katiyar, R.Schlegel, E.M.Rosen, J. Biol. Chem. 280 (2005) 33165-33177.

95. J.P.Vaughn, P.L.Davis, M.D.Jarboe, G.Huper, A.C.Evans, R.W.Wiseman, A.Berchuck, J.D.Iglehart, P.A.Futreal, J.R.Marks, Cell Growth Differ. 7 (1996) 711-715.

96. H.Ruffner, I.M.Verma, Proc. Natl. Acad. Sci. U. S. A. 94 (1997) 7138-7143.

97. M.Fabbro, K.Savage, K.Hobson, A.J.Deans, S.N.Powell, G.A.McArthur, K.K.Khanna, J. Biol. Chem. 279 (2004) 31251-31258.

98. K.Somasundaram, H.Zhang, Y.X.Zeng, Y.Houvras, Y.Peng, H.Zhang, G.S.Wu, J.D.Licht, B.L.Weber, W.S.El Deiry, Nature. 389 (1997) 187-190.

99. S.Li, P.L.Chen, T.Subramanian, G.Chinnadurai, G.Tomlinson, C.K.Osborne, Z.D.Sharp, W.H.Lee, J. Biol. Chem. 274 (1999) 11334-11338.

100. B.Xu, S.Kim, M.B.Kastan, Mol. Cell Biol. 21 (2001) 3445-3450.

101. B.Xu, A.H.O'Donnell, S.T.Kim, M.B.Kastan, Cancer Res. 62 (2002) 4588-4591.

102. Q.Zhong, C.F.Chen, S.Li, Y.Chen, C.C.Wang, J.Xiao, P.L.Chen, Z.D.Sharp, W.H.Lee, Science. 285 (1999) 747-750.

103. M.Ouchi, T.Ouchi, Genes Cancer. 1 (2010) 1211-1214.

104. J.H.Lee, T.T.Paull, Science. 304 (2004) 93-96.

105. X.Xu, Z.Weaver, S.P.Linke, C.Li, J.Gotay, X.W.Wang, C.C.Harris, T.Ried, C.X.Deng, Mol. Cell. 3 (1999) 389-395.

106. X.Yu, J.Chen, Mol. Cell Biol. 24 (2004) 9478-9486.

107. R.I.Yarden, S.Pardo-Reoyo, M.Sgagias, K.H.Cowan, L.C.Brody, Nat. Genet. 30 (2002) 285-289.

108. M.Fabbro, B.R.Henderson, Cancer Lett. 263 (2008) 189-196.

109. M.Takekawa, H.Saito, Cell. 95 (1998) 521-530.

110. J.M.Johnson, J.Castle, P.Garrett-Engele, Z.Kan, P.M.Loerch, C.D.Armour, R.Santos, E.E.Schadt, R.Stoughton, D.D.Shoemaker, Science. %19;302 (2003) 2141-2144.

111. A.Garcia-Sacristan, M.J.Fernandez-Nestosa, P.Hernandez, J.B.Schvartzman, D.B.Krimer, Cell Res. 15 (2005) 495-503.

112. F.Hirano, M.Chung, H.Tanaka, N.Maruyama, I.Makino, D.D.Moore, C.Scheidereit, Mol. Cell Biol. 18 (1998) 2596-2607.

113. J.P.Sleeman, K.Kondo, J.Moll, H.Ponta, P.Herrlich, J. Biol. Chem. 272 (1997) 31837-31844.

114. A.Ghosh, D.Stewart, G.Matlashewski, Mol. Cell Biol. 24 (2004) 7987-7997.

115. L.E.Jensen, A.S.Whitehead, J. Biol. Chem. 276 (2001) 29037-29044.

116. S.Mazoyer, N.Puget, L.Perrin-Vidoz, H.T.Lynch, O.M.Serova-Sinilnikova, G.M.Lenoir, Am. J. Hum. Genet. 62 (1998) 713-715.

117. E.Scholzova, R.Malik, J.Sevcik, Z.Kleibl, Cancer Lett. 246 (2007) 12-23.

118. Z.Wang, H.S.Lo, H.Yang, S.Gere, Y.Hu, K.H.Buetow, M.P.Lee, Cancer Res. 63 (2003) 655-657.

119. A.Sureau, R.Gattoni, Y.Dooghe, J.Stevenin, J.Soret, EMBO J. 20 (2001) 1785-1796.

120. B.M.Brinkman, Clin. Biochem. 37 (2004) 584-594.

121. J.M.Adams, Genes Dev. 17 (2003) 2481-2495.

122. D.Bentley, Curr. Opin. Cell Biol. 14 (2002) 336-342.

123. J.Y.Wu, T.Maniatis, Cell. 75 (1993) 1061-1070.

124. P.J.Grabowski, S.R.Seiler, P.A.Sharp, Cell. 42 (1985) 345-353.

125. E.J.Sontheimer, J.A.Steitz, Science. 262 (1993) 1989-1996.

126. A.M.Weiner, Cell. 72 (1993) 161-164.

127. H.D.Madhani, C.Guthrie, Cell. 71 (1992) 803-817.

128. R.Reed, Curr. Opin. Genet. Dev. 6 (1996) 215-220.

129. S.Valadkhan, J.L.Manley, RNA. 9 (2003) 892-904.

130. R.Reed, Curr. Opin. Genet. Dev. 6 (1996) 215-220.

131. A.E.Cowper, J.F.Caceres, A.Mayeda, G.R.Screaton, J. Biol. Chem. 276 (2001) 48908-48914.

132. A.M.Krecic, M.S.Swanson, Curr. Opin. Cell Biol. 11 (1999) 363-371.

133. X.D.Fu, RNA. 1 (1995) 663-680.

134. C.L.Will, R.Luhrmann, Curr. Opin. Cell Biol. 13 (2001) 290-301.

135. H.Shen, M.R.Green, Mol. Cell. 16 (2004) 363-373.

136. B.J.Blencowe, Trends Biochem. Sci. 25 (2000) 106-110.

137. W.G.Fairbrother, L.A.Chasin, Mol. Cell Biol. 20 (2000) 6816-6825.

138. S.Guil, R.Gattoni, M.Carrascal, J.Abian, J.Stevenin, M.Bach-Elias, Mol. Cell Biol. 23 (2003) 2927-2941.

139. S.Valadkhan, J.L.Manley, RNA. 9 (2003) 892-904.

140. J.D.Kohtz, S.F.Jamison, C.L.Will, P.Zuo, R.Luhrmann, M.A.Garcia-Blanco, J.L.Manley, Nature. 368 (1994) 119-124.

141. K.J.Hertel, T.Maniatis, Proc. Natl. Acad. Sci. U. S. A. 96 (1999) 2651-2655.

142. J.D.Kohtz, S.F.Jamison, C.L.Will, P.Zuo, R.Luhrmann, M.A.Garcia-Blanco, J.L.Manley, Nature. 368 (1994) 119-124.

143. P.Zuo, T.Maniatis, Genes Dev. 10 (1996) 1356-1368.

144. H.Shen, M.R.Green, Mol. Cell. 16 (2004) 363-373.

145. H.Shen, J.L.Kan, M.R.Green, Mol. Cell. 13 (2004) 367-376.

146. H.Shen, M.R.Green, Genes Dev. 20 (2006) 1755-1765.

147. J.Bi, H.Xia, F.Li, X.Zhang, Y.Li, Biochem. Biophys. Res. Commun. 333 (2005) 64-69.

148. van Der Houven Van Oordt, K.Newton, G.R.Screaton, J.F.Caceres, Nucleic Acids Res. 28 (2000) 4822-4831.

149. E.C.Ibrahim, T.D.Schaal, K.J.Hertel, R.Reed, T.Maniatis, Proc. Natl. Acad. Sci. U. S. A. 102 (2005) 5002-5007.

150. H.X.Liu, M.Zhang, A.R.Krainer, Genes Dev. 12 (1998) 1998-2012.

151. Y.He, R.Smith, Cellular and Molecular Life Sciences 66 (2009) 1239-1256.

152. Y.He, R.Smith, Cellular and Molecular Life Sciences 66 (2009) 1239-1256.

153. J.F.Caceres, S.Stamm, D.M.Helfman, A.R.Krainer, Science. 265 (1994) 1706-1709.

154. N.Matter, M.Marx, S.Weg-Remers, H.Ponta, P.Herrlich, H.Konig, J. Biol. Chem. 275 (2000) 35353-35360.

155. J.Zhu, A.Mayeda, A.R.Krainer, Mol. Cell. 8 (2001) 1351-1361.

156. N.Rooke, V.Markovtsov, E.Cagavi, D.L.Black, Mol. Cell Biol. 23 (2003) 1874-1884.

157. B.Charlet, P.Logan, G.Singh, T.A.Cooper, Mol. Cell. 9 (2002) 649-658.

158. M.Blanchette, B.Chabot, EMBO J. 18 (1999) 1939-1952.

159. N.Matter, M.Marx, S.Weg-Remers, H.Ponta, P.Herrlich, H.Konig, J. Biol. Chem. 275 (2000) 35353-35360.

160. R.Tacke, J.L.Manley, Curr. Opin. Cell Biol. 11 (1999) 358-362.

161. I.C.Eperon, O.V.Makarova, A.Mayeda, S.H.Munroe, J.F.Caceres, D.G.Hayward, A.R.Krainer, Mol. Cell Biol. 20 (2000) 8303-8318.

162. M.M.de la, C.R.Alonso, S.Kadener, J.P.Fededa, M.Blaustein, F.Pelisch, P.Cramer, D.Bentley, A.R.Kornblihtt, Mol. Cell. 12 (2003) 525-532.

163. S.Solier, A.Lansiaux, E.Logette, J.Wu, J.Soret, J.Tazi, C.Bailly, L.Desoche, E.Solary, L.Corcos, Mol. Cancer Res. 2 (2004) 53-61.

164. B.Li, C.Wachtel, E.Miriami, G.Yahalom, G.Friedlander, G.Sharon, R.Sperling, J.Sperling, Proc. Natl. Acad. Sci. U. S. A. 99 (2002) 5277-5282.

165. M.B.Stadler, N.Shomron, G.W.Yeo, A.Schneider, X.Xiao, C.B.Burge, PLoS. Genet. 2 (2006) e191-

166. H.X.Liu, S.L.Chew, L.Cartegni, M.Q.Zhang, A.R.Krainer, Mol. Cell Biol. 20 (2000) 1063-1071.

167. J.Wang, P.J.Smith, A.R.Krainer, M.Q.Zhang, Nucleic Acids Res. 33 (2005) 5053-5062.

168. R.H.Hovhannisyan, C.C.Warzecha, R.P.Carstens, Nucleic Acids Res. 34 (2006) 373-385.

169. M.Sironi, G.Menozzi, L.Riva, R.Cagliani, G.P.Comi, N.Bresolin, R.Giorda, U.Pozzoli, Nucleic Acids Res. %19;32 (2004) 1783-1791.

170. U.Pozzoli, M.Sironi, Cell Mol. Life Sci. 62 (2005) 1579-1604.

171. M.Sironi, G.Menozzi, L.Riva, R.Cagliani, G.P.Comi, N.Bresolin, R.Giorda, U.Pozzoli, Nucleic Acids Res. %19;32 (2004) 1783-1791.

172. Z.Wang, M.E.Rolish, G.Yeo, V.Tung, M.Mawson, C.B.Burge, Cell. 119 (2004) 831-845.

173. H.Sun, L.A.Chasin, Mol. Cell Biol. 20 (2000) 6414-6425.

174. R.H.Hovhannisyan, C.C.Warzecha, R.P.Carstens, Nucleic Acids Res. 34 (2006) 373-385.

175. M.Montes, S.Becerra, M.Sanchez-Alvarez, C.Sune, Gene. 501 (2012) 104-117.

176. L.P.Eperon, I.R.Graham, A.D.Griffiths, I.C.Eperon, Cell. 54 (1988) 393-401.

177. P.Cramer, J.F.Caceres, D.Cazalla, S.Kadener, A.F.Muro, F.E.Baralle, A.R.Kornblihtt, Mol. Cell. 4 (1999) 251-258.

178. M.M.de la, C.R.Alonso, S.Kadener, J.P.Fededa, M.Blaustein, F.Pelisch, P.Cramer, D.Bentley, A.R.Kornblihtt, Mol. Cell. 12 (2003) 525-532.

179. X.D.Fu, T.Maniatis, Nature. 343 (1990) 437-441.

180. S.H.Xiao, J.L.Manley, EMBO J. 17 (1998) 6359-6367.

181. J.M.Yeakley, H.Tronchere, J.Olesen, J.A.Dyck, H.Y.Wang, X.D.Fu, J. Cell Biol. 145 (1999) 447-455.

182. M.C.Lai, R.I.Lin, W.Y.Tarn, Biochem. J. 371 (2003) 937-945.

183. E.Allemand, S.Guil, M.Myers, J.Moscat, J.F.Caceres, A.R.Krainer, Proc. Natl. Acad. Sci. U. S. A. 102 (2005) 3605-3610.

184. K.Colwill, L.L.Feng, J.M.Yeakley, G.D.Gish, J.F.Caceres, T.Pawson, X.D.Fu, J. Biol. Chem. 271 (1996) 24569-24575.

185. K.Colwill, T.Pawson, B.Andrews, J.Prasad, J.L.Manley, J.C.Bell, P.I.Duncan, EMBO J. 15 (1996) 265-275.

186. M.Blaustein, F.Pelisch, T.Tanos, M.J.Munoz, D.Wengier, L.Quadrana, J.R.Sanford, J.P.Muschietti, A.R.Kornblihtt, J.F.Caceres, O.A.Coso, A.Srebrow, Nat. Struct. Mol. Biol. 12 (2005) 1037-1044.

187. H.Konig, H.Ponta, P.Herrlich, EMBO J. 17 (1998) 2904-2913.

188. J.H.Ding, X.Y.Zhong, J.C.Hagopian, M.M.Cruz, G.Ghosh, J.Feramisco, J.A.Adams, X.D.Fu, Mol. Biol. Cell. 17 (2006) 876-885.

189. C.Cheng, P.A.Sharp, Mol. Cell Biol. 26 (2006) 362-370.

190. J.Zhu, A.Mayeda, A.R.Krainer, Mol. Cell. 8 (2001) 1351-1361.

191. P.Klingbeil, R.Marhaba, T.Jung, R.Kirmse, T.Ludwig, M.Zoller, Mol. Cancer Res. 7 (2009) 168-179.

192. G.Merdzhanova, V.Edmond, S.De Seranno, B.A.Van den, L.Corcos, C.Brambilla, E.Brambilla, S.Gazzeri, B.Eymin, Cell Death. Differ. 15 (2008) 1815-1823.

193. A.A.Tesoriero, E.M.Wong, M.A.Jenkins, J.L.Hopper, M.A.Brown, G.Chenevix-Trench, A.B.Spurdle, M.C.Southey, Hum. Mutat. 26 (2005) 495-

194. A.Srebrow, A.R.Kornblihtt, J. Cell Sci. 119 (2006) 2635-2641.

195. D.R.Mercatante, C.D.Bortner, J.A.Cidlowski, R.Kole, J. Biol. Chem. 276 (2001) 16411-16417.

196. M.Krawczak, J.Reiss, D.N.Cooper, Hum. Genet. 90 (1992) 41-54.

197. C.Cheng, M.B.Yaffe, P.A.Sharp, Genes Dev. 20 (2006) 1715-1720.

198. E.Stickeler, F.Kittrell, D.Medina, S.M.Berget, Oncogene. 18 (1999) 3574-3582.

199. M.T.Pind, P.H.Watson, Breast Cancer Res. Treat. 79 (2003) 75-82.

200. D.S.Chandler, R.K.Singh, L.C.Caldwell, J.L.Bitler, G.Lozano, Cancer Res. 66 (2006) 9502-9508.

201. J.C.Bourdon, K.Fernandes, F.Murray-Zmijewski, G.Liu, A.Diot, D.P.Xirodimas, M.K.Saville, D.P.Lane, Genes Dev. 19 (2005) 2122-2137.

202. C.A.Pettigrew, J.D.French, J.M.Saunus, S.L.Edwards, A.V.Sauer, C.E.Smart, T.Lundstrom, C.Wiesner, A.B.Spurdle, J.A.Rothnagel, M.A.Brown, Breast Cancer Res. Treat. 119 (2010) 239-247.

203. L.Miao, Z.Cao, C.Shen, M.Gu, W.Liu, H.Li, C.Zheng, Biochemistry (Mosc.). 73 (2008) 1214-1223.

204. J.K.Pickrell, A.A.Pai, Y.Gilad, J.K.Pritchard, PLoS. Genet. 6 (2010) e1001236-

205. L.Perrin-Vidoz, O.M.Sinilnikova, D.Stoppa-Lyonnet, G.M.Lenoir, S.Mazoyer, Hum. Mol. Genet. 11 (2002) 2805-2814.

206. T.I.Orban, E.Olah, Biochem. Biophys. Res. Commun. 280 (2001) 32-38.

207. M.Lu, B.A.Arrick, Oncogene. 19 (2000) 6351-6360.

208. L.J.Huber, T.W.Yang, C.J.Sarkisian, S.R.Master, C.X.Deng, L.A.Chodosh, Mol. Cell Biol. 21 (2001) 4005-4015.

209. R.Bachelier, X.Xu, X.Wang, W.Li, M.Naramura, H.Gu, C.X.Deng, Oncogene. 22 (2003) 528-537.

210. E.Nakuci, S.Mahner, J.Direnzo, W.M.Elshamy, Exp. Cell Res. 312 (2006) 3120-3131.

211. K.Chock, J.M.Allison, W.M.Elshamy, Oncogene. 29 (2010) 5274-5285.

212. M.Lu, S.D.Conzen, C.N.Cole, B.A.Arrick, Cancer Res. 56 (1996) 4578-4581.

213. C.A.Wilson, M.N.Payton, G.S.Elliott, F.W.Buaas, E.E.Cajulis, D.Grosshans, L.Ramos, D.M.Reese, D.J.Slamon, F.J.Calzone, Oncogene. 14 (1997) 1-16.

214. J.E.Quinn, R.D.Kennedy, P.B.Mullan, P.M.Gilmore, M.Carty, P.G.Johnston, D.P.Harkin, Cancer Res. 63 (2003) 6221-6228.

215. M.Amarzguioui, H.Prydz, Biochem. Biophys. Res. Commun. 316 (2004) 1050-1058.

216. K.Ui-Tei, Y.Naito, F.Takahashi, T.Haraguchi, H.Ohki-Hamazaki, A.Juni, R.Ueda, K.Saigo, Nucleic Acids Res. 32 (2004) 936-948.

217. Flemington E., (2010)

218. E.Vondruskova, R.Malik, J.Sevcik, P.Kleiblova, Z.Kleibl, Neoplasma. 55 (2008) 130-137.

219. H.C.Wang, W.C.Chou, S.Y.Shieh, C.Y.Shen, Cancer Res. 66 (2006) 1391-1400.

220. B.Sobhian, G.Shao, D.R.Lilli, A.C.Culhane, L.A.Moreau, B.Xia, D.M.Livingston, R.A.Greenberg, Science. 316 (2007) 1198-1202.

221. J.N.Glover, R.S.Williams, M.S.Lee, Trends Biochem. Sci. 29 (2004) 579-585.

222. P.Duez, G.Dehon, J.Dubois, Talanta. 63 (2004) 879-886.

223. M.Falk, E.Lukasova, B.Gabrielova, V.Ondrej, S.Kozubek, Biochim. Biophys. Acta. 1773 (2007) 1534-1545.

224. M.E.Moynahan, T.Y.Cui, M.Jasin, Cancer Res. 61 (2001) 4842-4850.

225. Y.Lorat, S.Schanz, N.Schuler, G.Wennemuth, C.Rube, C.E.Rube, PLoS. One. 7 (2012) e38165-

226. B.M.Henrique, G.B.Garziera, R.Braga, V, M.P.Cesaro, R.Ferreira, J.F.Oliveira, P.B.Goncalves, V.Bordignon, Exp. Cell Res. (2012)

227. L.J.Barber, J.L.Youds, J.D.Ward, M.J.McIlwraith, N.J.O'Neil, M.I.Petalcorin, J.S.Martin, S.J.Collis, S.B.Cantor, M.Auclair, H.Tissenbaum, S.C.West, A.M.Rose, S.J.Boulton, Cell. 135 (2008) 261-271.

228. G.Bordeianu, F.Zugun-Eloae, M.G.Rusu, Rev. Med. Chir Soc. Med. Nat. Iasi. 115 (2011) 1189-1194.

229. M.H.Yun, K.Hiom, Nature. 459 (2009) 460-463.

230. B.Wang, S.Matsuoka, B.A.Ballif, D.Zhang, A.Smogorzewska, S.P.Gygi, S.J.Elledge, Science. 316 (2007) 1194-1198.

231. N.S.Ting, W.H.Lee, DNA Repair (Amst). 3 (2004) 935-944.

232. J.Lukas, C.Lukas, J.Bartek, Nat. Cell Biol. 13 (2011) 1161-1169.

233. K.A.Coleman, R.A.Greenberg, J. Biol. Chem. 286 (2011) 13669-13680.

234. L.J.Barber, S.J.Boulton, DNA Repair (Amst). 5 (2006) 1499-1504.

235. L.N.Burga, N.M.Tung, S.L.Troyan, M.Bostina, P.A.Konstantinopoulos, H.Fountzilas, D.Spentzos, A.Miron, Y.A.Yassin, B.T.Lee, G.M.Wulf, Cancer Res. 69 (2009) 1273-1278.

236. S.Furuta, X.Jiang, B.Gu, E.Cheng, P.L.Chen, W.H.Lee, Proc. Natl. Acad. Sci. U. S. A. 102 (2005) 9176-9181.

237. P.B.Mullan, J.E.Quinn, D.P.Harkin, Oncogene. 25 (2006) 5854-5863.

238. C.Y.Li, J.Y.Chu, J.K.Yu, X.Q.Huang, X.J.Liu, L.Shi, Y.C.Che, J.Y.Xie, Cell Res. 14 (2004) 473-479.

239. T.I.Orban, E.Olah, Mol. Pathol. 56 (2003) 191-197.

240. S.Debska, J.Kubicka, R.Czyzykowski, M.Habib, P.Potemski, Postepy Hig. Med. Dosw. (Online.). 66:311-21. (2012) 311-321.

241. P.Gottipati, B.Vischioni, N.Schultz, J.Solomons, H.E.Bryant, T.Djureinovic, N.Issaeva, K.Sleeth, R.A.Sharma, T.Helleday, Cancer Res. 70 (2010) 5389-5398.